INTERACTIONS OF QUINOLINE ANTI-MALARIALS WITH HAEMATIN AND THEIR EFFECT ON β-HAEMATIN FORMATION

BY

KANYILE K. NCOKAZI

Thesis Presented for the Degree of

DOCTOR OF PHILOSOPHY

in the Department of Chemistry

UNIVERSITY OF CAPE TOWN

May 2005

Supervisor: Associate Professor T. J. Egan

ABSTRACT

Thermodynamic compensation in the interaction of quinoline antimalarials with haematin in 40% (v/v) aqueous DMSO has been compared with that in pure aqueous solution. The data indicate that the degree of desolvation and loss of conformational freedom is identical in both systems. The nature of interactions between quinoline drugs and haematin was investigated spectroscopically in organic and mixed solvents. Free energies of association of chloroquine, quinine and quinidine with haematin are largely insensitive to the increasing concentration of $NaClO_4$. This demonstrates that electrostatic interactions play a minor role in the overall stability of these complexes under these conditions. Increasing concentration of DMSO weakens association of chloroquine, amodiaquine, quinine, quinidine and 9-epiquinine with haematin. These effects suggest that the interactions are hydrophobic. Furthermore, it has been demonstrated that free energy of association with haematin weakens as a function of decreasing solvent polarity in organic solvents. However, free energies of association are weaker in mixed aqueous solvents than in pure organic solvents. This indicates that dispersion and electrostatic interactions are relatively stronger in a non-aqueous environment.

A new assay has been developed for measuring inhibition of β-haematin formation using 5% (v/v) aqueous pyridine solution. This pyridine solution forms a low complex with haematin in aqueous solution but not with β-haematin. Formation of β-haematin is brought about in 4.5 M acetate, pH 4.5 at 60°C. The assay is rapid (60 min incubation) and requires no centrifugation or expensive radioactive material. This assay is compatible with high throughput screening and analysis can be done by visual inspection of β-haematin inhibitors. The IC_{50} values obtained were compared with those reported in other assays for 13 compounds investigated. There was generally a good correlation between the pyridine assay and other assays. Used qualitatively, the method was also employed for screening 48 compounds for β-haematin inhibition. All of these compounds produced results in agreement with expectation from previous investigations.

The pyridine assay was also used to investigate the strength of inhibition of β-haematin formation by chloroquine, amodiaquine, quinine and quinidine as a function of incubation time. This study has demonstrated that β-haematin eventually forms with long incubation times. This conclusion was supported by XRD, IR and SEM. It was further demonstrated that IC_{50} increases markedly with incubation time with 4-aminoquinolines such chloroquine and amodiaquine. By contrast, with quinine and quinidine the IC_{50} increases much more slowly with time, corresponding to slower β-haematin formation in the presence of these drugs. These findings suggest that quinoline drugs decrease the rate of β-haematin formation rather that irreversibly blocking its formation.

DECLARATION

I declare that this thesis is my own original research and all sources that I have used or quoted have been indicated and acknowledged by means of complete references.

Signed by candidate

Kanyile K. Ncokazi

ACKNOWLEDGEMENTS

I would like to thank my supervisor Professor Timothy J. Egan for his guidance, continual oversight of this work, many discussions of results and in help to shape me as a chemist, endless patience during the writing of this manuscript is warmly appreciated.

I would also like to thank the following people:

- Professor Peter Smith at the Division of Pharmacology, Department of Medicine for letting me use the 96 well plate reader.
- Mr Donelly van Schalkwyk for his kind assistance in the use of the plate reader and advice regarding the 96 well assays.
- Dr Gareth Arnott is also acknowledged for taking the digital photograph
- Mr Vincent Smith for assistance with collection of XRD data
- Ms Miranda Waldron for carrying out scanning electron analysis of my samples.
- To my former colleagues whom I met when I joined the group, Dr Winile Mavuso, Dr Catherine Kaschula and Mr Paul Swan.
- To my colleagues and fellow students Mmboneni Tshivhase, Katherine De Villiers and Tebogo Mabotha for their warm company and encouragement.
- To my parents for their moral support, even when the details of what I was doing remain somewhat a mystery.
- To my brother Kanya and my two sisters Kanyisa and Bukanyile for their endless support.

CONFERENCE PROCEEDINGS AND PUBLICATIONS ARISING FROM THIS WORK

CONFERENCE PROCEEDINGS

2000: 24 – 29th September, 35th Convention of the South African Chemical Institute, Potchestroom University, South Africa.
Poster – "Investigation of the thermodynamic interaction of anti-malarial drugs with haematin at different solvent systems".

2002: 1–5 July, 36th Convention of the South African Chemical Institute, University of Port Elizabeth, South Africa.
Poster – "Formation of β-haematin (haemozoin) on the surface of molecular imprinted polymer".

2003: 8 – 11 June, 11th Convention of the South African Chemical Institute in inorganic chemistry, Roode Vallei country lodge, Pretoria, South Africa.
Poster – "A new assay demonstrates delay but not inhibition of haemozoin formation by quinoline antimalarials". Winner of the 1st prize poster presentation competition.

2004: 4 – 9 July, 37th National convention of the South African Chemical Institute, CSIR, Pretoria, South Africa.
Poster – "Interaction of quinoline antimalarials with ferriprotoporphyrin IX is dominated by hydrophobic interactions".

PUBLICATIONS

Egan, T. J.; Mavuso, W. W.; Ncokazi, K. K. The mechanism of β-hematin formation in acetate solution. Parallels between hemozoin formation and biomineralization processes. *Biochemistry* **2001**, *40*, 204-213

Egan, T. J.; Ncokazi, K. K. Effects of solvent composition and ionic strength on the interaction of quinoline antimalarials with ferriprotoporphyrin IX. *J. Inorg. Biochem.* **2004**, *98*, 144-152.

Ncokazi, K.K.; Egan, T.J. A colorimetric high-throughput β-haematin inhibition screening assay for use in the search for antimalarial compounds. *Analytical Biochemistry* **2005**, *338,* 306-319.

Egan, T.J.; Ncokazi, K.K. Quinoline antimalarials decrease the rate of β-haematin Formation. *J. Inorg. Biochem.* **2005**, 99(7):1532-1539.

1. INTRODUCTION

ABBREVIATIONS

A	Absorbance
Å	Angstrom
Ala	Alanine
Asp	Aspartate
ATP	Adenosine triphosphate
BHIA	β-haematin inhibitory activity
^{13}C-NMR	Carbon -13 nuclear magnetic resonance
CHES	2-[N-cyclohexylamino]ethanesulphonic acid
DDT	Dichlorodiphenyltrichloroethane
DMSO	Dimethyl suphoxide
DNA	Deoxyribonucleic acid
EPR	Electron paramagnetic resonance
ESI	Electron spectroscopic imaging
ESR	Electron spin resonance
EXAFS	Extended X-ray absorption fine structure spectroscopy
Fg	Femtograms
Fe(III)PPIX	Ferriprotoporphyrin IX
Fe(II)PPIX	Ferroprotoporphyrin IX
Gly	Glycine
HAP	Histoaspartic protease
Hb	Haemoglobin
HPA	Haem polymerisation assay
HEPES	N-2-Hydroxyethylpiperazine-N'-2-ethanesulphonic acid
His	Histidine
HO-Fe(III)PPIX	Hydroxoferriprotoporphyrin IX
H_2O-Fe(III)PPIX	Aquaferriprotoporphyrin IX
HRP	Histidine rich protein
IC_{50}	50% inhibitory concentration
IR	Infrared spectroscopy
K	Molar equilibrium constant
μ	Ionic strength

MES	2-[N-Morpholino]ethanesulphonic acid
MOPS	3-[N-Morpholino]propanesulphonic acid
N-acetyl-MP8	N-acetylmicroperoxidase-8
NMR	Nuclear Magnetic Resonance
P	Plasmodium
PfCRT	Plasmodium falciparum chloroquine resistant transporter
pfmdr	*Plasmodium falciparum* multidrug resistance gene
Pgh 1	P-glycoprotein homologue 1
Phiβ	Pyridine haemochrome inhibition of β-haematin
RBC	Red blood cell
SEM	Scanning electron microscopy
TEM	Transmission electron microscopy
Uv-vis	ultraviolet / visible
VAR	Vacoular accumulation ratio
λ	Wavelength
ν	Wavenumber
WHO	World Health Organisation
XRD	X-ray (powder) diffraction
Zn(II)PPIX	Zinc protoporphyrin IX

CHAPTER 1

INTRODUCTION

1.1 HISTORY OF MALARIA

Malaria is one of the oldest diseases known to man, it is caused by a protozoan of the genus *Plasmodium*. Four species in this genus that infect man are *P. vivax, P. ovale, P. malariae* and *P. falciparum*. It is thought that malaria was prevalent in ancient China, Egypt, India and Greece where symptoms were described and documented. The disease supposedly had its origin in the jungles of Africa, where it is still very prevalent. The Romans named the disease *"mal' aria"* as at that time the disease was attributed to "*bad air"* surrounding stagnant water [1].

The antiquity of malaria is demonstrated by the host specificity of over 100 parasite species found in reptiles, birds and mammals. Of the four species of *Plasmodia* that infect man, *P. falciparum* is the most dangerous and is responsible for almost all deaths [2] .

1.1.1 Global efforts to eradicate malaria

Huge progress was made in the campaign of reducing the number of malaria cases in the 1950's following the discovery of the insecticide dichlorodiphenyltrichloroethane (DDT), chloroquine chemotherapy and the establishment of World Health Organisation (WHO) which embarked on a Global malaria eradication campaign. The aim of this campaign was to interrupt the transmission from vector to host by killing the attacking mosquitoes likely to contact humans at homes. This was done by employing a very large task force of people to spray DDT into houses in an infected area. Malaria was completely eliminated in Taiwan, the Caribbean, parts of North America, Europe, Northern Australia and a large part of the South Pacific [1].

By mid 1960's however, the WHO realised that malaria could not be eradicated but only controlled. The eradication campaign was put on hold

when mosquitoes developed resistance against DDT and malaria parasites to antimalarial drugs like chloroquine. These factors and others, such as degradation of environment which created more breeding grounds for mosquitoes, have led to an increase in malaria related deaths [3].

1.1.2 Magnitude of the malaria problem

Malaria remains the most serous parasitic disease in man, both from the point of view of mortality and morbidity and from its world-wide occurrence in tropical and subtropical regions (figure 1.1). It is estimated that about 300 million to 500 million people are infected annually with one to two million deaths [4]. The majority of these deaths occur in young children [5]. About two billion people are currently estimated to be at risk from malaria [5]. With increasing evidence of global warming, there is concern over the possibility of considerable growth in this number, with the prospect of malaria spreading to certain areas where it is currently absent [6].

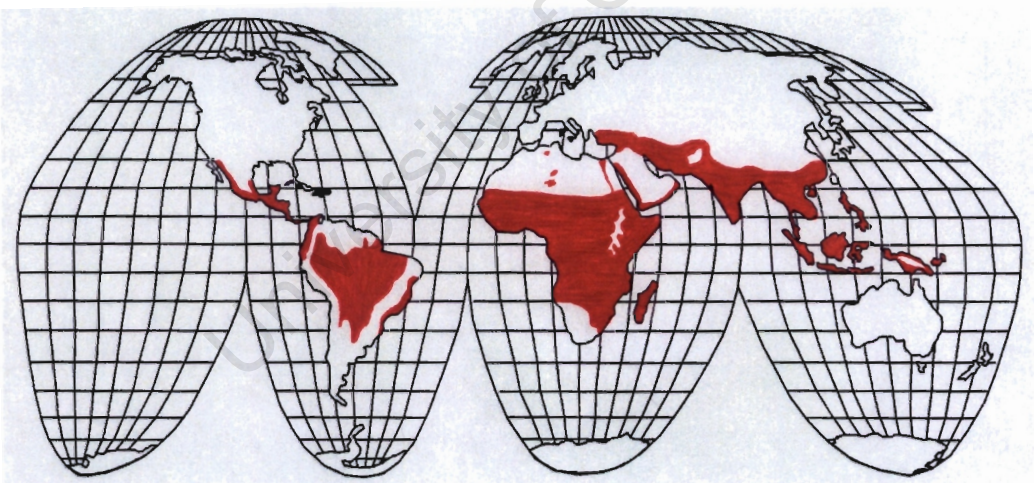

Figure 1.1 Worldwide distribution of malaria parasite [9].

1.2 LIFE CYCLE OF THE MALARIA PARASITE

Figure 1.2 illustrates the life cycle of *Plasmodium falciparum* [7]. The malaria parasite is transmitted by the female *Anopheles* mosquito. Of about 400 species of the *Anopheles* mosquito known, only about 60 transmit the disease [7]. An infected female *Anopheles* mosquito releases malaria sporozoites into the blood stream of the human host during its blood meal. Within 30 - 60 minutes after entering the host, the sporozoites invade parenchymal cells where they multiply and form schizonts. These burst open to release merozoites after 7-12 days in the case of *P. falciparum* [8]. The merozoites invade red cells and develop into small rounded bodies contained within a parasitophorous vacuole called rings, which develop into larger, more irregular shaped trophozoites. This stage of the life cycle is associated with host haemoglobin degradation and formation of the black, granular malaria pigment within an acidic secondary lysosome known as the food vacuole. This progressive invasion of red blood cells is repeated a number of times, giving rise to fevers which are the symptoms of malarial infection. The trophozoites divide asexually to form a blood schizont, which when matured causes the red blood cells to burst open and release more merozoites into the blood stream. These merozoites then invade fresh red blood cells to produce another generation of parasites leading to the progressive increase in parasitemia which continues until host response regulates the infection or death of the patient occurs. This blood stage of life the cycle takes 48 hours in *P. falciparum*, *P. vivax* and *P. ovale* and 72 hours in *P. malariae* [8].

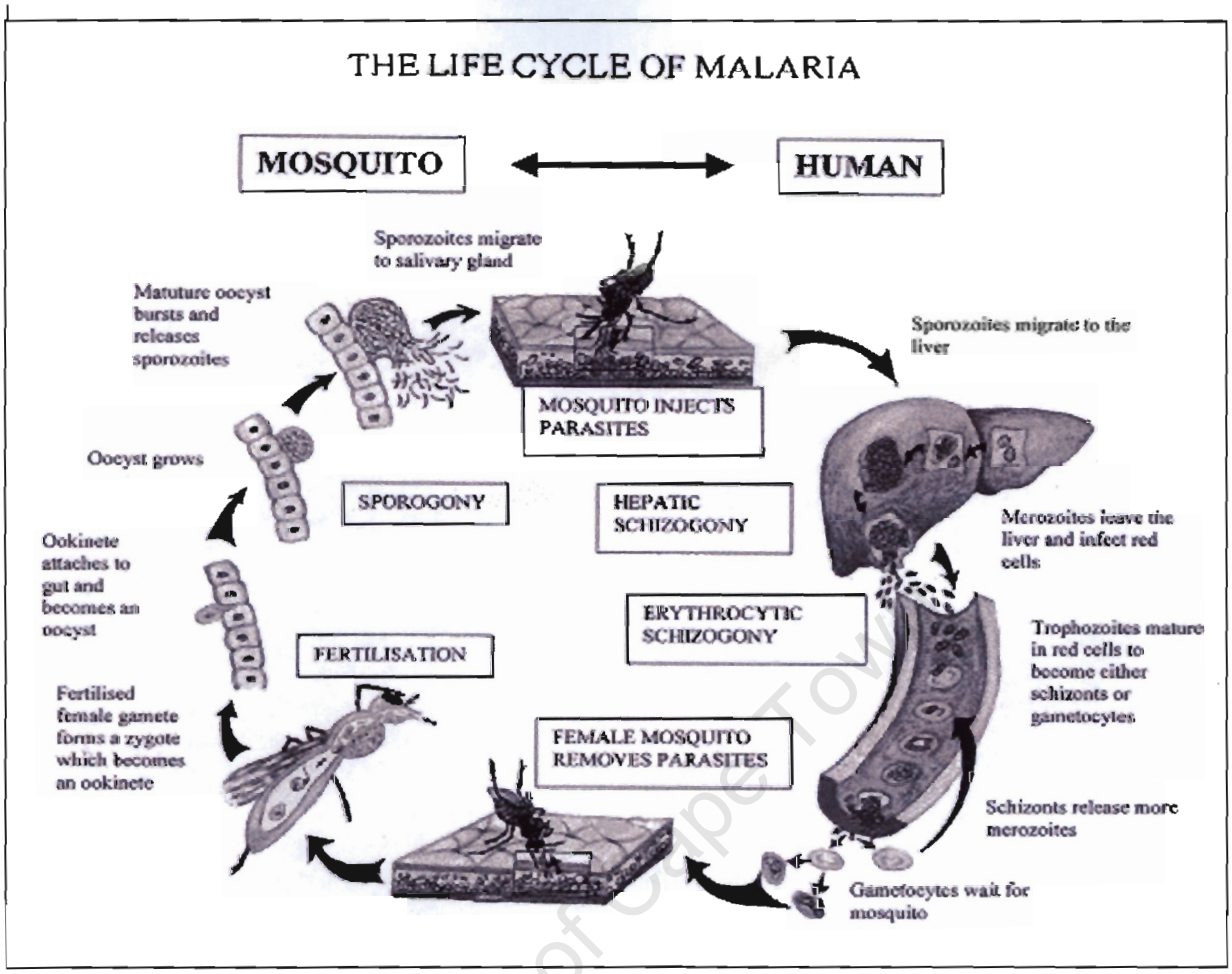

Figure 1.2. Life cycle of *Plasmodium falciparum* [9].

Some erythrocytic schizonts are intended to develop into male and female gametocytes which may be taken up by an *Anopheles* mosquito through its bite. Once inside the gut of the mosquito, male and female gametes fuse to form a zygote which develops into oocyst, and later into sporozoites. These sporozoites travel to the salivary glands where they wait to be discharged into the next human host when the mosquito takes another blood meal.

1.3 ERYTHROCYTIC HAEMOGLOBIN DEGRADATION AND HAEMOZOIN FORMATION

1.3.1 Haemoglobin degradation

As has been seen, a portion of the parasite life cycle occurs within the erythrocyte (red blood cell) of the human host. During this stage of the life cycle, the parasite utilises host haemoglobin as its primary food source [10]. In *Plasmodium falciparum* infection, about 60-70% of red blood cell haemoglobin is degraded by the parasite. Intriguingly, recent studies suggest that only a small fraction of the resulting amino acids are utilised by the parasite [11]. If confirmed, this would mean that the purpose for this large scale haemoglobin degradation is still not fully understood.

Haemoglobin is imported in transport vesicles into a specialised acidic compartment in the parasite, known as a food vacuole and degraded by four proteolytic enzymes which have been identified and characterised. These include four aspartic proteases, plasmepsin I, II [12-15] and IV [16] and histoaspartic protease (HAP) [17-19] three cysteine proteases, falcipain 1, 2 and 3 [20] and a metallopeptidase, facilysin [21]. Plasmepsin I and II are active in degrading haemoglobin, while plasmepsin IV has only weak proteolytic activity against the native protein but appears to act synergistically with plasmepsin I and II HAP is active against globin but not Hb [18]. Falcipain-2 is inactive against Hb unless a mild reducing agent is present and is more active against denatured globin [22]. Facilysin is active in cleaving Hb derived peptides to smaller fragments [22]. Thus, these enzymes appear to act in concert. The degradation process is summarised in figure 1.3.

1.3.2 Haemozoin formation

Haem is released in the process as a by-product which is then autoxidised to haematin which is known to be toxic to microorganisms [23]. Formation of haemozoin (malaria pigment) appears to be a detoxification mechanism for the parasite [24]. This material is responsible for the organ discolouration in malaria patients which was first noted by Lancisi in 1716 and later by Bright in 1831. Haemozoin formation is not unique to the malaria parasite, but has also been recently identified to other organisms that degrade haemoglobin where presumably it serves the same purpose. These organisms are the blood sucking insect *Rhodnius prolixus,* which is an important vector of *Trypanosoma cruzi,* the causative agent of Chaga's disease [25, 26], *Shistosoma mansoni*, a worm in humans causing schistosomiasis [27] and *Haemoproteus columbae* a protozoan parasite common in birds [28].

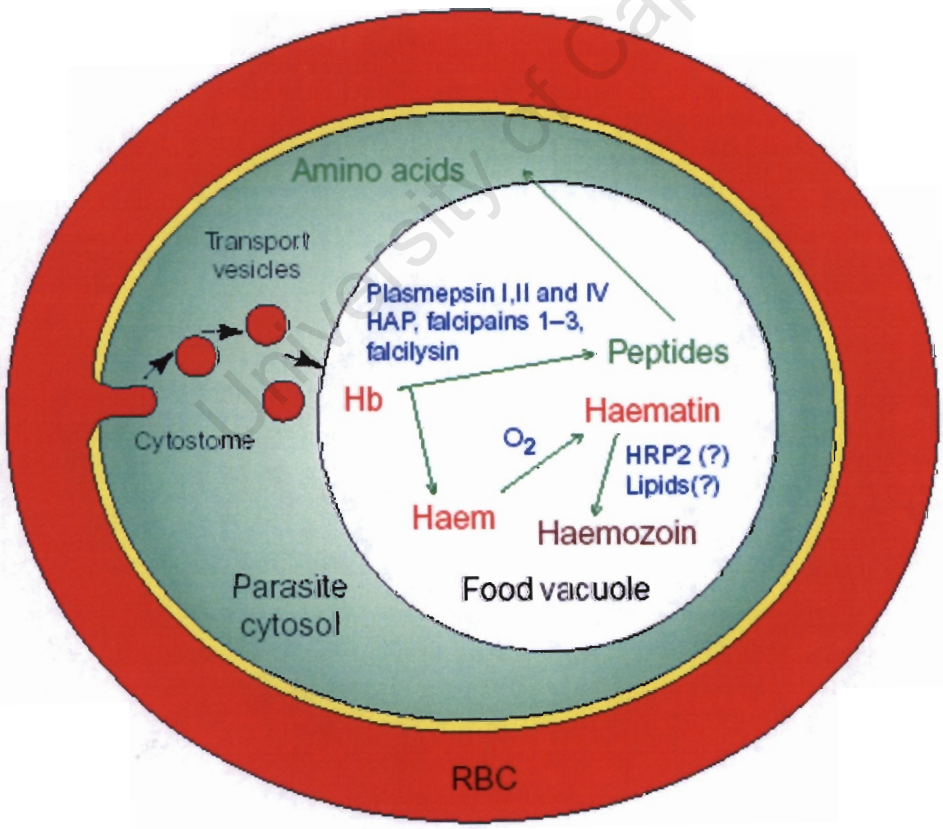

Figure 1.3 Schematic representation of haemoglobin degradation in the malaria parasite *P. falciparum* [29].

1.3.3 Haemozoin is identical to β-haematin

Malaria pigment (haemozoin) was believed to be melanin until in 1911 when Brown conclusively proved that the pigment in actually haematin [30]. Brown further suggested that the source of malaria pigment results from the action of proteolytic enzymes of the malaria parasite upon the haemoglobin of red cells. A few decades later Ghosh and Sinton demonstrated that such a pigment contained a non-ionizable Fe [31]. Warhurst and co-workers [32] made observations which suggested that haemozoin was a crystalline complex with a specially synthesized protein that detoxifies the iron porphyrin residue from haemoglobin digestion, but is incapable of cleaving the haem ring. Goldie et al. [33] characterised pigment granules of haemozoin and found them to be composed of 65% protein, 16% ferriprotoporphyrin IX, 6% carbohydrates and trace amounts of lipids and nucleic acids. They suggested that the overwhelming majority of the protein component is a mixture of native and denatured human globin non-covalently associated with the metalloporphyrin. Fitch and Kanjananggulpan [34] first demonstrated that ferriprotoporphyrin IX in fact is sequestered in malaria pigment as an insoluble aggregate of haematin, based on the electron absorption spectrum and insolubility in ethanol and aqueous sodium bicarbonate they proposed that malaria pigment is identical to β-haematin, a synthetic product prepared by treating erythrocytes with acetic acid at 75°C. Slater et al. [35] proposed that malaria pigment and β-haematin consist of a polymer of haems linked between the central ferric ion of one haem and the carboxylate side group oxygen of another and sequestered via this linkage into an insoluble product, a unique way of avoiding toxicity associated with soluble haem. For a number of years this material was thus believed to be a polymer of haematin, however, publication by Pagola et al. of the structure solved from the powder diffraction pattern demonstrated that malaria pigment is in fact a cyclic dimer of haem which involves reciprocal coordination of the ionised haem–propionate side chain of one haem to the iron centre of the other [36]. These dimer units interact in the crystal lattice via intermolecular forces that include hydrogen bonding of unionised haem propionates.

1.3.4 Spectroscopic and structural characteristics of β-haematin and haemozoin

Slater et al. [35] characterised haemozoin from trophozoites of the human malaria pathogen *Plasmodium falciparum*. Using chemical synthesis, IR, ESR and X-ray absorption spectroscopy they demonstrated that the haematin moieties are linked by a bond between the Fe(III) of one haem and the carboxylate side group oxygen of another. The IR spectra of haemozoin contain an intense absorbance peak at 1664 cm^{-1} that is absent in the spectrum of haematin (figure 1.4A). This strongly suggests the presence of a carboxylate bond between one haem propionate unit to the iron centre of the another. The other strong distinguishing IR absorbance in haemozoin at 1211 cm^{-1} can also be assigned to the axial carboxylate ligand. Figure 1.4B shows a spectrum of haemozoin and *β*-haematin.

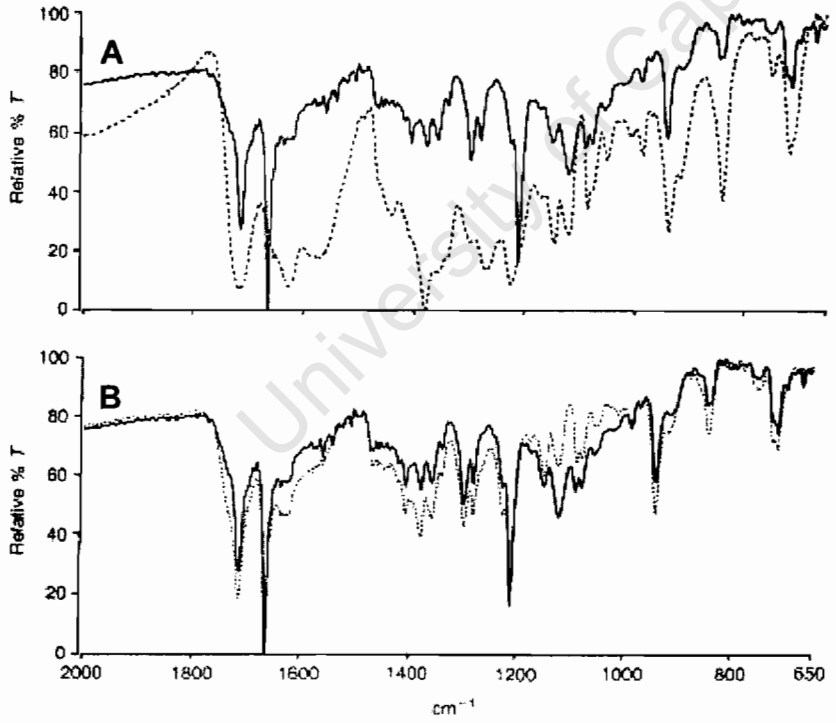

Figure 1.4 Comparison of FTIR of **(A)** Haemozoin (—) and haematin (·····). **(B)** Haemozoin (—) and *β*-haematin (·····) [35].

Wood et al. [37] demonstrated using Raman spectroscopy that the excitation profiles of β-haematin and haemozoin show an enhancement of the totally symmetric modes when excited with laser lines in the near IR region including 780 and 830 nm that indicate the existence of a z-polarised charge transfer band. On the basis of the Raman excitation profile of β-haematin, the UV-vis spectrum, and symmetry considerations, the band at 867 nm is assigned to the charge transfer band $d_{xy} \rightarrow e_g(\pi^*)$. They further suggested that the additional enhancement in the case of β-haematin is the result of excitonic coupling between covalently linked porphyrins which is absent in the case of monomeric haem. Figure 1.5 shows the similar spectra of β-haematin and haemozoin.

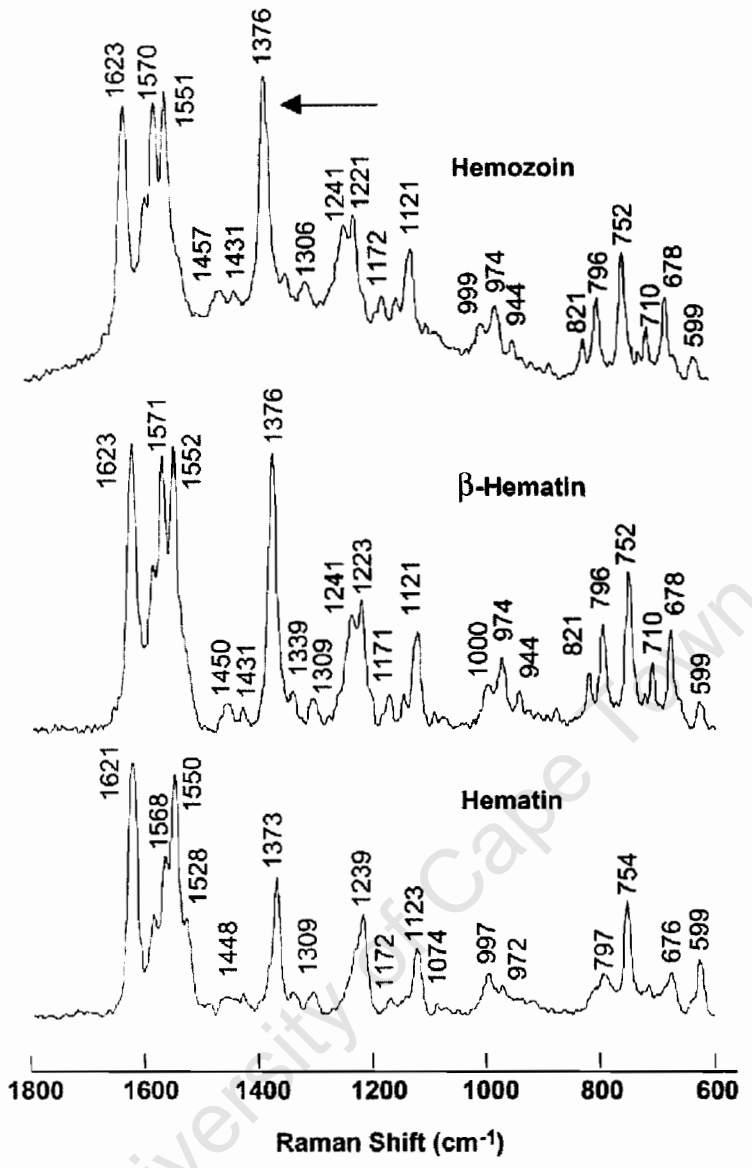

Figure 1.5 Raman spectra of haemozoin, *β*-haematin and haematin all obtained using 780 nm excitation. The arrow highlights the totally symmetric mode v_4 at 1374 cm^{-1} [38].

Bohle et al. [39] used X-ray diffraction to characterise *β*-haematin derived from both synthetic and natural sources and provide definitive evidence that the haem aggregate present in the late stages of trophozoites is *β*-haematin. Figure 1.6 provides compelling evidence that haemozoin from lyophilised late trophozoites of *Plasmodium falciparum* is identical to *β*-haematin, both of which are crystalline and have the same lattice [39].

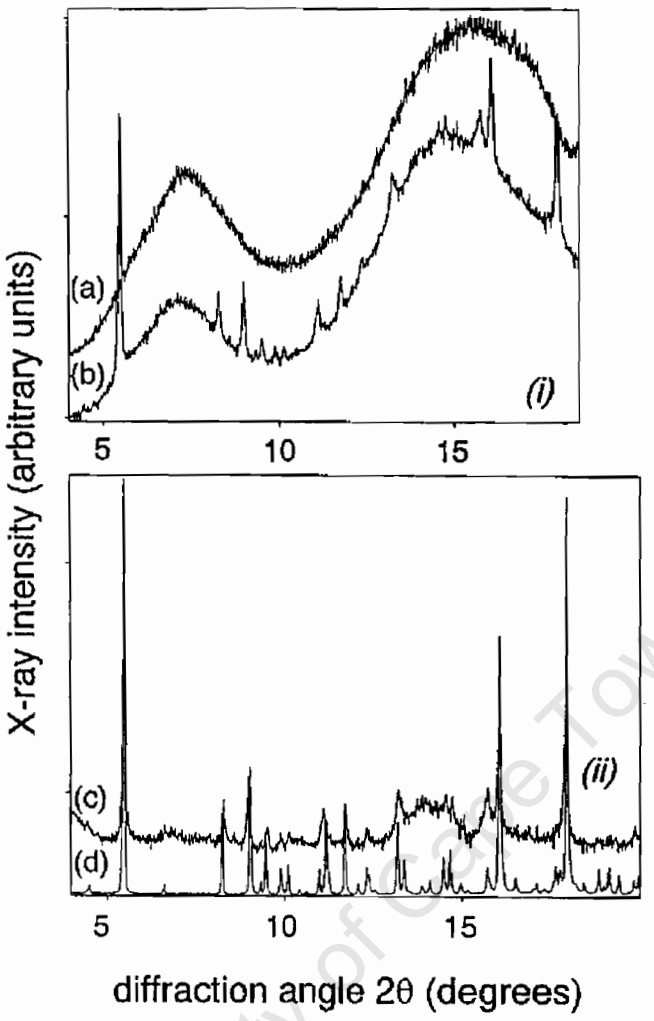

Figure 1.6 Powder diffraction patterns **(*i*)** (a) lyophilised uninfected erythrocytes (b) lyophilised late trophozoites of *Plasmodium falciparum* **(ii)** (c) difference between profile (a) and (b) in (*i*), and (d) β-haematin [39].

The solved X-ray diffraction pattern of β-haematin has demonstrated that it is a cyclic dimer of haematin (figure 1.7) [36].

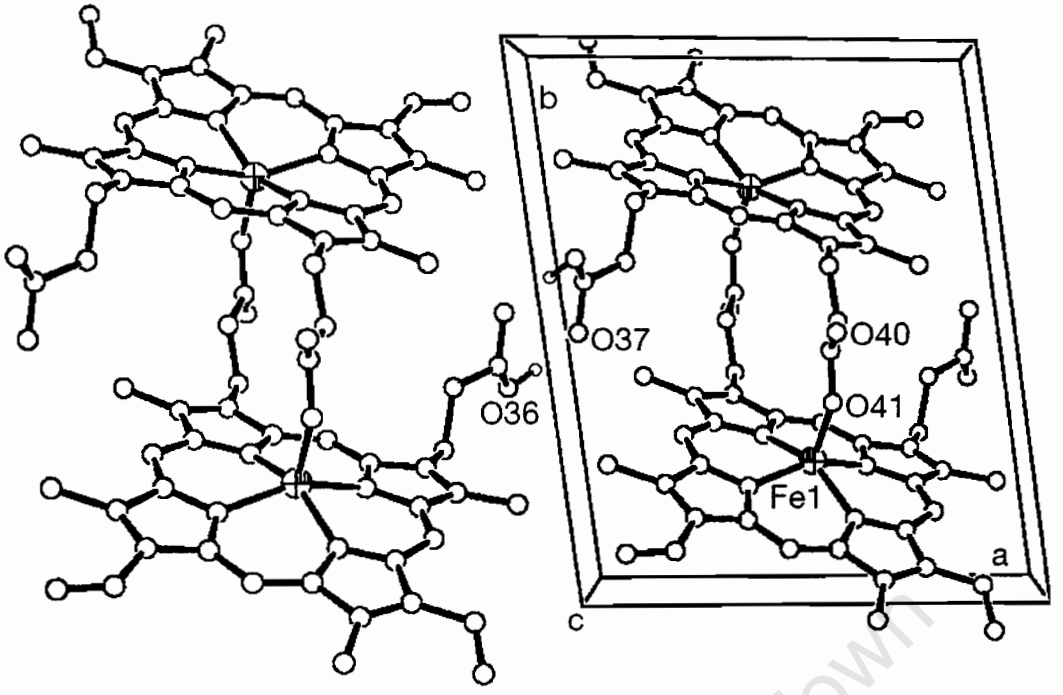

Figure 1.7. The crystal structure of β-haematin dimer reported by Pagola et al. [36]. Synchrotron radiation was used to collect the data which was then analysed by modelling the structure using a simulated annealing algorithm to reproduce the observed diffraction pattern.

1.3.5 Mechanism of haemozoin formation

Slater and Cerami [40] proposed that the malaria trophozoite uses a "haem polymerase" for haemozoin formation, however, this putative enzyme was never isolated. Numerous studies have indicated that lipids can promote haemozoin formation [41-43] and more recently the effect of lipids on the formation of haemozoin has been attributed to their ability to solubilise haematin [42] and in this respect they would appear to play a major role in the formation of haemozoin. Dorn et al. [44] confirmed that the "haem polymerase" activity observed in the parasite lysate is due to an autocatalytic chemical process of haem polymerisation onto haem-derived material associated with haemozoin, and is not due to enzyme catalysis. Sullivan et al. managed to identify and clone two histidine-rich proteins (HRP II and III) which occur in purified food vacuoles and which promote β-haematin

formation *in vitro* [45]. This protein, which bears a similarity to human histidine-rich glycoprotein, has been claimed to bind 50 haem units which all share a similar environment as indicated by electronic absorption, resonance Raman and EPR spectroscopy [46]. Choi et al. [46] found that all the ferrihaems in the HRP II-Fe(III)PPIX complex are low spin, and are six coordinate with two histidine ligands and that this complex is stable between pH 5.5 and 7.0. These results are at odds with the findings of Lynn et al. [47] who observed two pH dependent Fe(III)PPIX binding modes in HRP-II. Below pH 6, Fe(III) is supposedly coordinated to aspartate through a weak carboxylate-metal interaction which is capable of promoting haemozoin formation. Above pH 6, it is thought that formation of a strong Fe(III)-histidine complex correlates to the lack of haemozoin formation in this pH range [47]. The hypothesis that HRP II is responsible for haemozoin formation has been supported by studies using a peptide dendrimer [48]. Ziegler et al. [48] examined two first generation dendrimers with peptides consisting of the repeat sequence of HRP II from *P. falciparum* for their ability to bind haem units and perform β-haematin formation. These dendrimers bind about seven to ten haem units. These authors have shown that dendrimers containing four peptides with either the sequence of Ala-His-His-Ala-His-His-Ala-Ala-Asp or a duplication of this sequence linked to the dendrimer core bind haematin and form β-haematin. They also bind to metal free protoporphyrin IX. This seems to suggest that association is based on the porphyrin moiety rather than specific metal coordination which contradicts the proposal of Choi et al. This conclusion was further supported by the fact that Zn(II)PPIX as well as the structurally related metal free phthalocyanine and metallophthalocyanines, can bind to haem. In contrast, similar free linear peptides with the sequence Ala-His-His-Ala-Asp coordinate haematin, but do not form β-haematin. These studies appear contradictory, however it is interesting to note that Choi et al. [46] reported that β-haematin formation starts only once the specific haematin binding sites are saturated with Fe(III)PPIX at low pH. This indicates that HRPII behaves somewhat similarly to the linear peptide model until His residues have been saturated with haematin, only once no further bis-histidyl coordination can occur does β-haematin formation commence. Ziegler et al. [48] pointed out that steric effects in the dendrimers prevented His

coordination to Fe(III)PPIX. Thus it seems likely that interactions with polypeptide surfaces are important in facilitating β-haematin formation in these systems. Recent findings [49] have shown that the mechanism of β-haematin formation *in vitro* can be compared to a biomineralisation process, so it is possible that the role of HRP *in vivo* may provide a site on which nucleation of the crystal can occur. Further confusing issue however, a recent study of *Plasmodium falciparum* clones that lack HRP II and III can still form haemozoin [50], calling into question the role of HRP in haemozoin formation [51].

Thus, currently it is not clear which if any of these processes are in involved in haemozoin formation *in vivo.* It possible all occur together.

1.3.6 Haemozoin formation is the fate of almost all the haem released in the parasite

Haematin is known to be toxic to microogarnisms [23]. If the parasite did not have some mechanism of disposing this material, it would be overwhelmed by haematin when it digests large amounts of haemoglobin in the food vacuole. By converting haematin to haemozoin, the parasite removes it permanently from solution and deposits the iron porphyrin in a relatively innocuous solid form. Pagola et al. argued that the food vacuole of the parasite would contain well over 80 mM haematin if it were all dissolved, although this far exceeds the solubility limit of haematin, probably some would migrate to membranes, owing to its lipophilic nature [36].

In the past few years, two studies have proposed that most of the haem released as a by product of haemoglobin degradation is not in fact incorporated into haemozoin, but rather that close to 80% of the haem is degraded non-enzymically and iron is released [52, 53]. Recently, Egan et al. however, using a combination of chemical analysis of the elemental iron content of various cellular fractions, Mössbauer spectroscopy of freeze-dried whole parasites and electron spectroscopic imaging of parasitized red cells, have shown conclusively that the overwhelming proportion of haem is indeed

incorporated into haemozoin [54]. Elemental iron content of unparasitised red blood cells was found to be in excellent agreement with the accepted range of 90 – 111 fg/cell. Parasitised cells showed a similar quantity of iron, demonstrating no loss or gain of iron from the system in the presence of parasites within the red blood cell. Isolated trophozoites contained 61 ± 2% of the iron within the parasitized cell. This agrees with previous reports by Ginsburg and co-workers [11] who suggested that up to 65% of haemoglobin is digested. Egan et al. also found that 92 ± 6% of the parasite iron is in the food vacuole, which contradicts the hypothesis of Ginsburg and co-workers that more than 70% of the haematin is degraded outside the food vacuole, with the iron being deposited into the cytosol [52]. Finally 88 ± 9% of the iron inside the food vacuole is recovered with the haemozoin crystals, suggesting that this material contains the major portion of the iron in the parasite.

The findings obtained from ^{57}Fe-Mössbauer spectroscopy were completely consistent with these findings and led these authors to the inescapable conclusion that haemozoin is the only detectable iron species within the freeze-dried trophozoite. The advantage of Mössbauer spectroscopy is that it permits the species of iron in the parasite to be directly identified and does not require fractional isolation of material which leads to relatively large errors. It was concluded that at least 95% of the iron observed within the trophozoite is incorporated into haemozoin.

These findings were further supported by transmission electron microscopy (TEM) with electron spectroscopic imaging (ESI) as shown in figures 1.8 a-c illustrating iron distribution in trophozoites within an erythrocyte. Figure 1.8 c shows very little iron within the cytosol of the parasite. Haemozoin crystals are clearly discernible in the food vacuole by TEM and the ESI pictures convincingly show that major iron concentration is coincident with haemozoin.

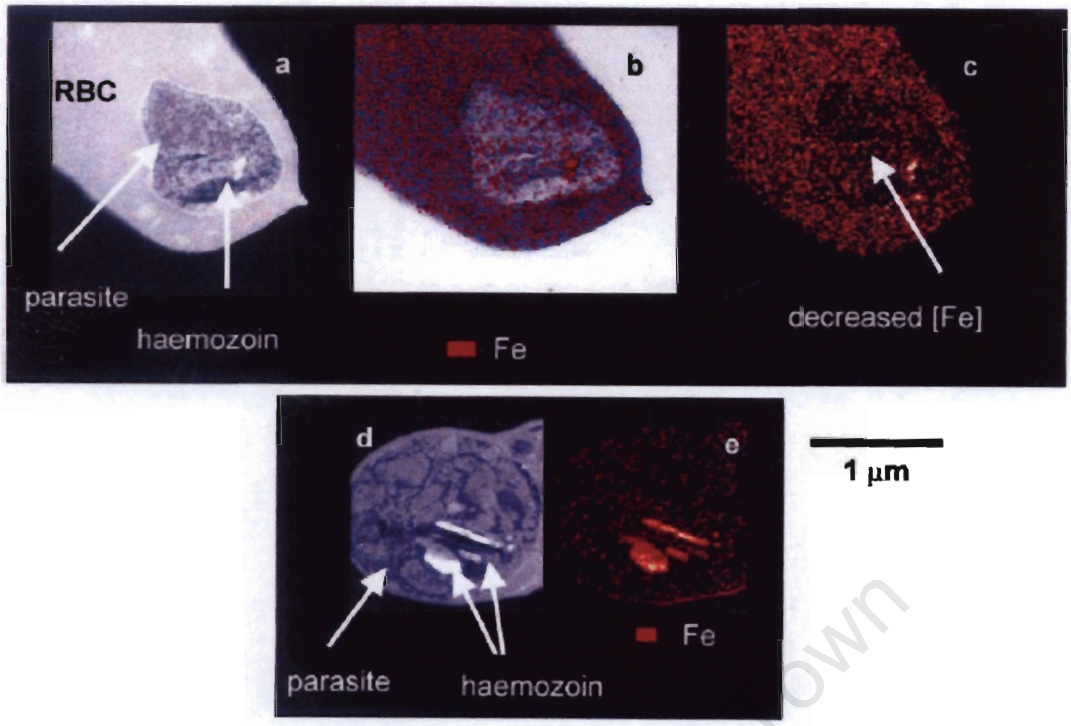

Figure 1.8 TEM and ESI of Plasmodium falciparum showing the distribution of elemental iron within the trophozoite and blood schizont **(a)** TEM of infected erythrocyte overlaid with distribution of iron determined by ESI **(b). (c)** The distribution of iron demonstrates that it is concentrated in haemozoin crystals within the trophozoite. The rest of the parasite is devoid of iron compared to the erythrocyte cytoplasm. **(d)** TEM of a schizont infected erythrocyte and distribution of elemental iron. **(e)** The distribution of iron coincides with haemozoin crystals [54].

1.4 MECHANISM OF ACTION OF QUINOLINE ANTIMALARIALS

Quinoline based antimalarial drugs such as chloroquine and quinine have a successful history in antimalarial chemotherapy. Their effectiveness however, especially that of chloroquine, has now been considerably reduced by the appearance of resistant strains of the malaria parasite. The mechanism of action of these drugs has been a subject of much debate over the last few decades. Although these drugs are believed to accumulate by a weak base mechanism in the acidic food vacuole of intraerythrocytic trophozoites and thereby interfere with haem detoxification, the mechanism of action and of

resistance is still not fully understood [55-58] (Chloroquine resistance will be discussed in the section 1.5).

1.4.1 DNA binding

Chloroquine was originally believed to exert antimalarial activity by intercalating into DNA [59]. It was thought that once chloroquine and quinine bind to DNA, important cell functions like DNA and RNA synthesis would be inhibited [7], ultimately leading to cell death. This hypothesis is no longer accepted on the basis that concentrations of chloroquine required to bind to DNA are significantly higher (100 μM) than the concentration required to inhibit parasite growth (10 nM) [40]. In addition, this theory does not explain why the quinoline antimalarial, mefloquine, which does not bind to DNA [60] is active. There is also no selectivity between the chloroquine-DNA interactions with host and parasite DNA.

1.4.2 Inhibition of protein synthesis

There are many important cell functions which when, disrupted could result in death of the parasite. One of these functions is protein synthesis. Some studies have shown that chloroquine does not to block protein synthesis in *P. falciparum* [61], *P. lophurae* and *P. berghei* [62]. On the other hand Surolia et al. [63] have reported that chloroquine is able to inhibit haem dependent protein synthesis in parasite lysate in situ at therapeutic concentrations. Since chloroquine had been reported to bind to haematin quite strongly [64] and protein synthesis in the trophozoite extract can reportedly be stimulated by haematin [63] it was then proposed that protein synthesis in the parasite could be decreased by chloroquine binding to haematin. This was found to be true at a high concentrations of chloroquine [63]. However, it is believed that the parasite could not possibly withstand the high haem concentrations required to stimulate protein synthesis without rupturing, as had been shown for *P. falciparum* [65, 66].

1.4.3 Inhibition of polyamine synthesis

Quinoline based antimalarials and related drugs like chloroquine have been reported to inhibit ornithine decarboxylase activity present in trophozoite extracts of infected red cells [67]. Since inhibition of this enzyme would block polyamine synthesis, it has been suggested that chloroquine may exert antiplasmodial activity through this effect. There has been no further follow up on the evidence which led to this hypothesis. However, it does not explain why chloroquine is only active on the erythrocytic stage [40] as liver stage parasites also presumably have ornithine decarboxylase.

1.4.4 Increased vacuolar pH

Since chloroquine is known to accumulate in the food vacuole of the parasite where it can achieve concentrations close to the millimolar range [57], this organelle is generally believed to be the locus of activity of these drugs. A number of authors have hypothesised that chloroquine raises the pH of the food vacuole as a result of its weak base properties [57]. This would have an effect of changing the conditions inside the food vacuole, so that the functioning of the enzymes inside the food vacuole is disrupted.

This hypothesis is no longer accepted because not all weak bases are antimalarials, in particular 9-epiquinine (a stereoisomer of quinine) is inactive in spite of having identical weak base properties to quinine [68]. The finding that external chloroquine concentrations of approximately 100 μM are required to raise the pH in lysosomes of mammalian cells (with similar pH as the food vacuole of parasite) by approximately one pH unit [69], makes it even more difficult to accept the hypothesis. This concentration is much higher than the external chloroquine concentration (10 nM) required for activity against the parasite *in vitro* [40]. In addition, active proton pumping in the vesicles ought to overcome the alkalining effects of the weak base. Nonetheless, these weak base properties probably account in part for accumulation of drugs in the food vacuole.

1.4.5 Inhibition of vacuolar lipases

Vacuolar phospholipase has been identified within the food vacuole where it responsible for degrading endocytic vesicle membrane in order to release the haemoglobin content into the food vacuole. Chloroquine has been shown to inhibit phospholipase activity *in vitro* [70] but at concentrations substantially higher than those likely to occur in the vacuole [40].

1.4.6 Inhibition of vacuolar proteolytic enzymes

Chloroquine has been shown to inhibit activity of purified aspartic proteinase from *P. falciparum* extracts [71], but at again at concentrations above the therapeutic range.

The hypothesis that chloroquine interferes with the parasite's feeding mechanism have further been questioned by Ginsburg and Krugliak who noted that treatment of chloroquine-treated parasites with membrane permeable amino acids, is unable to alleviate inhibition of parasite growth [70].

1.4.7 Interference with haematin detoxification

Haem-drug complex formation was first reported by Cohen et al. [72], who suggested that chloroquine acts by associating with haem. Slater and Cerami put forward a proposal that a haem polymerase enzyme [40] catalyses haemozoin formation. It was further suggested that inhibition of this enzyme by chloroquine would result in a build up of toxic haem in the parasite's food vacuole. Several studies emerged later suggesting that chloroquine and related drugs act by complexing with haematin and thus inhibit the conversion of haematin to haemozoin which is a process developed by the parasite for disposing of toxic haematin [44, 73-75], produced as a result of haemoglobin degradation. Additional interest in haemozoin formation has centred on the fact that drugs such as chloroquine inhibit its formation under synthetic

conditions, [44, 45, 73, 76] indicating that inhibition of haemozoin formation in the malaria parasite may be the basis of activity of these drugs. Furthermore, Ginsburg et al. [52] also proposed that chloroquine competitively inhibits degradation of haem by glutathione, thus allowing haem to accumulate in membranes. Tilley and co-workers [53] proposed a possible route for degradation of haem by reacting with H_2O_2 and undergoing rapid decomposition. It was then suggested that chloroquine and quinacrine are efficient inhibitors of this peroxidative destruction of haem by complex formation. However, the last two mechanisms appear unlikely given that haematin degradation appears to play little if any role in the haem pathways of the food vacuole [54].

1.5 PHYSICAL CHEMISTRY OF THE INTERACTION BETWEEN HAEMATIN AND CHLOROQUINE AND RELATED DRUGS

1.5.1 Association of chloroquine and related compounds with haematin

The ability of chloroquine to form a complex with haematin was first recognised by Cohen and co-workers in 1964 [72] and has led to the proposal that haematin is the target of chloroquine. These findings motivated a number of studies on antimalarial–haematin interactions in both aqueous and non-aqueous solution, as well as interactions with other iron porphyrins. Several early studies concentrated on obtaining spectroscopic evidence for drug-haematin interactions [68, 77, 78]. Association constants were not determined.

Fitch and co-workers [64] reported association constants in aqueous media based on an equilibrium dialysis method. These authors were able to determine the association constant of several antimalarials with haematin in aqueous solution at pH 7.4. Under these conditions haematin exists in an aggregated state [79]. This aggregated state was thought to probably consist at least partially of μ-oxo dimers [80] as well as further non-covalent aggregates [79], the structure and stoichiometry of which was not clearly defined. Moreau et al. [81] also studied interaction of chloroquine or quinine

with either haematin or uroporphyrin I in neutral aqueous solution using NMR, while Blauer [77, 82-84] used Mössbauer spectroscopy and uv-vis spectroscopy to study complex formation between haematin and amodiaquine, halofantrine, quinine or quinidine. Warhust [68, 85] studied these interactions in benzene using uv-vis spectroscopy. The solvent used in studying these interactions appears to be important, as demonstrated by amodiaquine [85] and 9-epiquinine [68]. These compounds were not found to bind to haematin in benzene, while quinine, mefloquine and cinchonine do. In aqueous and mixed aqueous solvents both amodiaquine and 9-epiquinine do bind to haematin [86]. Dorn et al. [74] reported association constants for chloroquine and several other antimalarial drug-haematin complexes also in aqueous solution at pH 6.5 using titration calorimetry. Enthalpies and entropies of association were also reported for these complexes. These results were interpreted as indicating that haematin itself exists almost exclusively as μ-oxo dimer under these conditions. Although this data provided information on the conditions that prevail under physiological conditions, interpretation of such data is likely to be complicated because of possible changes in the extent of non-covalent aggregation upon drug binding. In addition, there are several reports suggesting that studies performed on haematin in aqueous solution can be un-reliable and non-reproducible [87-89]. Egan et al. [86, 90] determined association constants for interaction between several quinoline antimalarials and haematin in 40% aqueous DMSO where it is monomeric. The association constants were determined by spectrophotometric titration, as the Soret band of haematin at 402 nm is strongly quenched upon association with quinoline drugs (figure 1.9). Enthalpies and entropies as well were also reported based on van't Hoff plots. These results are consistent with the titration calorimetric data. These authors also found that addition of acetonitrile to 40% DMSO weakens the association constants, at the least in the cases of chloroquine and quinine.

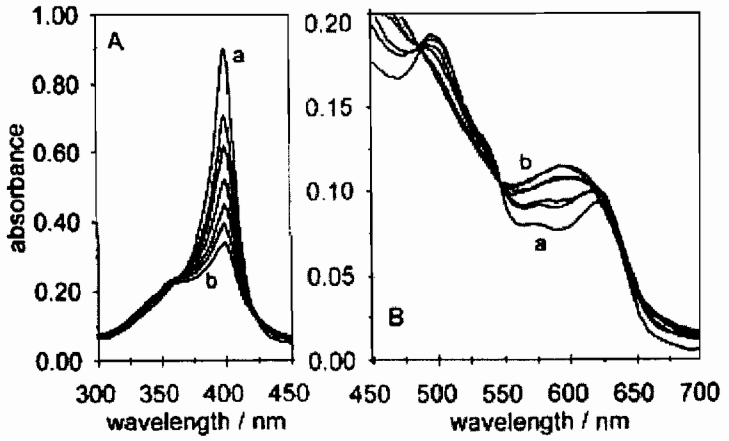

Figure 1.9 spectroscopic changes observed when haematin is titrated with chloroquine in 40% DMSO at pH 7.5, 25°C. **(A)** Shows a decrease in Soret band as a function of increasing concentration of chloroquine (from a-b). **(B)** Changes in the visible spectrum of haematin. The concentration of haematin was 3 times greater than in **(A)** [86].

Several interesting observations emerged from these studies. Association constants obtained by Dorn et al. [74] using titration calorimetry at pH 6.5 and those obtained by Egan et al. [86] in aqueous DMSO at pH 7.5 with monomeric haem show an excellent correlation (Table 1.1). More unexpectedly, the actual values are remarkably similar. In contrast, the association constant obtained by Chou et al. [64] using the dialysis method for measuring interaction of chloroquine with haematin in aqueous solution was found to be larger by 3 orders of magnitude than that obtained by Dorn et al. [74] using titration calorimetry. This discrepancy highlights the difficulty of investigating these interactions in an aqueous *milieu*. The difference in association constants can probably be ascribed to the different methods used to monitor these interactions. Marques et al. also reported association constants of chloroquine, quinine and 9-epiquinine interacting with N-acetyl-MP8 (N-acetylmicroperoxidase 8) [91] in aqueous solution. These are approximately two orders of magnitude weaker than those obtained with haematin in aqueous solution using titration calorimetry. The weaker association constant was attributed to the doming of porphyrin ring towards histidine and the presence of the axial water ligand in N-acetyl-MP8. The

increased distance between the porphyrin and the drugs would result in weaker complexes, and the presence of the axial ligand would limit the possible extent of π-π overlap.

Table 1.1 Log K values of antimalarial drugs with Fe(III)PPIX or N-acetyl-MP8

Compound	Fe(III)PPIX[a]	Fe(III)PPIX[b]	N-acetyl-MP8[d]	Fe(III)PPIX[e]
Chloroquine	5.52 ± 0.03	5.6 ± 0.2 {1:4}	3.08 ± 0.04[2:1]	8.46
Amodiaquine	5.39 ±0.04	5.0 ± 0.1 {1:4}	-	-
Quinine	4.10 ± 0.02	4.3 ± 0.04{1:5}	2.55 ± 0.02[1:1]	-
9-epiquinine	4.04 ± 0.03	-	2.42 ±0.05 [1:1]	-
Mefloquine	3.90 ± 0.08	4.1 ± 0.1[c] {1:3}	-	-
Quinacrine	-	5.69 ± 0.04 {1:4}	-	-
Pyronaridine	-	5.47 ± 0.03 {1:7}	-	-
Halofantrine	-	4.66 ± 0.07 {1:1}	-	-
Primaquine	-	4.2 ± 0.2 {1:7}	-	-
RO 48-6910	-	5.8 ± 0.1 {1:19}	-	-

[a] Association constants obtained in 40% DMSO using spectrophotometric titration. stoichiometry of drug:Fe(III)PPIX is 1:1 [86].

[b] Association constants obtained in aqueous solution at pH 6.5, 37°C using titration calorimetry reported by Dorn et al. [74]. Stoichiometry of drug:Fe(III)PPIX in {}.

[c] unbuffered

[d] Association constants obtained in aqueous solution at pH 6.25, 25°C (phosphate buffer) using spectrophotometric titration [91]. Stoichoimetry of drug:Fe(III)PPIX in[ ].

[e] Association constants obtained in aqueous solution pH 7.4, 4°C using dialysis method [64]. Stoichiometry of drug:Fe(III)PPIX is 4:1.

When Chou et al. first studied the interactions of chloroquine with haematin in aqueous media, they obtained a 4:1 stoichiometry of haematin to drug. This result was later supported by Moreau et al. [92] and Dorn et al [74] (table 1.1) and it was proposed that chloroquine is sandwiched between two haematin dimers. The same ratio was found with amodiaquine and quinacrine while ratios of 1:5 for quinine, 1:3 for mefloquine, 1:19 for the bisquinoline RO 48-6910, 1:7 for pyronaridine and 1:7 for primaquine were reported. The peculiar number of haematin molecules relative to drug suggests that the porphyrin

exists as a mixture of dimers, and monomers and even larger aggregates. Other porphyrins, like urohaemin I [93, 94] and N-acetyl–MP8 [91] remain monomeric in aqueous solution under controlled conditions, facilitating studies of their interactions with antimalarials. Monomeric urohaemin I in aqueous solution gave a 2:1 ratio with chloroquine or quinine while a 1:1 ratio was obtained with both drugs interacting with uroporphyrin I. Egan et al. [86] used non-aqueous solutions or mixed solvents to circumvent the problem of aggregation. Under these non-physiological, but partly aqueous conditions, binding stoichiometries are 1:1.

Initial studies of the structure of complexes between haematin and quinoline antimalarials were carried out by Moreau et al. [81, 92] using proton NMR. Shifts and broadening of NMR peaks of the drugs when they are titrated with small mole percentages of porphyrin compounds are indicative of complex formation. There was no evidence to suggest coordination between the Fe(III) centre and the quinoline nitrogen or alkyl nitrogen atoms as suggested by Chou et al. [64] since protons adjacent to these nitrogens did not shift significantly more than other protons. More importantly, metal free uroporphyrin I was also found to form complexes with chloroquine and quinine of comparable strength. This confirms that there is no coordination between the Fe(III) centre and N-atom. The geometry of the complex was proposed using a ring current model, suggested that the quinoline group is situated above the porphyrin ring rather than on the periphery. Constantinidis and Satterlee [93, 94] performed similar studies on the interaction of chloroquine and quinine with both Fe(III)uroporphyrin I and uroporphyrin I using ^{13}C-NMR. These also indicated co-facial complexation between the quinoline ring and Fe(III)uroporphyrin I. There was some evidence however, of coordination of the 9-hydroxyl group of quinine with the Fe(III) centre. Chloroquine was however, proposed to lie above the porphyrin ring with no coordination interactions. Marques et al. [91] observed a blue shift in the charge transfer band of the metalloporphyrin when N-AcMP8 s titrated with 9-epiquinine, which seems to support the suggestion that there is coordination of a deprotonated 9-hydroxyl group of quinine with the Fe(III) centre of the porphyrin. However, similar changes were subsequently observed in the

spectrum of haematin in 40% aqueous DMSO when titrated with chloroquine which has no hydroxyl group [86]. Thus evidence for coordination of the 9-OH group to Fe(III) remains weak.

In a study of a series of phenanthrolines, Shelnutt [95] found a correlation between the electron withdrawing strength of groups attached to the phenanthroline and the strength of the complex formed with various metalloporphyrins. The free energy of association of π-π complexes formed with these metalloporphyrins was found to be directly proportional to the Hammett constants of substituents on the neutral aromatic phenanthroline rings [95-97]. The shifts in Raman lines of porphyrins indicated transfer of electron density from the porphyrin ring to the phenanthroline. Shelnutt [98] noted that cationic species of methyl viologen and protonated chloroquine formed substantially stronger complexes than the phenanthrolines. It was proposed that these interactions are essentially electrostatic cation-π-attractions and so for viologen and chloroquine the same trends are not observed. This appears to be supported by observation that there is no simple correlation between association constant of quinoline antimalarial drug–Fe(III)PPIX complexes and the identity of quinoline ring substituents [86].

Molecular modelling studies have also been carried out in attempt to further understand the interactions between iron porphyrins and chloroquine and other related drugs. Marques et al. [91] studied the interactions between a simplified model of N-acetyl MP8 and quinine, 9-epiquinine or chloroquine in vacuum. The structures of the porphyrin and drugs were initially optimised individually and then the structures of drug and porphyrin complexes were modelled using molecular mechanics. Quenched dynamics and simulated annealing techniques were used to identify flexible regions in the complex. The study showed that coordination of the 9-hydroxyl group of quinine and 9-epiquinine to the Fe(III) centre is possible with considerable flexibility in the complex. The plane of the porphyrin ring and the quinoline ring are parallel to each other, with the pyridine ring of the quinoline lying over the pyrrole β-carbon in the porphyrin ring and benzene ring of the quinoline over the meso carbon atom in the porphyrin ring. The quinuclidine ring is pointed up and

away from the porphyrin ring. The complexes of both quinine and 9-epiquinine were found to be quite similar, which makes it difficult to easily account for the inability of 9-epiquinine to inhibit β-haematin formation. The minimum energy structure of the interaction of the quinoline ring of chloroquine with the porphyrin ring was found to be unstable in molecular dynamics simulations because there is no bond holding them together. O'Neal et al. [99] also carried out molecular modelling of quinoline drug-haematin complexes. The structures of the drug and Fe(III)PPIX were optimised prior to modelling the interactions. The drug structures were further optimised using semi-empirical molecular orbital calculations. The interactions of the drug and Fe(III)PPIX were simulated by molecular mechanics calculations using molecular dynamics with simulated annealing. The minimised structures obtained at the end of the calculation also showed co-facial interactions between haematin and amodiaquine or tebuquine. Hydrogen bonding and ionic interactions between the two propionate groups of haematin and charged protonated tertiary nitrogen of the drugs were also suggested. These structures were stable when immersed in a cube of TIP3 water (a cube of TIP3 water is a simple molecular mechanics simulation model for water molecules).

A recent NMR study by Leed et al. [100] has suggested a 1:1 association between the μ-oxo dimer of haematin and chloroquine quinine and quinidine in aqueous solution. Leed et al. [100] have used paramagnetic relaxation effects in the of NMR spectrum to determine distance constrains for the solution structures formed between μ-oxo dimers of haematin and the three quinoline drugs chloroquine, quinine and quinidine at several pHs. Using these distance constraints and molecular mechanics and dynamics, they have deduced the solution structure of antimalarial drug-haematin complexes at atomic resolution. They confirmed that the quinoline ring lies over the porphyrin, although often tilted at an angle so that the two systems are not completely co-facial. The calculated structures suggested a significant interaction between the side - chain and haematin molecule. (figure 1.10).

It is however, difficult to believe that the interactions of the terminal amino group in the side chain of the drug with propionate group of Fe(III)PPIX is

essential for strong complex formation. De et al. [101] have shown that chloroquine analogs with side chains ranging from ethyl to dodecyl all containing a terminal diethylamino group are equally active against chloroquine resistant parasites. Vippagunta et al. [102] performed initial calculations to optimise the structures of both haematin and chloroquine or its analogues for their modelling studies. They found that an electron withdrawing group (chloro-) at the 7-position is required for the correct distribution of electrons on the quinoline ring. A reduced electrostatic potential surface is obtained when the chloro – group is moved to the 6-position, explaining the inability of this analogue to bind to haematin or inhibit β-haematin formation.

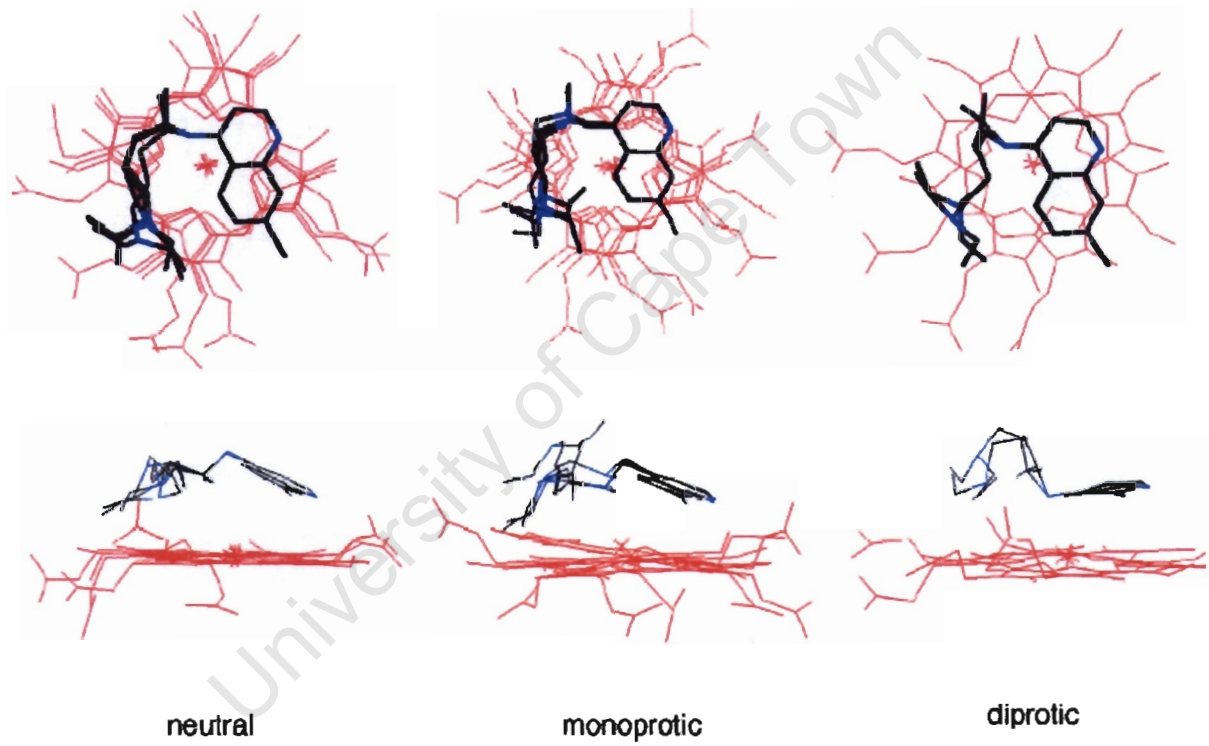

Figure 1.10 Axial and side views of superpositioned lowest-energy complexes formed between haematin μ-oxo dimer and neutral, monoprotic and diprotic forms of chloroquine. Blue denotes N atoms on the drug, and red denotes the haematin. The protons and the second haematin monomer are omitted for clarity [100].

Egan et al. [103] have recently synthesised a series of cationic 2,2-bipyridyl- and 1,10-phenanthrolineplatinum(II) benzoylthiourea complexes which inhibit β-haematin formation and exhibit *in vitro* antimalarial activity. They confirmed that the phenanthroline ligands form complexes with haematin as reported by

Shellnutt and the association constants were obtained. These were found to be weak and fall in a narrow range. Shellnutt [97] reported that the interaction of copper uroporphyrin increases as electron withdrawing groups are attached to the phenanthroline, but similar effects were not observed in the haematin complexes in aqueous DMSO. The bipyridyl ligands were found not to form complexes with haematin at all, and this could be ascribed from the fact that these compounds are non-planar in nature and are likely to be twisted around the bond linking the two pyridyl rings. Benzoylthiourea associated with haematin only very weakly and this could be ascribed to the lack of an extended aromatic system. Interestingly, cationic mixed-ligand platinum benzoylthioureas interacted strongly with haematin. This was even found with bipyridyl complexes, which is probably due to the enforced planar conformation of the bipyridyl and the presence of an extended planar system which allows delocalisation of electrons in all these complexes. The cationic nature of the platinum complexes may enhance association with haematin via cation-π interaction.

1.5.2 Thermodynamic compensation

Egan et al. [86] observed a thermodynamic compensation phenomenon for the interaction between chloroquine and related compounds with haematin in 40% aqueous DMSO. This may provide a means to gain further insight into these interactions. Thermodynamic compensation is often observed in weak complexes and this can provide information about the flexibility of these complexes and the degree of desolvation which occurs upon their formation [104]. Thermodynamic compensation is a linear experimental relationship between ΔH and ΔS values of complexation of a series of structurally related complexes. This relationship holds for weak interactions but not for strong interactions such as those where chemical bonding takes place. Under certain circumstances this phenomenon can be an artefact, as randomly chosen ΔH values and corresponding ΔS values calculated from Van't Hoff plots ($\Delta G = \Delta H - T\Delta S$), have also been shown to give a significant linear correlation [105].

Recent advances have however been made in understanding this phenomenon allowing such relationships to be more fully interpreted. The relationship need not be linear, as has been demonstrated for interactions in the gas phase and for monatomic sublimation. Recently, using theoretical considerations, the existence of thermodynamic compensation has been justified. In the case of weak complexes, a decrease in enthalpy correlates to an increase in the energy spacing of vibrational modes in the energy well, which restricts vibrations of the complex resulting in a corresponding decrease in entropy (figure 1.11). Inoue and co-workers have published papers explaining that this relationship is common in most weak host-guest interactions [106, 107]. The enthalpy-entropy compensation relation is obtained from experiment and is not derived from equations of thermodynamics and is described by equation 1.1

$$T\Delta S = \alpha\Delta H + T\Delta S_o \quad \text{.....(1.1)}$$

A plot of TΔS against ΔH is linear, where α is the slope of the plot and suggested to indicate the extent to which conformational freedom decreases when the complex is formed. The intercept, $T\Delta S_o$ is related to the extent of desolvation during the formation of the complex. Inoue and Wada [104] have investigated thermodynamic compensation for a wide range of supramolecular systems. These systems include among others, cations binding to glymes, crown ethers, cryptands or ionophores, interactions between porphyrins and quinones and interactions between metalloporphyrins and pyridines. A thermodynamic compensation plot (ΔH against TΔS) for the one of the supramolecular systems mentioned above is shown in figure 1.12. Since the interactions between antimalarial quinolines and haematin are weak, thermodynamic compensation is also expected. Figure 1.13 shows a plot of α values versus $T\Delta S_o$ values for a series of different supramolecular systems in both aqueous and organic solvents.

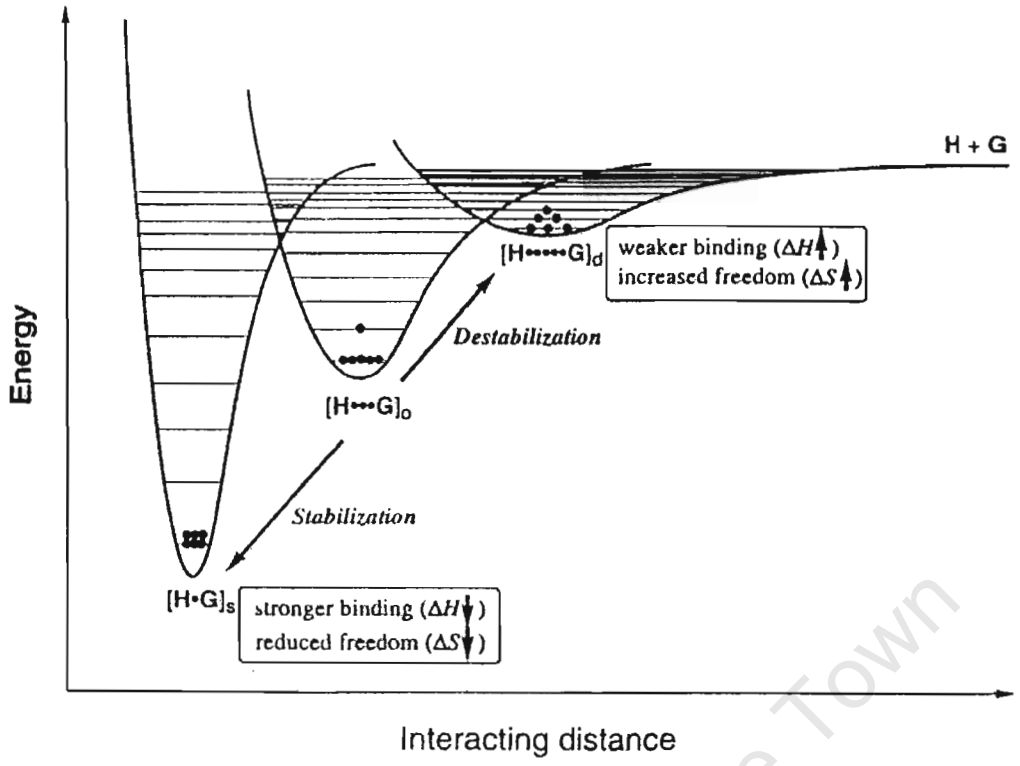

Figure 1.11 The energy wells for typical weak complex formation interactions [104] showing the relationship between the depth of the well (a measure of ΔH) and the number of accessible vibrational levels (a measure of ΔS) [104].

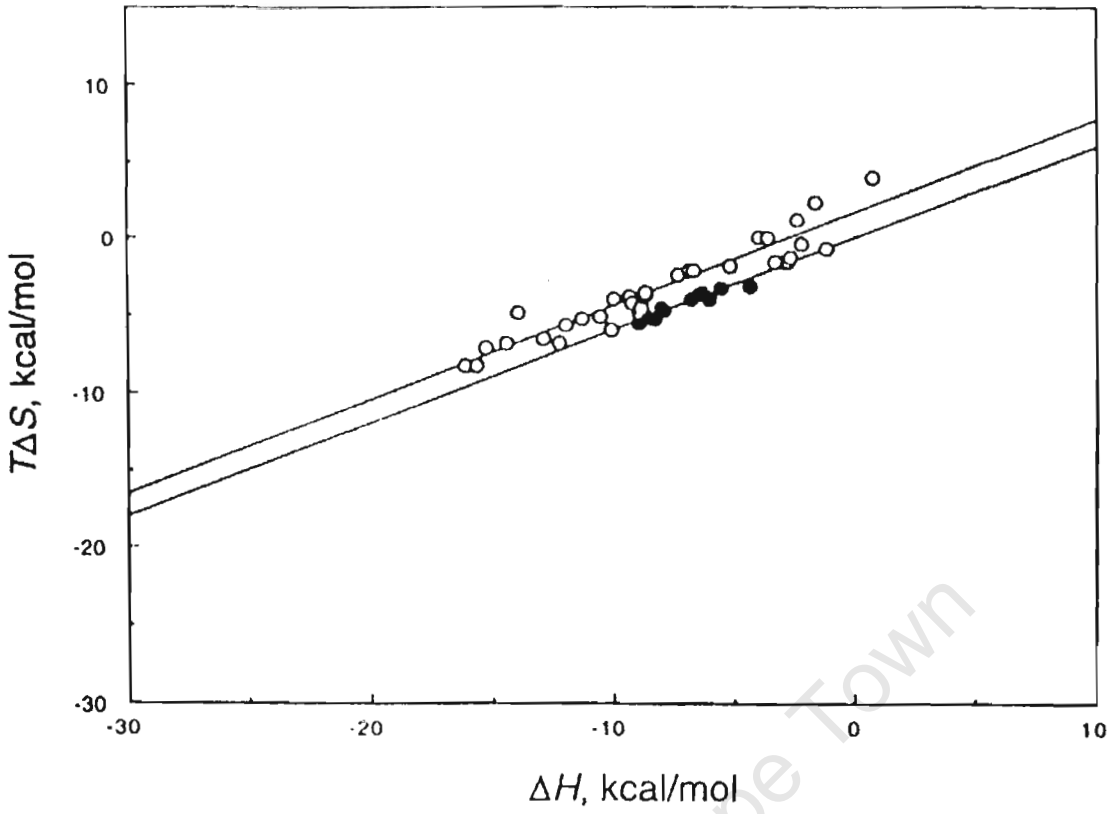

Figure 1.12 Thermodynamic compensaton plot for the interactions of quinones with receptor porphyrins (●) and of pyridines with metalloporphyrins (○) [104].

Inoue and Wada showed that the value of α for non-covalent interactions between quinones and porphyrins is 0.6 and the value for $T\Delta S_o$ for such interactions is approximately zero. The corresponding values for metalloporphyrin-pyridine interactions that involve chemical bond formation are 0.61 and 1.6 kcal/mol respectively. These relatively low values (see figure 1.13) could be ascribed to the fact that the porphyrins are already rigid molecules, so the loss of flexibility upon complex formation is low. While the long acyclic glyme which possess an extended chain will have to encircle the guest and then suffer a most comprehensive conformational change resulting in a rigid structure with restricted motion. The resulting slope α is 0.89 and the intercept $T\Delta S_o$ is 2.0 kcal/mol. Furthermore, the type of solvent seems to play a significant role in the interactions of these complexes.

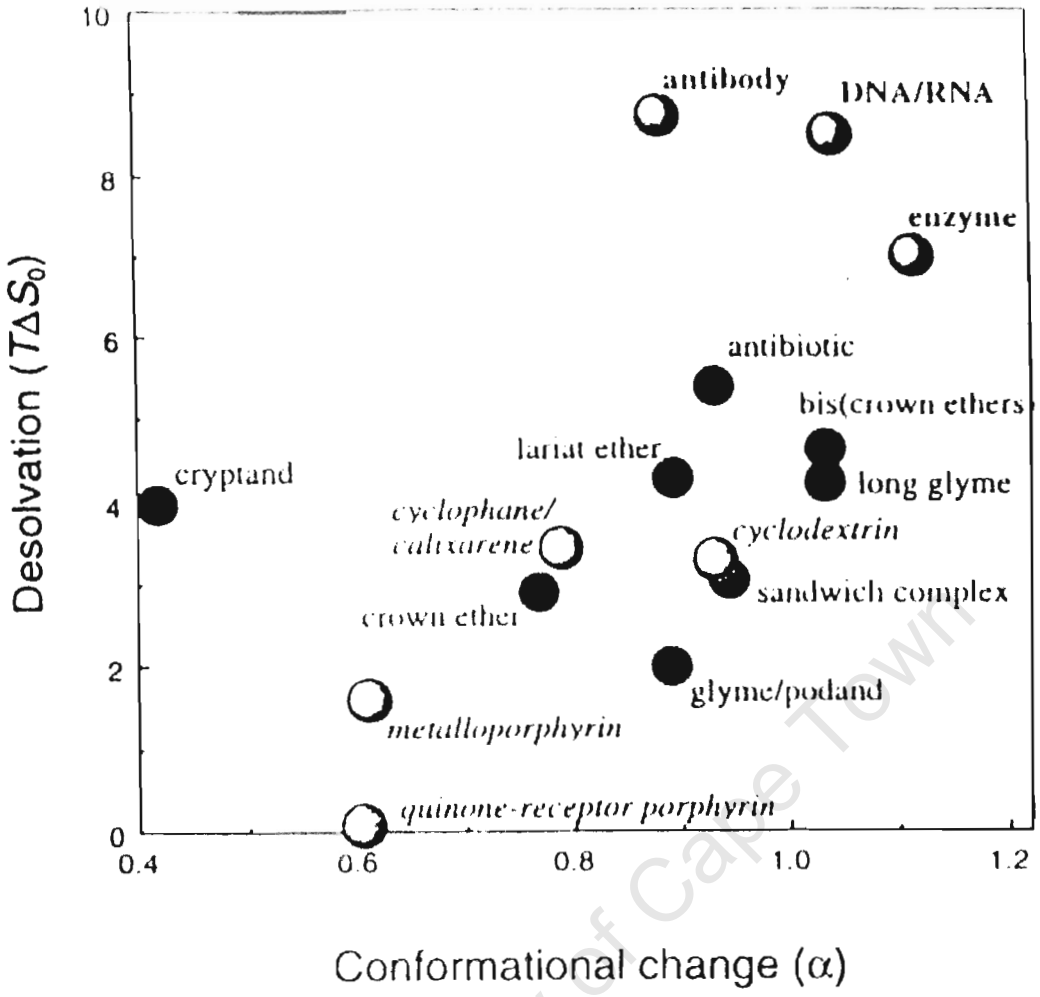

Figure 1.13 plot of intercepts $T\Delta S_0$ as function of conformational change (α) obtained from cationic binding or molecular inclusion shown by open circles. Solid symbols represent supramolecular interactions [104].

1.5.3 Inhibition of β-haematin formation

Slater and Cerami [40] originally observed that chloroquine and related antimalarials inhibit β-haematin formation in the presence of parasite extracts. This led them to propose that this class of antimalarials act via inhibition of haemozoin formation. However, these authors suggested that the effect is indirect, in that chloroquine was proposed to act by inhibiting haem polymerase, a putative enzyme that was postulated to catalyse haemozoin formation. On the other hand, various studies have indicated that 4-

aminoquinolines form complexes with haematin in solution [64, 74, 86], suggesting that the inhibitory effect is direct.

Studies by Dorn et al. [44] showed that β-haematin formation in parasite lysate is not enzyme catalysed, but suggested that it is autocatalytic. They also confirmed the earlier observation by Egan et al. [73] that this could be inhibited by chloroquine and suggested that the process is the target of this drug in vivo. They later tested more drugs including quinacrine, amodiaquine, quinine, pyronaridine, halofantrine and the bisquinoline, Ro 48-6910 for inhibition of β-haematin formation in a reaction mixture containing trophozoite lysate, food vacuole extract, haemozoin or acetonitrile extract of parasite lysate. In agreement with Egan et al., primaquine was found not to inhibit β-haematin formation [43, 74]. Sullivan et al. [108] reported that the haematin-quinoline complex "caps" the growing β-haematin product, now interpreted as evidence that it incorporates into a growing crystal face and blocks further crystal growth [45, 109-111]. They further suggested that chloroquine and quinidine have similar potency on the inhibition of crystal growth, while quinine is over 10 times less potent. This is indicative of an additional haem crystal inhibition step in addition to haematin binding affinity.

Pagola et al. [36] have pointed out, however, that since haematin is present in large molar amounts over chloroquine, it is difficult to imagine how such interactions could significantly inhibit haemozoin formation if the interaction is stoichiometric. Egan et al. [29] pointed out that it may be possible that chloroquine forms an irreversible complex with a small fraction of haematin, which exerts a toxic effect on the parasite, but this would mean that the haematin-chloroquine complex is thermodynamically more stable than haemozoin. This is unlikely because the log of the association constant for this complex is only 5.5, typical of reversible complex formation [74, 86].

Leiserowitz and co-workers [111] have used computer simulations to model the external morphology of haemozoin crystals based on the molecular structure previously reported by Bohle and co-wokers [36]. The computational study was used to reproduce the appearance of haemozoin crystals and

allowed the smallest, but fastest growing face to be related to the molecular structure. This face was found to be corrugated. By docking chloroquine with it, they showed that the drug can fit the surface and probably thereby block haemozoin formation (figure 1.14).

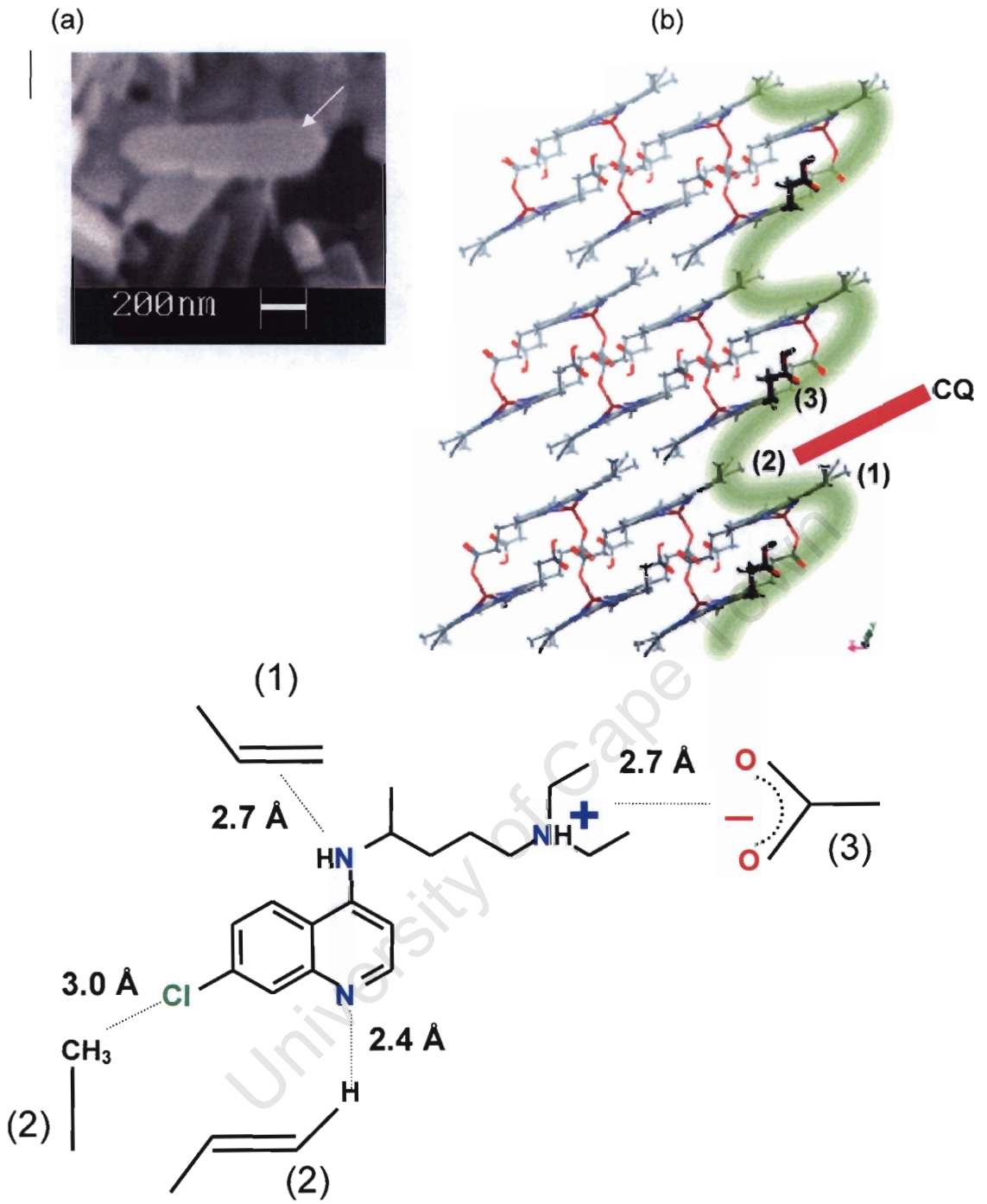

Figure 1.14 (cont. next page). The external morphology of the haemozoin crystal. The arrow represents the smallest face of the crystal **(a)** [29] and the proposed interaction of chloroquine with the fastest growing face of the crystal **(b)**. The schematic representation in **(b)** and **(c)** show a summary of the proposal of Leiserowitz and co-workers. **(b)** Shows haemozoin with a corrugated surface (green) in which chloroquine intercalates, interacting with three porphyrin groups marked 1-3 [111]. **(c)** Proposed interaction of haemozoin with chloroquine. The 4 amino group of chloroquine interacts with the vinyl group of the porphyrin(1). The Cl group on the

quinoline interacts with a porphyrin methyl group and the quinoline N with vinyl group on porphyrin (2). The positively charged terminal amino group interacts with the negatively charged propionate group and forms a salt bridge with porphyrin (3) (numbers represent porphyrins in (b)) [29].

These findings account directly for the essential role of the groups in the 7-position, i.e Cl in the case of chloroquine. Recent studies of chloroquine analogues have shown that the group at this position is essential for inhibition of β-haematin formation [102, 112, 113]. One aspect of this model appears problematic however, the quinoline ring has to be unprotonated, which is unlikely at the pH of the food vacuole. On the other hand, this may be possible in the immediate micro-environment of the crystal.

Detoxification of haematin to haemozoin has long been thought to be exclusive to *Plasmodium*. Recently, it has been shown to occur in the blood sucking insect *Rhodnius prolixus* [26] and in the parasite worm Schistosoma mansoni [27]. In both cases the dark brown crystalline material has been characterised either by transmission electron microscopy or polarised light microscopy and infrared spectroscopy and was found to be identical to haemozoin found in *Plasmodium*. In *R. prolixus* chloroquine was found to inhibit haemozoin formation and resulted in the build up of haem in the insect haemolymph which caused lipid peroxidation, thus modelling the proposed mechanism of action of chloroquine *in vivo*.

1.6 STRUCTURE ACTIVITY RELATIONSHIPS IN QUINOLINES

1.6.1 Association between quinoline antimalarials and haematin

As discussed above, a number of studies have provided conclusive evidence that quinoline antimalarials form complexes with haematin. Other studies have shown that the activity of the 4-aminoquinoline antimalarials, chloroquine and amodiaquine as well as quinoline methanols, quinine and quinidine are dependent on haemoglobin degradation [114, 115]. Recent studies have thus

investigated the structural requirements for association of quinolines with haematin. Egan et al. [112] investigated structural changes and reported the essential functional groups that are required for the association of amino-quinolines with haematin in 40% aqueous DMSO, pH 7.5. They have shown that 2- and 4-aminoquinolines have a unique affinity for haematin with association constants approximately 3 orders of magnitude stronger than quinoline, 3-, 5-, 6-, 8-aminoquinoline or 4,7-dichloroquinoline. Quinoline itself does in fact form a complex with haematin but the association constant is thousand times weaker than that found for 2- and 4-aminoquinoline. Attachment of the alkyl side chain to the 2- or 4-amino group of aminoquinolines was found to have only a very small effect on the association constant, even when a chlorine atom is placed at the 7-position of the quinoline ring. The 4-aminoquinoline nucleus of chloroquine was thus identified to be a necessary but not sufficient requirement for antiplasmodial activity. These authors have shown that the 2-aminoquinoline (figure 1.15A), 4-aminoquinoline (figure 1.15B) and 4-amino-7-chloroquinoline (figure 1.15C) interact with haematin within the range of other antimalarials. Attachment of a hydroxylethyl group to the terminal end of the alkyl chain causes a decline in log K in the case of 4-aminoquinoline but a small increase when the 7-chloro group is attached. When an amino-alkyl side chain is attached to the 4-amino-7-chloroquinoline it was found to cause an increase in log K and the effect is much bigger when the terminal amine was ethylated (figure 1.15 (D)). The molecular basis of specific interactions remains unknown, although it was suggested that the difference may involve the ability of partial charges on quinoline to form strong interactions with haematin by matching opposite charges on haematin and minimising repulsive electrostatic interactions of the π-clouds. Portela et al. [116] supported this idea using molecular orbital calculations and suggested that the amino group connected to the quinolinic ring, corresponding to a positive electrostatic potential, interacts with the central negative zone of the haematin dimer. The negative potential located over the aromatic area of the quinoline ring also interacts with the peripheral positive area of the μ-oxo dimer.

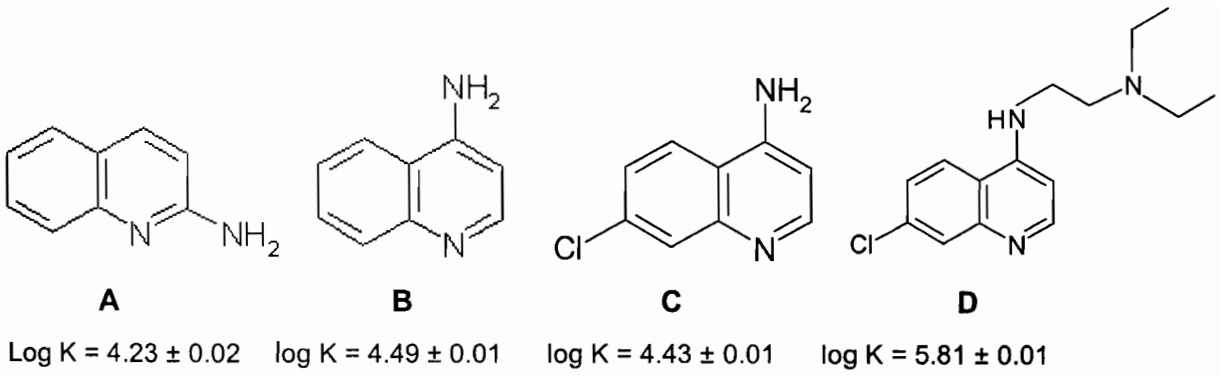

A Log K = 4.23 ± 0.02 **B** log K = 4.49 ± 0.01 **C** log K = 4.43 ± 0.01 **D** log K = 5.81 ± 0.01

Figure 1.15 A selection of 2-, and 4-aminoquinoline compounds used to investigate structure activity relationships for haematin-quinoline association [112] Log K values were obtained from [112].

Chloroquine and its analogues were found to exhibit stronger association constants with haematin than any other quinolines, indicating that there is some additional interaction of the side chain of the quinoline with haematin. Although the explanation of this effect remained unclear, it was argued that there may be hydrogen bonding between the tertiary amino group of the quinoline interacting with haematin propionic acid group, although it seems unlikely that this will occur more readily in the case of compound **D** which has a bulky tertiary amino group than in *N*-(7-chloro-4-quinolinyl)-1,2-ethanediamine which has a primary terminal amine group and where the effect is not seen. The other possibility is that Van der Waals forces may be involved between the side chain of the quinoline and porphyrin ring. As seen in figure 1.10, this is supported by structural studies by Leed et al. [100]. Finally the tertiary amino group could coordinate with the iron centre of haematin, although this seems unlikely as no evidence was found of triethylamine interacting with haematin. Vennerstrom and co-workers [117] have recently synthesised carbon isosteres of chloroquine in which the aniline N is replaced with a methylene carbon (figure 1.16A) and the pyridine N is replaced with a carbon atom (figure 1.16B). They found that the binding affinity of compound A (figure 1.16) decreased by 6.4 fold compared to that of chloroquine, while there was no measurable binding interaction observed between chloroquine isostere B and the haematin μ-oxo dimer, which

indicates that the pyridine N atom is essential to this binding interaction. They further compared the IC_{50} values for β-haematin inhibition of chloroquine to that of chloroquine isostere A, and found it to be a much weaker inhibitor of β-haematin formation with an IC_{50} value of 1500 μM (IC_{50} of chloroquine = 80 μM). The carbon isostere B had no effect on β-haematin formation at concentrations of up to 2500 μM.

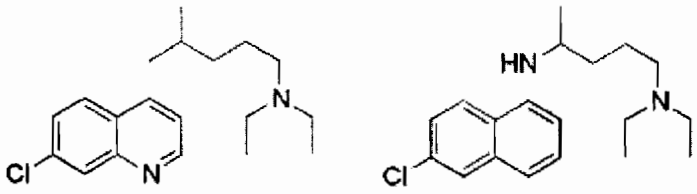

Figure 1.16 Carbon isosteres of the 4-aminopyridine substructures of chloroquine [117].

1.6.2 β-haematin inhibitory activity

Recent investigations of the effect of quinoline antimalarial-haematin interactions have centred on the hypotheses that these drugs inhibit β-haematin formation or have the ability to inhibit the breakdown haematin by glutathione [52] or hydrogen peroxide [53]. The ability of these quinoline antimalarials to inhibit haemozoin formation was first proposed by Slater and Cerami in 1992 as described in section 1.5.3. At that time it was believed that β-haematin is a polymer and that the drugs inhibit a haem-polymerase enzyme. It was then shown that these drugs inhibit β-haematin formation in the absence of biological materials [73]. It was suggested that inhibition occurs when the drug forms a complex with haematin, with the resulting complex not being capable of forming β-haematin.

A number of studies have now shown that a wide range of quinoline, and phenanthrene antimalarials and antiplasmodials inhibit β-haematin formation [43-45, 73-75, 90, 102, 110, 112, 118, 119]. However, it is now clear that

inhibition of β-haematin formation is not merely a result of association with haematin. Quinolines including 9-epiquinine as well as certain 4-amino quinolines have been shown not to inhibit β-haematin formation despite forming complexes with haematin [102, 112]. Egan et al. [102, 112] have shown that the key feature for inhibition of β-haematin formation by 4-aminoquinolines appears to the presence of the 7-chloro group. The identity of the group at this position was identified as a critical feature in determining the strength of inhibition of β-haematin formation. This conclusion has recently been supported by Cheruku et al. [117] who have confirmed that the 4-amino-7-chloroquinoline substructure of chloroquine is essential for inhibition of β-haematin formation.

1.6.3 Antiplasmodial activity

It has been found that antiplasmodial activity of 4-aminoquinolines depends both on the strength of β-haematin inhibition and on the accumulation of the compound in the food vacuole through pH trapping. The extent of pH trapping depends on the basicity of the quinoline ring and of the side-chain amino group. Replacement of the 7-chloro group with a bromo-, or nitro group has been shown to result in complexes that are still active, while 7-amino and 7-hydro are not. This seems to suggest that groups that are π- electron withdrawing are successful inhibitors [102]. This is consistent with a recent report on the antiplasmodial activity of aminoquinolines with fluoro-, chloro-, bromo-, iodo-, trifluoromethyl and methoxy- substituents in the 7-position [120]. The fluoro and methoxy derivative were found to be less active than chloro-, bromo-, iodo-, and trifluoromethyl derivatives. The nature of the group at 7-position has only a small influence on the association constant with haematin compared to the effect of the presence and position of the amino group. Kaschula et al. [113] reported that the pK_a is strongly dependent on the nature of the group at the 7-position on the quinoline ring in short chain analogues of chloroquine (figure 1.17). Groups that are electron withdrawing such as NH_2 and OCH_3 raise pK_{a1} relative to that of the 7-H derivative. By

contrast, strongly electron-withdrawing groups such as NO_2 cause considerable decrease in pK_{a1}.

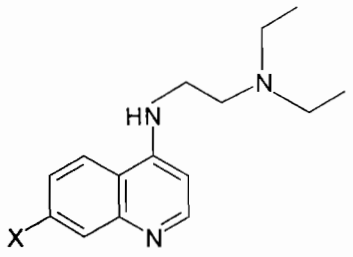

X = a) NH_2, b) OCH_3, c) H, d) F, e) Br, f) I, g) Cl, h) NO_2

Figure 1.17 Short chain analogues of chloroquine studied by Kaschula et al. [113].

De et al. [120] also found that the most active aminoquinolines were those with two or three carbon diaminoalkane side chains especially those that have chloro-, bromo- or iodo- groups in the 7-position. These authors also found that these aminoquinolines are active against chloroquine resistant *P. falciparum* because they avoid the mechanism responsible for resistance to chloroquine [121]. They suggested that the side chain length (carbons between the two nitrogens in the diaminoalkane side chain of 7-bromo- and 7-iodo- of 4-aminoquinolines) is the major determinant of activity against chloroquine-resistant *P. falciparum* as it is with 7-chloro-4-aminoquinoline.

Egan [122] has proposed a series of features of aminoquinolines that are important for antiplasmodial activity. He suggested that compounds that do not associate with haematin do not inhibit β-haematin formation and have essentially no antiplasmodial activity. Those that do associate with haematin, but are unable to inhibit β-haematin formation and lack the side-chain amino group essential for accumulation in the acidic food vacuole are also inactive. Aminoquinolines that can inhibit β-haematin formation, but lack the amino group and those that do not inhibit β-haematin formation but can accumulate through pH trapping due to the presence of amino group exhibit weak antiplasmodial activity. In contrast, those that inhibit β-haematin formation and contain an amino alkyl side chain exhibit strong activity. The proposed structure activity relationship is shown in figure 1.18

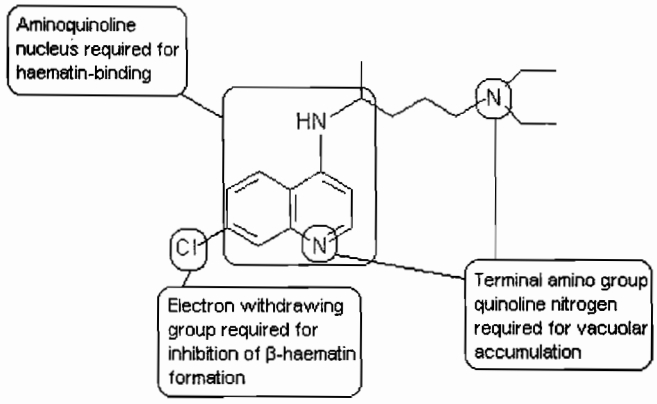

Figure 1.18. Proposed structure-activity relationship for chloroquine [112].

1.7 MECHANISM OF CHLOROQUINE RESISTANCE

Drug resistance in *Plasmodium falciparum,* especially resistance to 4-aminoquinolines, has proved to be a major obstacle in controlling this life threatening disease. *P. falciparum* possesses a transmembrane glycoprotein, Pgh 1 (P-glycoprotein homologue 1) coded for by the pfmdr 1 gene [123] which resembles the mammalian multi-drug resistance protein implicated in drug resistant cancer. This led to the suggestion that Pgh 1 is responsible for chloroquine resistance. Mutations at codon 86 were found to be associated with chloroquine resistance in a number of isolates [124-128]. Later, little support for this correlation could be found in epidemiological studies [129-135] and a genetic cross between chloroquine-resistant and sensitive parasites showed no evidence of association with mutations in this gene at all [136]. There is some evidence that mefloquine resistance may be related to an increase in Pfmdr1 copy number [137-140], while mutations at codon 86 are associated with increased sensitivity to mefloquine [138]. Thus, there is evidence that multi-drug resistance to quinoline methanols may be associated with the Pgh 1 protein, which is located primarily in the food vacuole membrane [141].

Recently, it has been demonstrated by Cooper et al. [142] that point mutations in PfCRT are associated with chloroquine resistance. It has now been established that chloroquine resistant strains share a common K76T mutation in the *Plasmodium falciparum* chloroquine resistant transporter

(pfcrt) gene, but with other groups of point of mutations in this gene also necessary for chloroquine resistant strains to appear. The pattern of these mutations is specific to regions of the Globe that are coincident with the independent appearance of chloroquine resistance, namely in South America and Southeast Asia [143]. These strains exhibit different sensitivities to various drugs and different susceptibilities to resistance reversal agents. There is now also evidence that resistance is related to levels of expression of PfCRT [144]. Mutations in pfcrt can apparently alter susceptibility to mefloquine and quinine [142, 145]. Based on this evidence, it seems likely that while Pgh 1 may have some role in chloroquine resistance in at least some strains, it is possibly involved mainly susceptibility to quinoline methanols and related compounds while, PfCRT is the primary protein involved in chloroquine resistance.

While there has been major progress in identifying the genes responsible for quinoline drug resistance in *P. falciparum*, the cellular mechanism of resistance is still unclear. While Pgh 1 is similar to mammalian multidrug resistance proteins and presumably acts by pumping out drugs from the site of action, the role of PfRCT is unclear. It is well established that parasitized red blood cells accumulate less chloroquine in resistant parasites [146, 147]. Suggestions that a Na^+/H^+ exchanger is involved in drug uptake [148, 149] or that a Cl^-/HCO_3^- antiporter is responsible for maintaining pH gradients in the food vacuole [150] appear to have been disproved [115, 151], or do not find strong support [115]. An increase in food vacuole pH would be expected to cause decrease in pH trapping of the drugs in the food vacuole and has been proposed as the mechanism of chloroquine resistance, but there is no definitive evidence of increased pH to date [56]. Other studies have suggested that there is in fact a decrease in food vacuole pH in resistant parasites resulting in a decrease in haematin available as a target for chloroquine as a result of increased haematin aggregation and precipitation [152]. The latter study has been under criticism regarding interpretation of microscopic images used to determine the pH [153]. Recently, Sanchez et al. [154] proposed that the rapid rise in accumulation of chloroquine inside the food vacuole after glucose addition in chloroquine sensitive strains is

activated at low levels of intracellular ATP and a small rise in intracellular ATP level is sufficient to deactivate chloroquine accumulation. They proposed that this is consistent with increased chloroquine uptake after glucose addition in chloroquine sensitive strains being dependent on energy input for haemoglobin degradation and hence the production of free haem as a target for chloroquine binding or, alternatively, being dependent on proton accumulation in the vacuolar compartment into which it accumulates [155] with proton pumping being performed by a pump of high affinity for ATP. In chloroquine resistant strains they proposed that the activation of a chloroquine efflux carrier by glucose addition counteracts the effect of the increased driving force for chloroquine accumulation [154]. However, this proposal appears to be disproved by the observation by Bray et al. [153] that deoxyglucose also stimulates chloroquine efflux, despite being unable to generate ATP.

In addition, general changes in pH are difficult to reconcile with the observation that closely related dibasic 4-aminoquinolines, differing only in side-chain length exhibit major differences in activity against chloroquine resistant parasites. Increased parasite sensitivity to quinine, but decreased sensitivity to its enantiomer quinidine is consistent with the protein influencing the sensitivity of the parasite to these drugs acting by a mechanism other than effects on food vacuole pH [142]. Ward and colleagues [151] have suggested that the accessibility of free haem to chloroquine, and not necessarily the total amount of haem or of drug, is a relevant parameter for determining reduced net chloroquine accumulation in resistant strains. Recently, Martin and Kirk [156] have conducted a bioinformatics analysis of the pfcrt gene. This study indicates that the normal function of the protein may be to export peptides from the food vacuole. The mutant is predicted to allow chloroquine to flow down its concentration gradient out of the food vacuole. This is proposed to be the result of the exchange of the positively charged lysine side chain at position 76 (predicted to lie on the vacuolar side of the food vacuole membrane) for a neutral serine side chain. This would permit the positively charged diprotonated chloroquine molecule to pass through the food vacuole.

Regardless of the mechanism of resistance, analogues of chloroquine with altered side–chains [101, 157, 158] remain active against chloroquine–resistant parasites, so this class of compounds remain of considerable interest. As far as this is concerned. A significant number of studies have been reported on the activity of 4-aminoquinoline analogues of chloroquine in which the aminoalkyl-side chain is substantially altered. These are highly active against chloroquine-resistant parasites. This is observed in compounds with shortened side chains and with bulky groups attached to the terminal amine [157]. They include compounds containing groups such as ferrocene in the side chain [158, 159]. In contrast, changes in the 7-position of the aminoquinoline result in either moderate effects or no effects at all [120, 152]. Compounds with linear side chains slightly shorter or longer than chloroquine show cross resistance [120]. Cross resistance between chloroquine and quinoline methanols such as mefloquine is not ruled out [137], but often an inverse relationship is observed with chloroquine-resistant parasites showing enhanced sensitivity to mefloquine. However, mefloquine resistance appears to be correlated with decreased sensitivity to quinine [137]. These findings seem to support proposals that resistance mechanisms in quinoline methanols are different to that of chloroquine-resistance. The question as to whether structural changes to mefloquine can circumvent this type of resistance does not appear to have been investigated [51].

1.8 METHODS OF SCREENING FOR β-HAEMATIN INHIBITION

Kurosawa et al. [160] tested more 100 000 non–quinoline compounds for *β*-haematin inhibition in order to identify new possible antimalarials. The compounds included among the others indoles, carbonyls, piperizines, imides and benzophenones. The assay involves overnight incubation and makes use of radioactive materials. Egan et al. [73] used an infrared technique to measure qualitatively the inhibition of β-haematin formation by various quinoline drugs. However, owing the need for the sample to dry over a period of two days, and the inability to measure quantitatively the inhibition of β-haematin formation using this method it is unsuitable for screening large

numbers of compounds or for obtaining strengths of β-haematin inhibition [113]. Basilico et al. [119] first developed a haem polmerisation inhibitory assay activity (HPIA) that makes use of no radioactive substances. However, interference by salts was later noted. To circumvent this artefact, Parapini et al. [161] modified the assay to the so-called β-haematin inhibitory activity (BHIA) assay based on the differential solubilisation of haematin, but not β-haematin in DMSO. However, this assay involves long reactions (about 16-24hrs) and also two centrifugation steps and so is compatible with medium throughput screening, but not high throughput screening. Deharo et al. [162] adapted the BHIA technique to a high-throughput screening method that avoids centrifugation but instead employs a vacuum filtration method using a 96-well multi-screen plate, but again it involves long reactions (18-24hrs).

Even a recent assay from Chong and Sullivan [108] that is useful as a high-through-put screening method, does not require use of radioactive materials and multiple centrifugation steps and makes use of cheap materials is not ideal. It is fairly slow (12 hour incubation) and is inconvenient because it does not use directly commercially available products and requires dispensing of solid material which is less convenient than a liquid or solution.

Thus none of the β-haematin inhibition assays are ideal. While Kurosawa et al. [160] have demonstrated that screening for β-haematin inhibition is a fruitful method for identifying new antimalarials, cheaply and easily, there is still a clear need for a simple, cheap and rapid method for screening compounds for β-haematin inhibition.

1.9 AIM AND SCOPE OF THIS PROJECT

The overall aims of this project are to investigate the role of hydrophobic interaction in complex formation between quinoline antimalarials and haematin, to develop a new method of screening compounds for inhibition of β-haematin formation and to investigate the dependence of β-haematin inhibition on incubation time.

1.9.1 Effect of solvent composition on the association of quinoline antimalarials with monomeric haematin

Specific objective: To investigate the interactions of quinoline antimalarials with haematin in aqueous DMSO of varying composition and in a series of non-aqueous solvents (figure 1.19 shows compounds to be investigated) in order to obtain more information about the role of solvation and electrostatic interactions in these complexes.

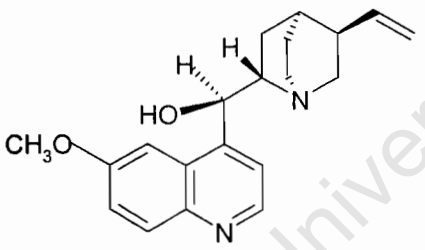

A

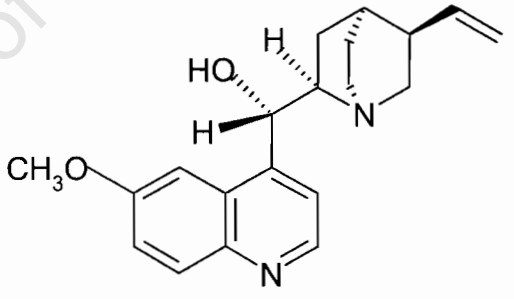

B

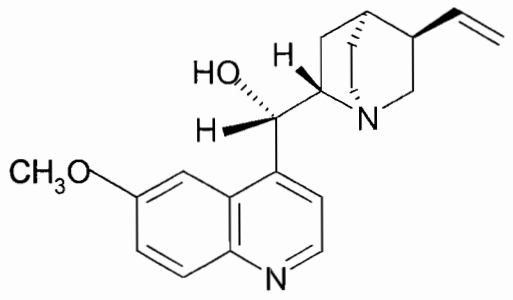

C

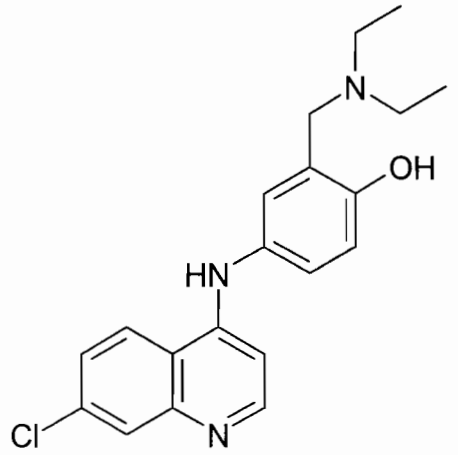

D

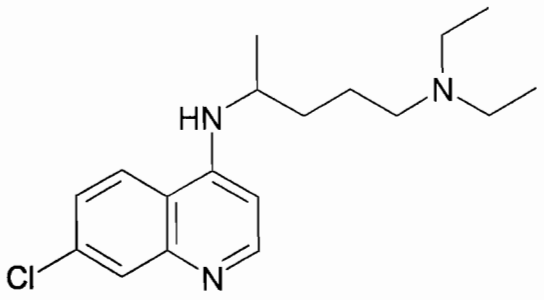

E

Figure 1.19 Some of the compounds investigated **(A)** quinine. **(B)** quinidine, **(C)** 9-epiquinine, **(D)** amodiaquine and **(E)** chloroquine.

1.9.2 Development of a potential high throughput screening method for detecting β-haematin inhibition

The specific objective: To develop a cheap, rapid potentially, high throughput method for screening antimalarial compounds for *β*-haematin inhibition.

1.9.3 Investigation of the effect of incubation time on β-haematin inhibition

The specific objective: To determine whether the strength of *β*-haematin inhibition by quinoline antimalarials depends on incubation time.

CHAPTER 2

MATERIALS AND GENERAL METHODS

2.1 INTRODUCTION

This chapter contains a comprehensive list of materials used in this work, as well as equipment and methods used in more than one chapter in the thesis. Detailed methods specific to a chapter are listed in that particular chapter.

2.2 MATERIALS

All water used in this work was distilled in glass. The materials given in table 2.1 were analytical grade or of highest purity commercially available.

Materials	Supplier
2-[N-cyclohexylamino]ethanesulphonic acid (CHES)	Sigma chemical company
2-[N-morpholino]ethanesulphonic acid (MES)	Sigma chemical company
2-aminoquinoline	Aldrich chemical company
3-[N-morpholino]propanesulphonic acid (MOPS)	Sigma chemical company
3-aminoquinoline	Aldrich chemical company
4,7-dichloroquinoline	Aldrich chemical company
5-aminoquinoline	Aldrich chemical company
6-aminoquinoline	Aldrich chemical company
8-aminoquinoline	Aldrich chemical company
8-hydroxyquinoline	Aldrich chemical company
9-epiquinidine	Buchler GmbH
9-epiquinine	Buchler GmbH
Absolute ethanol	Kimix Laboratory suppliers
Acetonitrile	Scharlau Chemie Reagent grade

Amodiaquine dihydrochloride	Sigma chemical company
Bovine haemin	Sigma chemical company
Buffer solution (phosphate) pH 4	BDH Laboratory suppliers
Buffer solution (phosphate) pH 7	BDH Laboratory suppliers
Chloroquine diphosphate	Sigma chemical company
Dimethylsulphoxide (DMSO)	BDH Laboratory suppliers
Ethyl acetate	Lasechem
Glacial acetic acid	Saarchem Laboratory suppliers
Halofantrine hydrochloride	Glaxo-SmithKine
Hydrochloric acid	BDH Laboratory suppliers
Mefloquine hydrochloride	Roche S.A Ltd
MicroSep,Cellulosic, White, Plain 0.22 Micron, 25 mm membrane filters	Millipore Corporation, Osmonics
N-[2-hydroxyethyl]piperizine-N-[2-ethanesulfonic acid] (HEPES)	Sigma chemical company
n-octanol	BDH Laboratory suppliers
Nujol	Merck
Phosphorus pentoxide	Riedel-de Haën
Porcine haematin	Sigma chemical company
Potassium bromide	Merck
Primaquine diphosphate	Aldrich chemical company
Pyridine	BDH Laboratory suppliers
Quinidine sulphate	Sigma chemical company
Quinine sulphate	BDH Laboratory suppliers
Quinoline	Aldrich chemical company
Silica gel	Merck
Sodium acetate trihydrate	Sigma chemical company
Sodium chloride	Saarchem chemical suppliers
Sodium hydrogen phosphate	Saarchem Laboratory suppliers
Sodium hydrogen sulphate	Aldrich chemical company
Sodium hydroxide	Saarchem

2.3 METHODS

2.3.1 pH measurement

All pH measurements were carried out using a Crison micropH 2000 pH-meter. Standard buffer solutions were used to calibrate the pH meter before use. The temperature of the laboratory was taken into account when calibrating the instrument.

2.3.2 Temperature control

A YIH DER BL-710 thermostated water bath was used to keep temperatureS stable. A thermometer was used to confirm that the solutions under study were at required temperatures.

2.3.3 Infrared Spectroscopy

Samples were thoroughly washed with distilled water and then dried in a desiccator for 48 hours over phosphorus pentoxide and silica gel. KBr discs were then prepared using a mixture of approximately 2.0 mg of sample and 200 mg of KBr. A homogeneous mixture of the sample and KBr was obtained by grinding with an agate mortar and pestle, and this was pressed into a pellet under 10 ton for 3 minutes. An infrared spectrum of the sample in the pellet was obtained using a Perkin-Elmer 983 infrared spectrophotometer, Perkin Elmer PARAGON 1000 FTIR Spectrometer or Spectrum one Perkin Elmer FTIR Spectrometer. This was carried out in transmittance mode.

2.3.4 X-ray powder diffraction

Approximately 100 mg of sample was finely ground into a powder to avoid preferred orientation effects, and was then carefully packed into a glass sample holder. Diffraction patterns were recorded using a Philips PW3710

mpd controlled goniometer connected to a PW3830 X-ray generator, with copper (λ = 1.5418 Å) as a source of X-rays between 2θ values of 5-40°.

2.3.5 UV-Visible spectroscopy

A Beckman DU68 or Varian Cary 100 UV-visible spectrophotometer fitted with a thermostated cell holder was used. Spectrophotometric titrations were carried out at fixed wavelength at 402 nm when chloroquine and related antimalarials were titrated against haematin. Absorbance measurements were carried out at 405 nm for data collected to obtain IC_{50} values for β-haematin inhibition using pyridine-haematin complex for quantitation. Wavelengths ranging from 300 to 700 nm were scanned to confirm the monomeric and dimeric nature of haematin in pure and mixed-solvents, and when observing spectroscopic changes brought about by interaction of the drug with haematin and co-ordination of pyridine with haematin.

2.3.6 Scanning electron microscopy

Samples were sent to the Electron Microscope Unit at the University of Cape Town for scanning electron microscopy studies. Finely ground samples were sprinkled onto aluminium stubs pre-coated with an almost dry carbon and glue mixture. Excess sample was then removed before the samples on the stubs were sputter-coated with gold-palladium, and finally examined with a Leica S440 scanning electron microscope.

CHAPTER 3

EFFECT OF SOLVENT, pH AND IONIC STRENGTH ON THE INTERACTIONS OF QUINOLINE ANTIMALARIALS WITH Fe(III)PPIX

3.1 INTRODUCTION

Egan et al. have studied the interaction of quinoline antimalarial drugs with haematin in buffered 40% (v/v) aqueous dimethyl sulfoxide (DMSO) [86, 90] (see chapter 1). This solvent system has the advantage of controlling the aggregation state of haematin and drugs, maintaining haematin in a monomeric state [163]. Furthermore, association of drugs with haematin can be studied using Uv-Visible spectroscopy under these conditions. By contrast, spectroscopic changes in aqueous solution are very small, with the result that quantitative investigation is not feasible owing to an unfavourable signal to noise ratio in the titration data. However, while interaction of antimalarial drugs with Fe(III)PPIX cannot be studied in pure aqueous solution by Uv-Vis spectroscopy, it has been successfully studied by titration calorimetry by Dorn and co-workers [74]. Other porphyrins, like uroporphyrins [93, 94] which remain monomeric in an aqueous environment have also been used to avoid aggregation.

Despite the non-physiological nature of 40% (v/v) DMSO solvent system, Egan et al. have shown that spectroscopic observations made in this mixed aqueous solvent where haem is monomeric, models the molar free energies of interactions of haematin with the quinoline drugs very well. They have shown that the association constants for this class of compound with Fe(III)PPIX in 40% (v/v) aqueous DMSO are remarkably similar to those reported in purely aqueous medium where Fe(III)PPIX is believed to exist as a μ-oxo dimer [74].

A thermodynamic compensation in the 40% (v/v) aqueous DMSO has been observed for these drugs [86]. Subsequent to the original study, there have been considerable advances in the interpretation of thermodynamic compensation phenomena from the work of Inoue and Wada [104] who compared this phenomenon in many classes of host- guest interactions. The phenomenon has been proposed as method of determining the degree of desolvation and tightness of complexes (i.e loss of flexibility) in such interactions from a plot of $T\Delta S$ versus ΔH. The intercept ($T\Delta S_o$) provides an indication of desolvation, while the slope (α) is a measure of tightness of the complexes formed in solution (see chapter 1).

In this study the thermodynamic compensation has been examined in the light of the Inoue and Wada interpretation and the role of electrostatic interactions and solvent hydrophobicity on the strength of these complexes has been investigated by varying the solvents, ionic strength and pH.

3.2 METHODS

3.2.1 Preparation of 200 mM buffer stock solutions

There were four buffers used in this work. These were prepared by weighing out 4.776g (HEPES); 3.904g (MES); 4.186g (MOPS) and 4.146g (CHES). These masses were dissolved in less than 100 ml of water. A slurry of NaOH solution was used to adjust the pH to required values (7.5, 5.5, 8.5 and 9.5 respectively). The solutions were made up to 100 ml with water.

3.2.2 Preparation of buffered aqueous DMSO solutions

Spectrophotometric titrations were carried out in solutions consisting of 40% DMSO (v/v) by mixing 4 ml DMSO, 1 ml of 0.2 M HEPES, 50% DMSO (5 ml DMSO, 1 ml HEPES); 60% DMSO (6 ml DMSO, 1 ml HEPES); 70% DMSO (7 ml DMSO, 1 ml HEPES) and 80% DMSO (8 ml DMSO, 1 ml HEPES). All

these solutions were made up to 10 ml with distilled water. All pH studies were carried out in 40% DMSO (v/v) using the buffers mentioned in section 3.2.1. Furthermore, an ionic strength study was carried out in 40% (v/v) DMSO at pH 7.5

3.2.3 Preparation of 2 mM quinoline drug solutions in aqueous DMSO

The required amount of each drug (Table 3.1) was weighed out and dissolved in 10 ml of 40; 50; 60; 70 and 80% (v/v) aqueous DMSO containing 0.02 M HEPES buffer (pH 7.4). These solutions were used in the binding study. For solutions containing $NaClO_4$, a stock solution of this salt was prepared in water (2.0 M). This was used to prepare working solutions and quinoline solutions with $NaClO_4$ concentrations ranging between 0.125 and 1.0 M.

Table 3.1 Masses of quinolines used to prepare 2 mM solutions

Compound	Mass /g
Amodiaquine dihydrochloride dihydrate	0.009296
Chloroquine diphosphate	0.01032
Quinine sulphate	0.007470
Quinidine sulphate	0.007469
9-epiquinine hydrochloride	0.007217

3.2.4 Preparation of 2mM chloroquine solutions in organic solvents

The drug solutions were prepared by dissolving 6.397 mg of chloroquine free base in 10 ml of ethyl acetate, DMSO, acetonitrile, ethanol or n-octanol. These solutions were not buffered.

3.2.5 Preparation of haematin solutions in aqueous DMSO

A stock solution of haematin was prepared by dissolving 8 mg of haemin chloride in 10 ml of DMSO, the solution was covered with aluminium foil and stored in the dark. No significant changes have been observed on the spectrum of this solution even if it was allowed to stand for several days. New stock solutions were prepared every week. Working Fe(III)PPIX solutions in aqueous DMSO were prepared in situ in the cuvette by mixing 5 μl of haemin stock solution with 200 μl of the appropriate buffer and 795; 995; 1195; 1395 or 1595 μl of DMSO for (40; 50; 60; 70 and 80% (v/v) of DMSO respectively) and 200 μl of HEPES buffer (0.2 M, pH 7.5)

3.2.6 Preparation of haematin solutions in organic solvents

A stock solution of haematin was prepared by dissolving 8.0 mg of haematin in 10 ml of absolute ethanol, the solution was covered with aluminium foil and stored in the dark. Working Fe(III)PPIX solutions (2.0×10^{-6} M) in ethylacetate, DMSO, acetonitrile, absolute ethanol and n-octanol were prepared by mixing 3.4 μl of the haematin stock solution with 1995 μl of the appropriate solvent in situ.

3.2.7 The spectrum of haematin in 40% DMSO

Spectra were recorded on a Beckman DU68 or a Varian Cary 100 UV- visible spectrophotometer fitted with a thermostated cell holder at 25°C. A 2 ml blank solution of 40% (v/v) aqueous DMSO (0.02 M, HEPES at pH 7.5) was pipetted into a 1 cm cuvette and placed into the sample compartment of the instrument. The solution was allowed to equilibrate to 25°C for five minutes and was then stirred until the initial absorbance was stable before the absorbance was zeroed. The cuvette was emptied, rinsed and dried. A 2 ml haematin solution in 40% (v/v) DMSO, 0.02 M HEPES at pH 7.5 was pipetted into the cuvette and placed into the sample compartment. After the solution

was equilibrated for 5 minutes, it was stirred. The absorbance spectrum of this solution was recorded over wavelengths ranging from 300 – 700 nm.

3.2.8 Effect of chloroquine on the spectrum of haematin in 40% DMSO

A 2 ml volume of the haematin solution described in section 3.2.7 was delivered to a clean dry cuvette and placed in the sample compartment of the spectrophotometer. After this solution had been temperature equilibrated, 5μl of the buffered chloroquine solution in the same solvent system and at the same pH was added to the haematin solution using a Hamilton syringe. The mixture was stirred and the spectrum was recorded. Further aliquots of chloroquine were added in this way, followed by stirring and recording of the spectrum between 300 – 450 nm. (The effect of chloroquine on the spectrum of haematin was also measured between 450 – 700 nm. In the latter case the concentration of haematin solution used was increased by 5 fold). Aliquots of the same volume of buffered chloroquine solution were added to a blank solution of aqueous DMSO (without haematin) in the reference cuvette. After stirring, the spectrum was recorded after each addition of chloroquine solution. The resulting difference spectra were corrected for dilution by multiplying by the dilution factor.

3.2.9 *Titration of haematin with quinoline antimalarials*

Spectrophotometric titrations were carried out on a DU 68 Beckman or Varian Cary 100 UV-visible spectrophotometer fitted with a thermostated temperature control. The instrument was zeroed using the appropriate buffer solution or solvent as mentioned above. Predetermined aliquots of the quinoline solution were added to 2.00 ml of the haematin solution. The resulting solution mixtures were stirred and their absorbance measured and recorded after each addition. Care was taken to ensure that the solution had equilibrated after each addition. Where the quinoline solution absorbs in the area of interest, the reference cell was titrated. A 2.00 ml solution of the blank was delivered into the cuvette in the reference beam of the instrument. The same volumes of

quinoline solution as in the sample cuvette, were also added to the cuvette in the reference cell. Both cuvettes were treated the same throughout the titration.

3.2.10 Data analysis

The absorbance readings obtained at 402 nm were corrected for dilution as shown in equation 3.1 below

$$A_{corr} = \frac{2000 + V}{2000} \times A_{402} \quad \text{.....(3.1)}$$

Where A_{corr} is the corrected absorbance at 402 nm, V is the total volume of quinoline solution added to the haematin solution (in μl) and A_{402} is the measured absorbance at 402 nm.

The concentration of the quinoline at each data point was calculated as indicated below, in equation 3.2

$$[D] = \frac{V}{V_{total}} \times [D]_{stock} \quad \text{.....(3.2)}$$

Where [*D*] is the concentration of the quinoline in the cuvette, V_{total} is the sum of the volume of haematin and that of the quinoline (in μl) and $[D]_{stock}$ is the concentration of the stock quinoline solution.

Titration data obtained were analysed using non-linear squares fitting methods. The model of association of haematin and quinoline compounds that was found to fit the data was a 1:1 model [164]. Absorbance observed using this model is described by equation 3.3

$$A = \frac{A_o + A_\infty K[D]_{free}}{1 + K[D]_{free}} \quad \text{.....(3.3)}$$

Where A is the corrected absorbance at 402 nm, A_o is the absorbance before the quinoline solution is added, A_∞ is the corrected absorbance at the end of the titration, at which point addition of more quinoline solution does not alter the absorbance further, K is the association constant under the specific conditions used and $[D]_{free}$ is the concentration of uncomplexed quinoline.

Non-linear squares fitting of a 1:1 model was performed as described previously [164]. The free quinoline concentration was determined numerically for each titration point during each iteration of the non-linear least squares fitting procedure using Newton's method. In order for this method to be used, the polynomial form of the expression for free quinoline (eq. 3.4) is required. This has been derived previously [164].

$$K[D]_{free}^{2} + (K[M]_T - K[D]_T + 1)[D]_{free} - [D]_T = 0 \quad \text{.....(3.4)}$$

Here $[M]_T$ is the total haematin concentration and $[D]_T$ is the total quinoline concentration.

3.3 RESULTS AND DISCUSSION

3.3.1 Changes in the spectrum of haematin due to interaction with quinoline antimalarials

The spectrophotometric titration of haematin with compounds under investigation, including chloroquine was performed by monitoring the absorbance of the Soret band at 402 nm. Figure 3.1(A) shows the decrease in the absorbance spectrum of haematin as aliquots of choloroquine are added. The decrease in the intensity of the Soret band has been reported to be due to complex formation of haematin with the drug [86]. In the 450 –700 nm region, the haematin spectrum shows absorbance peaks at 498 nm, 535 nm and 620 nm (Figure 3.1(B)). The progressive addition of the drug results in the

disappearance of the 498 nm and the 535 nm peaks and appearance of the broad peak at 598 nm.

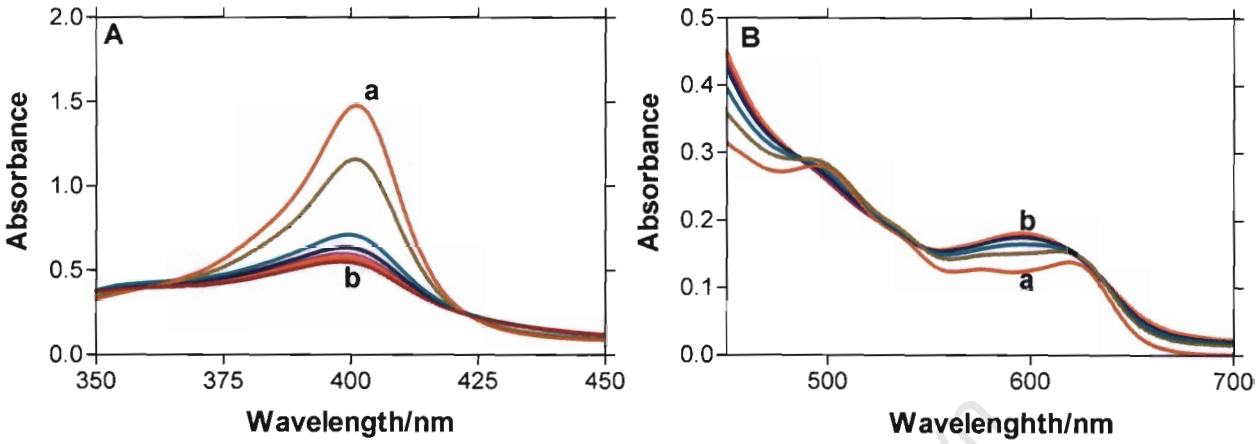

Figure 3.1 Spectral changes as a function of increasing concentration of chloroquine (from a to b) **(A)** Decrease in the Soret band of haematin in 40% (v/v) aqueous DMSO centred at 402 nm upon titration with chloroquine at pH 7.5 (0.02 M HEPES), 25°C **(B)** Changes in the visible region of a spectrum of haematin as a function of increasing concentration of chloroquine

Changes in the spectrum are also observed with increasing ionic strength (figure 3.2(A)). A non-coordinating salt (sodium perchlorate) was used to observe the effect of ionic strength on the spectrum of haematin. However, increasing ionic strength resulted in a decrease in the Soret band and a small blue shift was observed in the absorption maximum ($\lambda_{0.00M\ NaClO4}$ = 402.5 nm, $\lambda_{1.00\ M\ NaClO4}$= 400 nm). An effect is also observed in the long wavelength region. Increasing ionic strength causes an apparent disappearance of the 498 nm and 535 nm peaks and appearance of the new peak at 571 nm with a small shoulder at 602 nm (figure 3.2(B)). The spectrum of haematin in high concentrations of $NaClO_4$ is identical to that of the μ-oxo dimer [79]. Similar effects have also been observed in the spectrum of haematin with increasing concentration of sodium chloride. This indicates that increasing ionic strength induces the formation of μ-oxo dimer at pH 7.5. A significant decrease in intensity and shift in Soret band occurs in purely aqueous medium as well. These changes are believed to be as a result of aggregation [165]. Comparing spectral changes resulting from the progressive addition of chloroquine to

haematin solution are significantly different to those observed in the presence of salt. This confirms that these changes are due complex formation and not μ-oxo dimer formation.

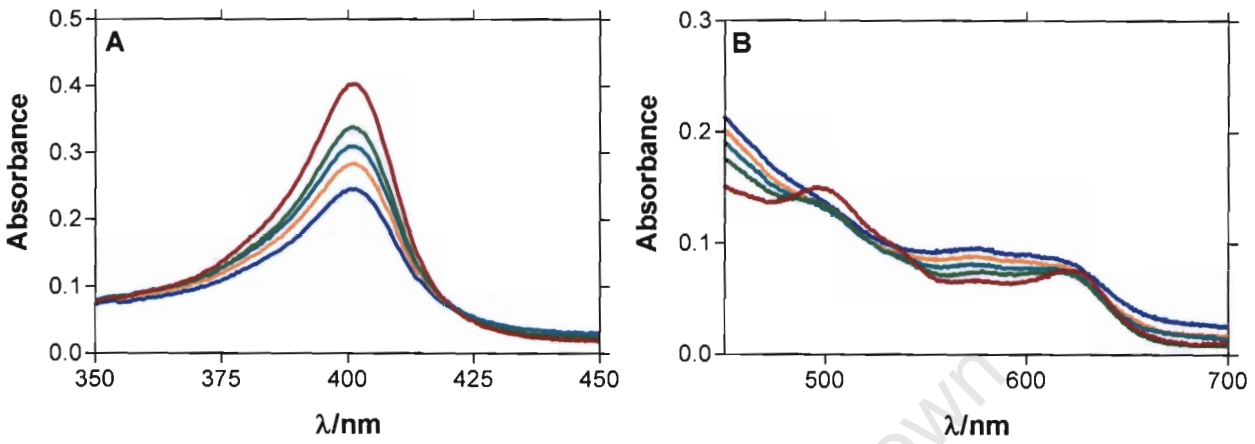

Figure 3.2 (A) A decrease in the Soret band as a function of increasing concentration of $NaClO_4$ and **(B)** visible spectra of haematin in 40% (v/v) aqueous DMSO, in the presence of $NaClO_4$. (—) 0.00 M; (—) 0.25 M; (—) 0.5 M; (—) 0.75 M and (—)1.00 M.

Spectral changes were also observed in 40% aqueous DMSO when the apparent pH was varied from 5.5 –10 (figure 3.3). The decrease in Soret band when the pH is increased appears to be due to changes of a monomeric species to a dimeric species. The absorption maximum also experience a blue shift ($\lambda_{pH\ 5.5}$ = 401 nm, $\lambda_{pH\ 10}$ = 396 nm) (figure 3.3A). This is confirmed in the region between 450 –700 nm where peaks observed at 500 nm, 535 nm and 623 nm at pH 5.5, 6.5 and 7.5 respectively demonstrate the presence of the monomeric species. At pH 8, 9 and 10 there is an apparent disappearance of these peaks with an appearance of a peak at 571 nm with a shoulder at 599 nm (figure 3.3B). At pH 9 and 10 the spectrum is identical to that of a μ-oxo dimer. No significant fraction of μ-oxo dimer is observed below pH 8.0. The conditions chosen for the study of interactions of quinoline antimalarials with haematin were thus selected to avoid μ-oxo dimer formation.

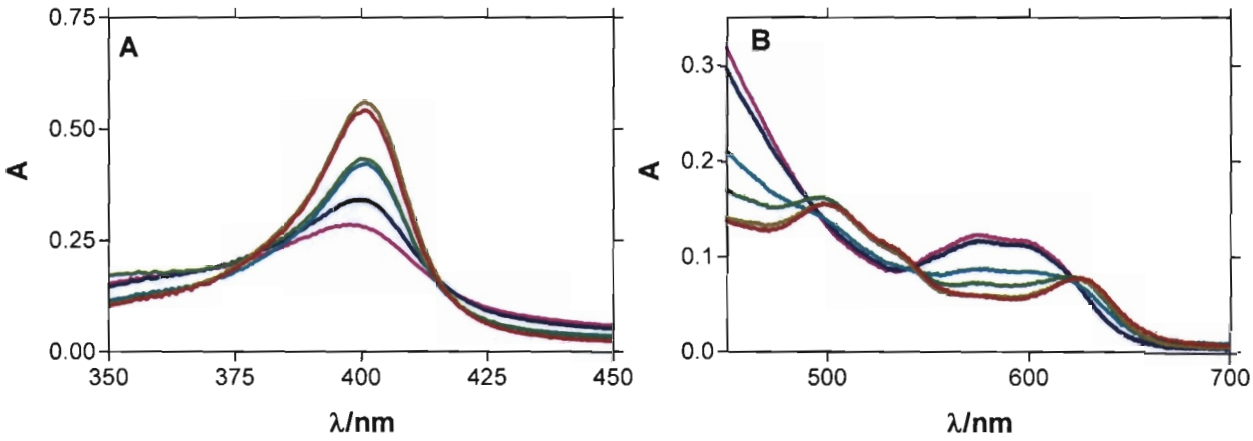

Figure 3.3 Spectra of haematin in 40% (v/v) DMSO as function of increasing pH. **(A)** Shows a decreasing absorbance from (—) pH 5.5; (—) pH 6.5; (—) pH 7.5; (—) pH 8.0; (—) pH 9.0; (—) pH 10.0 at 25°C. **(B)** Spectral changes in long wavelength region

3.3.2 Thermodynamic compensation

In previous studies it has been shown that there is a thermodynamic compensation phenomenon in the association of various quinoline drugs with Fe(III)PPIX in 40% aqueous DMSO [86]. Subsequently, there has been a considerable advance in the understanding of this phenomenon from the work of Inoue and Wada [104]. As described in the introduction, these authors have suggested that this phenomenon can provide information about the degree of desolvation of the guest ($T\Delta S_o$) and the loss of flexibility of the host (α), where α is the slope of a plot of $T\Delta S$ versus ΔH.

The thermodynamic compensation effect for a series of quinoline and related antimalarials observed in 40% aqueous DMSO has been compared with that in pure aqueous solution. The enthalpy and entropy data for the association of quinoline drugs with Fe(III)PPIX under these conditions have been collected and are plotted in figure 3.4(A) for the interactions in 40% DMSO. Thermodynamic compensation observed in thermodynamic data reported for the interaction of the quinoline drugs with Fe(III)PPIX in purely aqueous

medium by titration calorimetry [74] is shown in figure 3.4(B). In 40% aqueous DMSO the slope α of a plot of $T\Delta S$ versus ΔH is 1.1 and the intercept $T\Delta S_o$ is 29 kJ/mol. In pure aqueous medium essentially identical values were obtained (α = 1.0 and $T\Delta S_o$ = 29 kJ/mol).

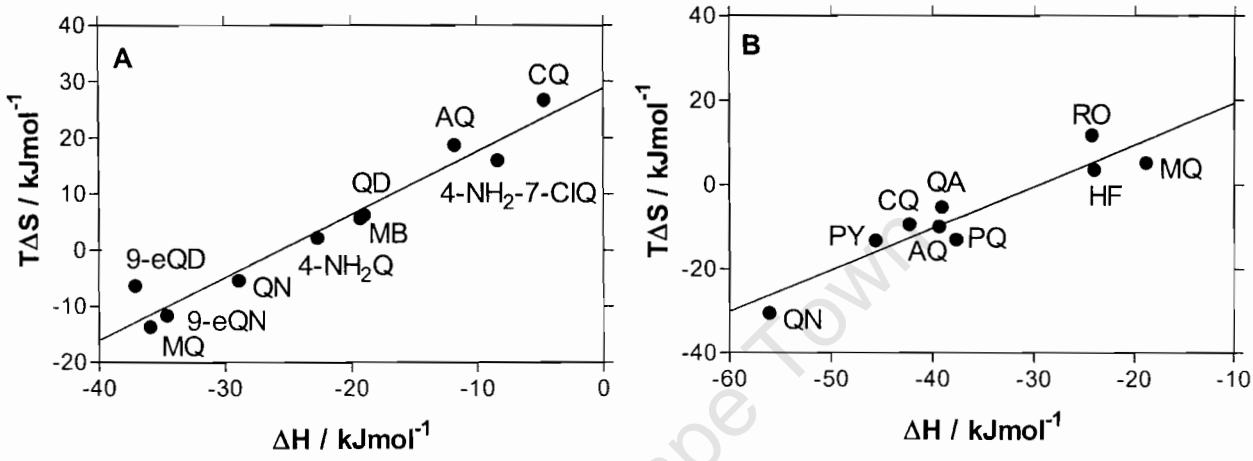

Figure 3.4 Thermodynamic compensation plot for the interaction of quinoline antimalarials with Fe(III)PPIX in **(A)** 40% v/v aqueous DMSO, pH 7.5 (0.02 M HEPES), 25°C and **(B)** aqueous solution, pH 6.5 (0.25 M phosphate), 37°C. The data in **(A)** were obtained in our laboratory from Van't Hoff's plots and most ΔH and ΔS values were previously reported [86]. The plot in **(B)** was constructed using calorimetric data reported by Dorn et al. [74]. The slopes (α) and intercepts ($T\Delta S_o$) of both plots are identical within experimental error (α = 1.1 ± 0.1 and 1.0 ± 0.1 and $T\Delta S_o$ = 29 ± 2 kJ/mol and 29 ± 5 kJ/mol respectively). The abbreviations in (A) and (B) are AQ – (amodiaquine); CQ–(chloroquine); QD – (quinidine); 4-NH_2-7-ClQ – (4-amino -7-chloro quinoline); 4-NH_2Q – (4-aminoquinoline); QN – (quinine); 9-eQN – (9-epiquinine); MQ – (mefloquine); 9-eQD – (9-epiquinidine); PY – (pyronaridine); PQ – (primaquine); QA – (quinacrine); HF – (halofantrine); RO – (RO 48-6910); MB – (N-[2-(7-chloro-4-quinolinyl)]-2-(4-methylpiperazin-1-yl)ethanamide)

The value of $T\Delta S_o$ is a measure of the degree of desolvation where ΔS_o is the value ΔS corresponding to a ΔH value of zero and the slope (α) of a plot of $T\Delta S$ versus ΔH is a measure of loss of flexibility of the host. These α and

$T\Delta S_o$ values are relatively large in both 40% (v/v) aqueous DMSO and in pure aqueous solutions, indicating that there is a considerable degree of desolvation (large $T\Delta S_o$) and a large loss of flexibility. The compensation plot reported by Inoue and Wada for the association of porphyrins with quinones in organic solvents showed that the value of α for such non-covalent interactions is 0.6 and the value of $T\Delta S_o$ is 0 kJ/mol. The value of α and $T\Delta S_o$ for coordination of metalloporphyrins with pyridine are 0.61 and 1.6 kJ/mol respectively. The small values of α and $T\Delta S_o$ in pure organic solvents in these studies were ascribed to the fact that there is little desolvation and the porphyrins are already rigid and this results in relatively little loss of flexibility upon complex formation. The values of α and $T\Delta S_o$ obtained in 40% aqueous DMSO and in pure water appear to be very large owing to the different solvent environment. It appears that in aqueous media there is a high degree of desolvation and a large loss of flexibility resulting in a complex that is much more restricted in its motion. This suggests that water plays a major role in locking the conformation of the quinoline –Fe(III)PPIX complex. The low degree of desolvation in non-aqueous media is to be expected, as organic solvents generally solvate solutes rather weakly. Interestingly, similar entropy –enthalpy effects have also been reported for the interaction of amino acids and amino esters with a series of zinc porphyrins in aqueous solution [166]. In that case, intermediate α and $T\Delta S_o$ values were observed (0.81 and 13.0 kJ/mol respectively). The close similarity of the thermodynamic compensation plots for Fe(III)PPIX-quinoline interactions in 40% aqueous DMSO and pure water further underline the similarity of the interactions under both sets of conditions, going beyond the mere similarity in the strength of interaction previously noted [4]. However, the ΔH and ΔS data collected in 40% aqueous DMSO are generally more positive for monomeric Fe(III)PPIX than for dimeric Fe(III)PPIX in aqueous solution. Thus the interactions in aqueous DMSO are more entropy driven while in aqueous solution appears to be more enthalpy driven. This probably reflects tighter interaction in pure aqueous solution. This tightness results in more favorable enthalpies of interaction but less favorable entropies.

The drug receptor site on monomeric Fe(III)PPIX in 40% DMSO is probably similar to that of dimer in aqueous solution. In the μ-oxo dimer it is believed to be an open face of the five coordinate porphyrin [81, 102]. If Fe(III)PPIX is similarly five coordinate in 40% aqueous DMSO, one face will be occupied by an $-OH^-$, $-H_2O$ or –DMSO ligand, while the other will be open as in the μ-oxo dimer. By contrast, it should be noted that it has previously been found in aqueous solution that the association constants of chloroquine, quinine and 9-epiquinine with the six coordinate Fe(III)PPIX group of the haem peptide N-acetyl micro-peroxidase-8 are about 2-3 orders of magnitude weaker supporting the argument that association with Fe(III)PPIX occurs with the open face of the porphyrin. Finally, similarity of the interactions in pure aqueous medium and in 40% aqueous DMSO emphasises the fact that the solvent environment in 40% DMSO, which is about 86% by mole water, is probably a reasonable approximation to aqueous solution.

3.3.3 Effect of the fraction of DMSO in DMSO/water mixtures on the interaction of quinoline antimalarials with Fe(III)PPIX

Spectrophotometric titration of haematin with chloroquine, amodiaquine, quinine, quinidine and 9-epiquinine in DMSO/water mixtures ranging from 40 – 80% (v/v) where haematin is strictly monomeric were performed. The free energy of association decreases linearly with increasing mole fraction of water in the solvent mixture in this range. Titration data of these quinoline drugs are shown in figure 3.5.

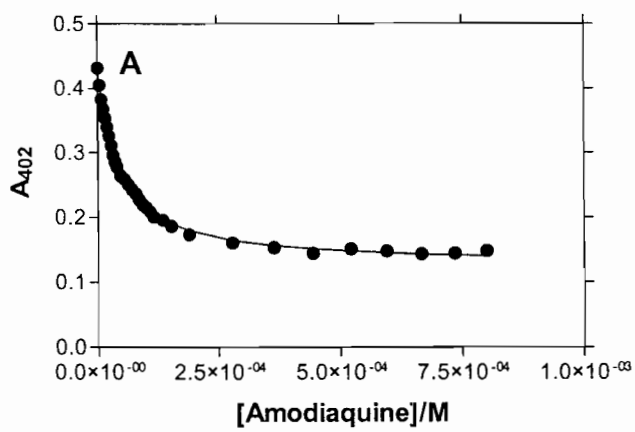

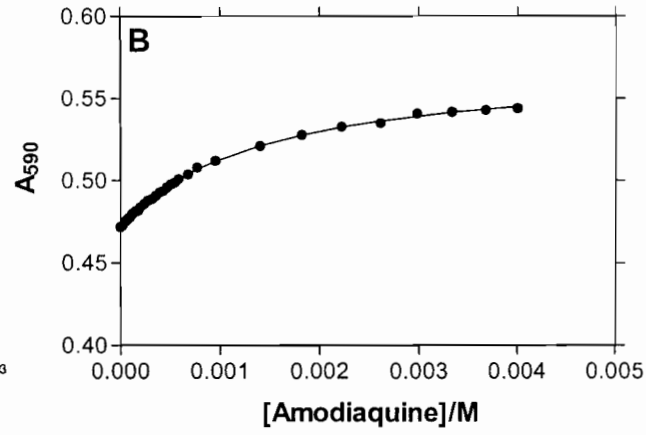

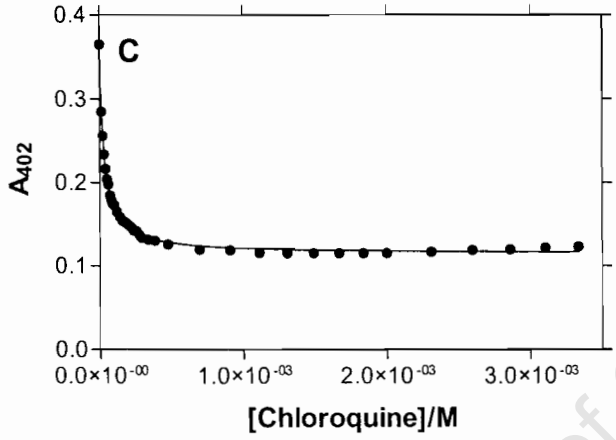

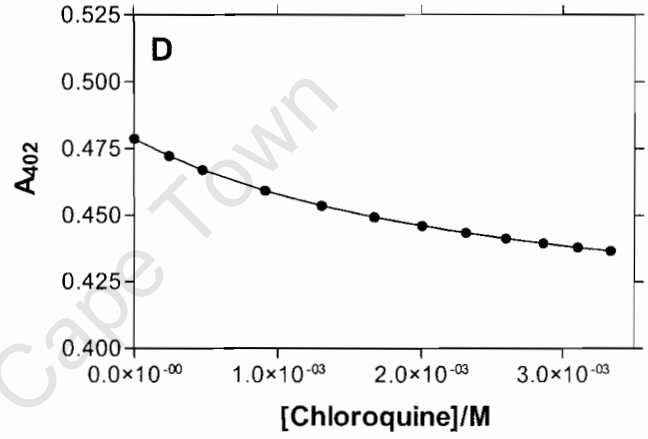

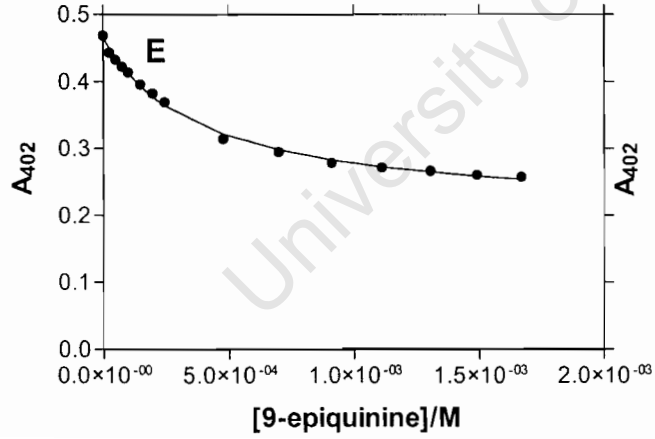

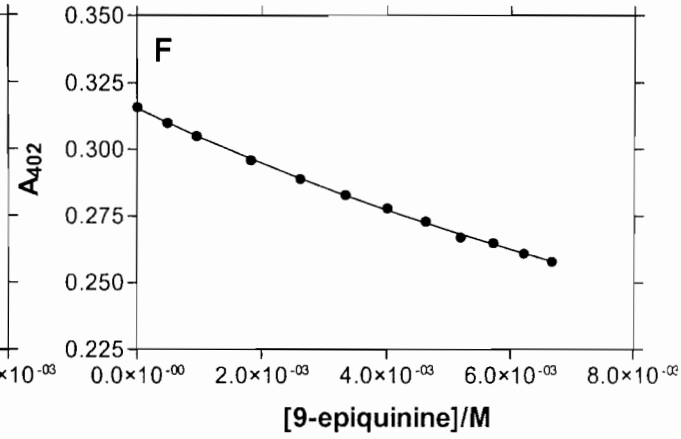

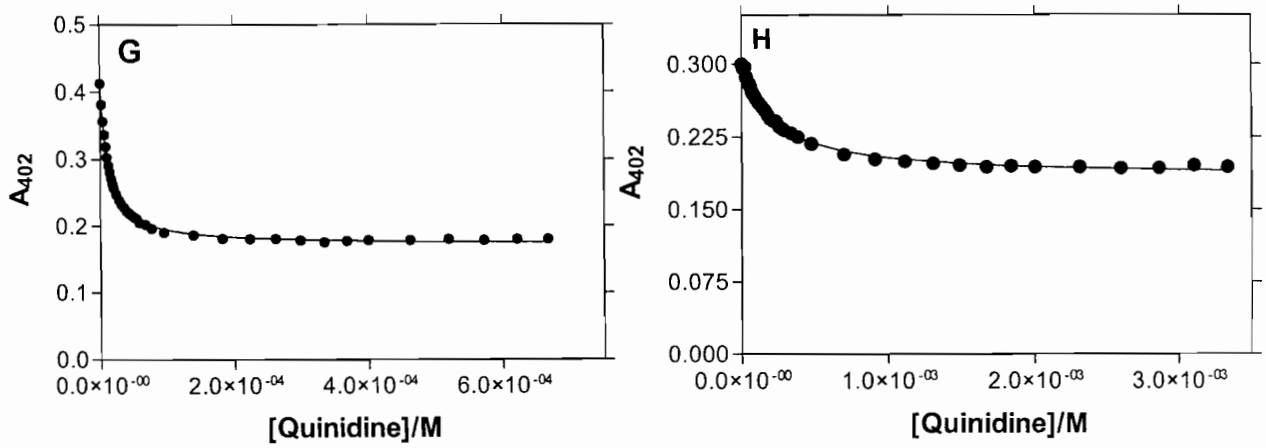

Figure 3.5 Titration curves of haematin with quinoline compounds in 40% and 80% aqueous DMSO, 0.020 M HEPES at pH 7.5 and 25°C. **(A)** is curve of amodiaquine in 40% DMSO, **(B)** amodiaquine in 80% DMSO, **(C)** chloroquine in 40% DMSO, **(D)** chloroquine 80% DMSO, **(E)** 9-epiquinine in 40% DMSO, **(F)** 9-epiquinine in 80% DMSO, **(G)** quinidine in 40% DMSO and **(H)** quinidine in 80% DMSO all fitted to a 1:1 (haematin to drug) association model as given by equation 3.3. Solid lines are best fits of the data to the 1:1 association model.

Quantitative measurement of association constants of chloroquine, amodiaquine, quinidine and quinine with haematin were conducted in five different DMSO/water mixtures Table 3.2. Chloroquine was found to be the most strongly associating quinoline drug in 40% DMSO followed by amodiaquine, quinidine, quinine and 9-epiquinine. The strength of interaction of these drugs with haematin decreases with increasing DMSO concentration. When the association constants were converted into molar free energy values, a plot of a free energy of association against mole fraction of water was found to decrease linearly (figure 3.6).

Table 3.2 Log K values for the association of quinoline antimalarials with Fe(III)PPIX in aqueous DMSO[a]

Quinoline	log K				
	40% DMSO	50% DMSO	60% DMSO	70% DMSO	80% DMSO
chloroquine	5.41	4.56	4.01	3.50	2.64
amodiaquine	5.18	4.39	3.82	3.19	2.96
quinidine	5.02	5.01	4.64	4.22	3.52
quinine	4.14	3.94	3.54	3.27	2.75
9-epiquinine	4.04	3.53	2.93	2.52	1.87

[a]% DMSO is v/v

Two interpretations of these results can readily be imagined. The decreased stability of the complex as the solvent polarity decreases could indicate a hydrophobic effect. The interpretation of this result would be that the change in solvent environment implies that water plays a major role in determining the strength of the complex with haematin. This suggests that replacing water with a less polar solvent would result in a substantial weakening in the complex. Alternatively, it could be that there is a change in coordination of $^{-}OH/H_2O$ to the haematin Fe(III) with increasing concentration of DMSO. DMSO is known to coordinate to haematin [167] in aqueous DMSO and may displace OH^{-}/H_2O from the Fe(III) centre of the pophyrin or form a 6-coordinate complex at higher concentration of DMSO. Similar behaviour was observed by Smithrud and Diederich in the spectral changes of haematin in basic solution of $DMSO/H_2O$ mixtures at constant $[OH^{-}]$ by increasing the mole fraction of water. They suggest that it is unlikely that the changes are due to ligand displacement involving OH^{-} ion, but that the spectral changes are caused by ligand replacement of DMSO by water [167].

Weak complexes with quinoline drugs could be a result of coordination of DMSO to the vacant sixth coordination site at higher concentrations of DMSO, sterically destabilising the interaction.

Plots of ΔG versus mole fraction of water for amodiaquine, chloroquine and quinine indicate that the extrapolated log K values in pure water are reasonably close to those published by Dorn. et.al, for the observed association of these drugs with μ-oxo dimer of haematin in pure aqueous solution obtained by titration calorimetry (figure 3.6) [74].

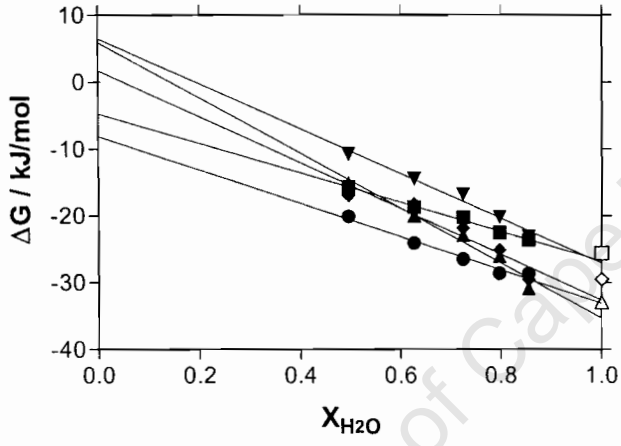

Figure 3.6 A plot of the change in free energy of association (ΔG) versus mole fraction of water (X_{H20}) in DMSO/water mixtures for the complexation of haematin with antimalarial quinolines at pH 7.5 (0.02 M HEPES) at 25°C. Open symbols represent pure aqueous solvent (□ quinine, ◊ amodiaquine and Δ chloroquine) and are from Dorn et al. [74]. Solid symbols represent DMSO/water mixtures (▼ 9-epiquinine, ■ quinine, ♦ amodiaquine, ▲ chloroquine and ● quinidine)

In order to attempt to distinguish between these two alternatives, spectra of haematin in varying percentages of DMSO were compared, (figure 3.7). The visible spectrum of haematin shows very little change when the percentage of DMSO is decreased from 80% to 50%. This indicates that there is probably no change in coordination over this range (although, it cannot be ruled out that the spectra of these species are very similar). The effect of percentage DMSO on association constants thus suggests that an increasing mole fraction of

water probably results in stronger interaction of quinoline antimalarials with haematin due to strengthened hydrophobic effect.

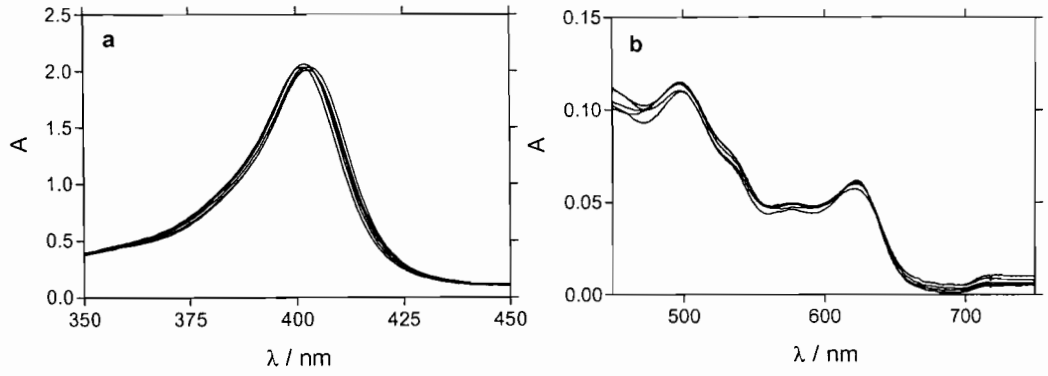

Figure 3.7 Spectra of haematin in 50%, 60%, 70%, and 80% (v/v) aqueous DMSO at pH 7.5

3.3.4 Effect of pH on the interaction of quinoline antimalarials with haematin

Lowering the pH environment in which interactions take place between haematin and drugs (amodiaquine, chloroquine and quinine) causes only small changes to the values of the binding constant. The value of the binding constant for chloroquine changed by 0.6 log units in changing the pH from 7.5 to 5.5 (% increase in ΔG is approximately equal to 12%), amodiaquine and quinine experienced a small change of 0.3 (% decrease in ΔG is approximately equal to 7%). This insensitivity to pH has been confirmed by Vippagunta et al. [168] for chloroquine. It suggests that electrostatic interactions probably do not play a major role in the stability of these complexes as changes in the protonation state and hence charge on Fe(III)PPIX with pH has little effect on the interaction

3.3.5 Effect of ionic strength on the association of quinoline compounds with Fe(III)PPIX

Further, spectrophotometric titration data was collected in the presence of non-coordinating sodium perchlorate. The effect of sodium perchlorate concentration on the association of chloroquine, amodiaquine, and quinine with Fe(III)PPIX in 40% aqueous DMSO is given in Table 3.3. This serves as a useful probe to determine whether electrostatic effects play a major role in these interactions. Free energy of association of these drugs with Fe(III)PPIX shows only a small dependence on the ionic strength. This suggests that electrostatic interaction makes a relatively small contribution to the association energy, as a considerable weakening of the interaction would otherwise be expected as ionic strength increases. The relative insensitivity to ionic strength confirms that hydrophobic effect probably plays a dominant role in the association of these quinolines with Fe(III)PPIX in an aqueous mileu. However, it should be noted that interpretation may be complicated by formation of the μ-oxo dimer at high ionic strength.

Table 3.3 Log K values for the association of quinoline antimalarials with Fe(III)PPIX in 40% aqueous DMSO pH 7.5, 25°C as a function of ionic strength.

Quinoline	log K[a]					
	0.000 M[b]	0.125 M[b]	0.250 M[b]	0.500 M[b]	0.750 M[b]	1.000 M[b]
chloroquine	5.41(5)	5.17(2)	5.15(2)	5.17(4)	5.07(2)	5.11(7)
amodiaquine	5.18(6)	—	4.83(4)	4.99(5)	4.99(4)	4.93(2)
quinine	4.14(2)	—	4.14(2)	4.159(7)	4.27(3)	4.24(4)

[a]mean ± standard error of the mean (in the last decimal place shown in parentheses) for 3 determinations; [b]concentration of $NaClO_4$ = μ.

3.3.6 Effect of solvent polarity on the interaction of quinoline drugs with Fe(III)PPIX

If this weakening of association between the drugs and haematin as the fraction of DMSO increases is due to DMSO coordination to the Fe(III) center, the shape of the dependence of ΔG on DMSO concentration in the solvent can be easily modeled on the basis of law of mass action. This modeling suggests that the increase in ΔG with increasing DMSO concentration is not due to changes in coordination. Such a change would show a hyperbolic dependence on DMSO (and strongly curved dependence on mole fraction, figure 3.8) which is not observed. Indeed this conclusion is consistent with earlier studies suggesting that the under the conditions used in this study it is likely that the species of haematin present is a DMSO complex throughout the experimental range of DMSO concentration [167]. Thus, the data indicate that the decrease in association strength of these drugs with haematin with increasing mole fraction of DMSO appears to be a result of decreased solvent polarity. Free energy of association values of these drugs have been plotted against $E_T(30)$ values (Figure 3.9(A)). $E_T(30)$ (the Dimroth-Reichardt parameter) is an empirical measure of solvent polarity based on changes in electronic transition energies of a standard betaine dye (called $E_T(30)$) measured in solvents of different polarity. Experimental $E_T(30)$ values have been extensively reported in the literature for both pure solvents and binary solutions (including DMSO/water mixtures) [169, 170].

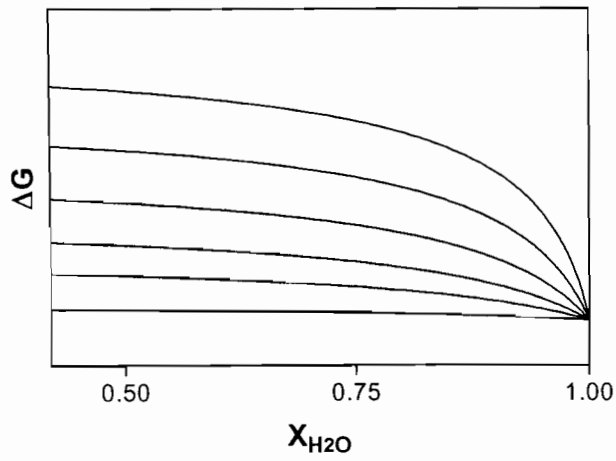

Figure 3.8 The modeled dependence on mole fraction of DMSO expected if the weakening (increase in ΔG) were due to an equilibrium change in axial coordination owing to increased concentration of DMSO. Here it is assumed that haematin exists as an equilibrium mixture of haematin-H_2O and haematin-DMSO with increasing proportions of the latter as the mole fraction of water decreases. It is further assumed that the quinoline complex with haematin-DMSO is weaker than that with hematin, giving rise to two association constants. The apparent value of ΔG is obtained from a weighted average of the two association constants. This average is what would be observed as a result of fitting the data to a 1:1 association model. The family of lines shows the effect of decreasing the association constant for coordination of DMSO to haematin (top to bottom).

These parameters have successfully been used in the correlation analysis of solvent effects on chemical equilibria, reaction rates, and spectral absorption [170]. A plot of ΔG versus $E_T(30)$ for the data obtained in 40% DMSO is shown in figure 3.9(A). There is a straight line correlation as expected, implying that the interactions of these drugs with haematin are predominantly due to hydrophobic effect. The slopes of the plot for quinine and quinidine are significantly smaller than those of chloroquine and amodiaquine, implying that hydrophobic effect play a somewhat smaller role in the interactions of these compounds with haematin. This is in agreement with previous results suggesting that these quinoline methanols, which form complexes with haematin which are typically about an order of magnitude weaker than chloroquine and amodiaquine [171] may weakly coordinate to the Fe(III)

centre of haematin via the hydroxyl group. There is evidence from NMR and visible spectroscopy for this [91, 93, 94]. The contribution of coordination of quinoline methanols to haematin is not expected to be as sensitive to the solvent environment. Nonetheless, this contribution appears to be small, as the association constants of these complexes also weaken greatly when the DMSO concentration increases. In the case of 9-epiquinine this coordination contribution may be lacking altogether (it appears to behave very similarly to chloroquine and amodiaquine) possibly suggesting a different structure for this complex. This difference may explain its inability to inhibit haemozoin formation [73] and consequently its lack of antimalarial activity [172].

Despite the above evidence, the possibility that DMSO coordination contributes to the weakening of the interaction of these drugs with haematin as the mole fraction of DMSO increases cannot be ruled out completely. The interaction of chloroquine base with haematin in pure organic solvents was thus also investigated (example of titration curve in ethanol is shown figure 3.10(C)). The solvents chosen were ethanol, *n*-octanol, acetonitrile, DMSO and ethylacetate. Data in pure water were taken from Dorn et al. [74]. A plot of ΔG shows a linear increase with decreasing $E_T(30)$ (Figure 3.9(B)), although the slope for pure solvents is much lower than that of aqueous DMSO.

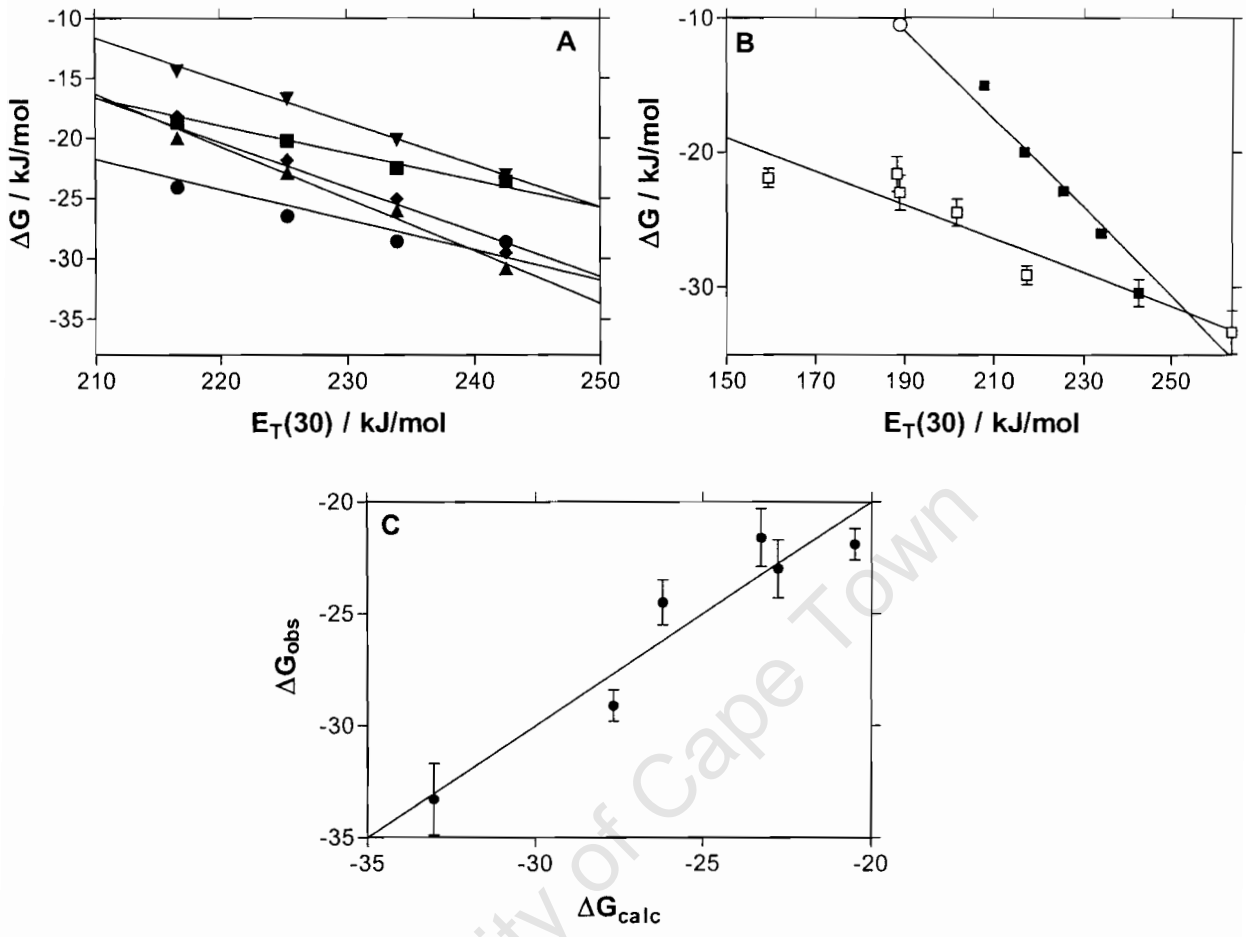

Figure 3.9 The linear free energy relationship between ΔG and $E_T(30)$ for the association of quinoline antimalarials with Fe(III)PPIX. In **(A)** ΔG results for haematin-quinoline interactions in DMSO/water mixtures at (pH 7.5 0.02 M HEPES) are correlated with Dimroth-Reichardt parameter ($E_T(30)$ in kJ/mol). Solid symbols represent (▼ 9-epiquinine, ■ quinine, ♦ amodiaquine, ▲ chloroquine and ● quinidine). In **(B)** solid symbols represent a data for chloroquine as in (A) and the open circle symbols represent data for chloroquine in pure solvents. The solvents are from the lowest $E_T(30)$ to highest: ethyl acetate, DMSO, acetonitrile, *n*-octanol, ethanol and water. The open circular symbol represents the predicted value for pure DMSO obtained from the DMSO/water mixtures. In **(C)** a plot of the observed ΔG values for the association of chloroquine with Fe(III)PPIX in pure solvents against calculated values obtained by fitting to the Kamlet-Taft LFER equation is shown. The fitted equation is $\Delta G = -17.7\alpha - 8.4\pi^* - 5.0$ ($n = 6$, $F = 15.2 > F_{crit} = 9.55$ at 95 % confidence level, $r^2 = 0.91$)

Figure 3.10 shows spectroscopic changes of haematin with increasing concentration of chloroquine base in absolute ethanol. The interaction of the quinoline antimalarials with Fe(III)PPIX depend on the solvent environment. The decrease in absorbance as a function of increasing concentration of chloroquine base results in a small red shift (from 398.8 nm to 400 nm) with prominent isosbestic points at ~ 373 nm and 408 nm (figure 3.10 (A)). In the higher wavelength region there is a decrease in the charge transfer band with a small shift from 596 nm to 598 nm and a shift of the broader peak at 489 nm which sharpens at 494 nm is also observed. There are well defined isosbestic points at ~ 630.5 nm (figure 3.10(B)).

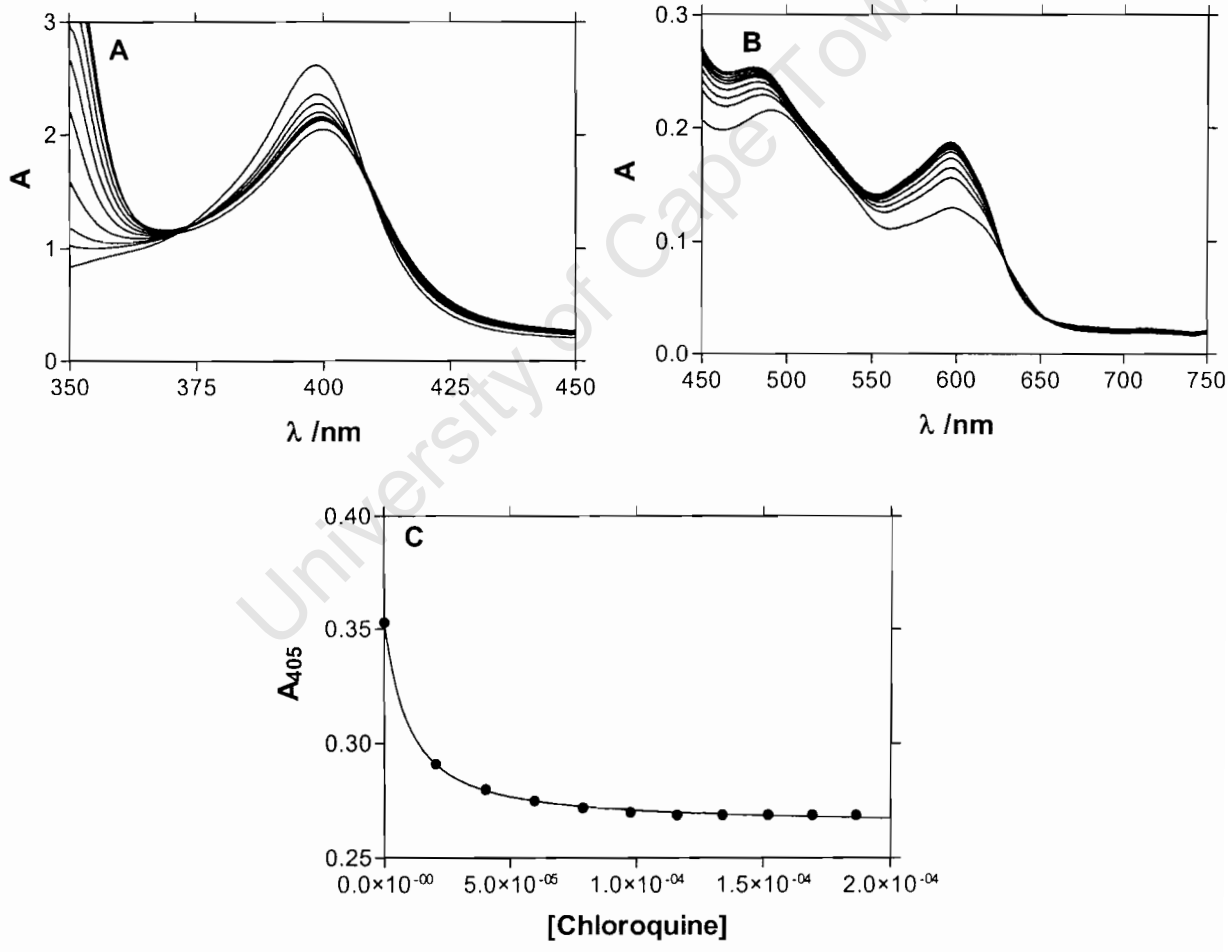

Figure 3.10 Spectroscopic changes in Soret band **(A)** and long wave region **(B)** of the spectrum of Fe(III)PPIX (6.85 x 10^{-6} M) upon addition of chloroquine free base in absolute alcohol. In **(C)** titration curve of chloroquine base in ethanol is fitted to a 1:1 association model. Chloroquine diphosphate could not be used due to insolubility in absolute ethanol.

This shows that the interactions of these drugs are weaker in mixed solvents than in pure organic solvents. The interpretation of this result could be a difference in charges on haematin in pure organic solvents as opposed to buffered aqueous DMSO solution resulting from differences in protonation. Interestingly, Cubberley and Iverson [173] observed a similar behavior when they were investigating solvent effects on aromatic stacking interactions using ^{1}H NMR. These authors observed a linear increase in ΔG with decreasing solvent polarity in mixed protic solvent systems, namely methanol/water mixtures with a greater slope compared to pure organic solvents. This indicates a stronger hydrophobic effect in protic solvents as well weaker interactions in mixed solvents. Solvent molecules such as water have the highest cohesive interactions and possess the lowest molecular polarisability. This results in stronger interactions between the host and the guest in pure aqueous compared to apolar solvents. Thus, energy is gained upon the release of solvating molecules during complexation [169].

The data can also be correlated with other hydrophobicity parameters namely the Kamlet - Taft and the Hildebrand equations. The Kamlet – Taft equation is the most extensively applied method of obtaining values for intermolecular solute/solvent interactions. The Kamlet-Taft parameters are α, a measure of the hydrogen bond donor ability of the solvent, β, a measure of the hydrogen bond acceptor ability of the solvent and π^*, a measure of dipole moment and polarizability of the solvent. The observed free energies of association are modeled according to the expression in equation 3.1 [174].

$$\Delta G = \Delta G^o + a\alpha + b\beta + p\pi^*, \quad \ldots\ldots (3.1)$$

where ΔG^o, a, b, and p are fitted coefficients. A significant fit was found using α and π^* terms. This suggests that the association of chloroquine with Fe(III)PPIX is strengthened by increased solvent dipole moment and polarizability and by increased hydrogen bond donor ability. There is no significant correlation with hydrogen bond acceptor ability of the solvents on the interactions. Figure 3.8(C) shows a plot of observed ΔG versus calculated

ΔG (from the fit to equation 3.1). The fit is better than that of ΔG versus $E_T(30)$ (r^2 = 0.91, p= 0.003 versus 0.88, p = 0.006). The Hildebrand parameter (δ) is a measure of the cohesion of solvents (energy required to create a cavity in a solvent). The Hildebrand parameter is sometimes also used as a measure of hydrophobicity of a solvent [175, 176]. A statistically reasonable correlation is also observed with the observed association data, but it is a much weaker correlation (r^2 = 0.70, p = 0.04). The correlations with three different measures of solvent polarity strongly suggest that hydrophobic effect play a major role in the formation of these complexes. Obviously, the correlation of free energy of association with Hildebrand parameter is not as good as their correlation with $E_T(30)$ since solvent cohesive interactions represent only one major solvent property that reflects solvation effects. However, a clear trend is visible that the association strength increases with solvent cohesive interactions.

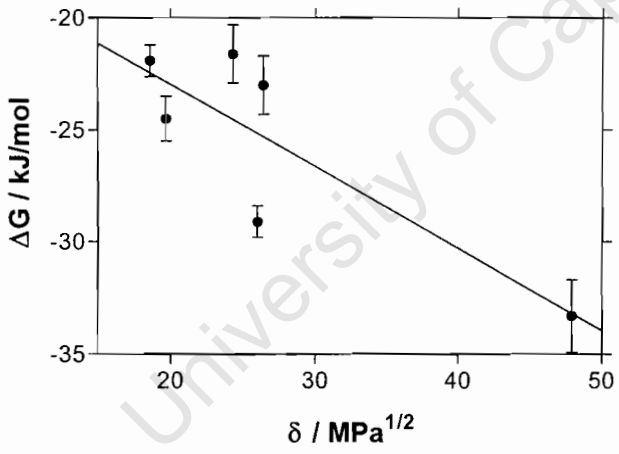

Figure 3.11 Free energy of association of chloroquine with haematin in pure solvents are plotted against the Hildebrand parameter (r^2 = 0.70, p = 0.04)

By contrast no correlation was observed with donor number (a measure of Lewis basicity) [177] or the molar volume of the solvent (or a combination of the two). This supports the argument that the differences in the free energy of association of chloroquine with haematin are not a result of solvent coordination to the metalloporphyrin or differences in the Steric bulk of any coordinated solvent molecules.

Interestingly, chloroquine associates more strongly with haematin in pure organic solvents or pure aqueous solvents than it does in mixed systems. This behaviour has been observed in other systems. Mizutani et al. [166] have investigated the interactions of amines and amino-esters with synthetic zinc porphyrins. These were found to interact strongly in dichloromethane and water, but much more weakly in aqueous methanol. This was attributed to the predominance of desolvation and dispersion interactions in aqueous solution and of strong dispersion interaction and electrostatic interactions in non-aqueous solution. The weaker interaction in the mixed solvents was ascribed to weakening of both effects. Similar behaviour has also recently been observed in the dependence of energy of formation of donor-acceptor complexes of aedamer monomer on solvent polarity [173]. In that case the slope of ΔG versus $E_T(30)$ was found to be distinctly steeper for methanol mixtures than for other solvents. It was suggested that hydrophobic effect is considerably stronger in protic solvents. It seems likely that similar factors lie behind the differences in non-aqueous and mixed solution in the case of the interaction of the antimalarials with haematin.

3.4 CONCLUSIONS

The thermodynamic compensation phenomenon in aqueous solution and 40% aqueous DMSO, as well as studies of interactions of quinoline antimalarials with Fe(III)PPIX in solvents of lower polarity suggests that water plays a major role in the stability of these complexes. The small effect of ionic strength on these interactions suggests that electrostatic interaction contributes little to the overall stability of these complexes.

These findings have important consequences for any effort to model such interactions of antimalarial drugs with haematin under physiological conditions. Firstly, as water plays a critical role in these interactions, any successful computational model will likely have to either explicitly include solvent molecules or experimental constraints to obtain reliable structures.

Secondly, as previous SAR studies [102, 112] suggest that electrostatic and orbital interactions do appear to play a major role in the geometry of these interactions and hence in the ability of these compounds to inhibit β-haematin formation, these will need to be included in a successful computational model. Thirdly, studies in non-aqueous solvents suggest that chloroquine-Fe(III)PPIX complexes and possibly other complexes of quinoline antimalarials, if implicated, may indeed survive in the cell membrane. Fe(III) is high spin, in this state Fe(III) has five unpaired electrons (d^5). In this case the protonation state is likely to be critical in developing a useful model, as ion pairing may be important in determining the stability of the complex under these conditions. Thus any successful model will also need to consider the protonation state of both Fe(III)PPIX and drug.

CHAPTER 4

A POTENTIAL HIGH-THROUGHPUT SCREENING ASSAY FOR β-HAEMATIN INHIBITION

4.1 INTRODUCTION

As discussed in the introduction (chapter 1), one approach to the discovery of new compounds with antimalarial activity is to search for those substances that inhibit β-haematin formation. Currently there are numerous methods for detecting and measuring inhibition of β-haematin formation [44, 45, 73, 76, 161, 178-180] but most of these have certain disadvantages for high throughput screening. For example Egan et al. have used in the past an infrared based assay for detecting *β*-haematin inhibition. However, this method cannot be used for quantitating β-haematin inhibition and requires 48 hours of drying before recording infrared spectra. The BHIA assay [161] which is based on the differential solubility of haematin, but not β-haematin in DMSO requires overnight reaction and involves two centrifugation steps. The assay used for high throughput screening developed by Roche uses radio-labelled haematin which is expensive. This is an important consideration for studies relating malaria which is a predominantly a Third-world disease. Furthermore, radioactivity assays require specialized equipment for analysis and may be problematic in some countries as they have strict legislation regulating the use of radioactive materials. Other assays make use of materials that are not commercially available such as histidine rich protein or peptide bionucleating template dendrimer [178]. These assays also require between 12 and 48 hours of reaction respectively. Even the recent assay by Chong and Sullivan [108] that is compatible with high throughput screening is fairly slow (12 hours incubation). It also requires preparation of β-haematin, which though easy, is inconvenient to dispense because it is a solid material. Liquids or solutions

are more suitable for automated dispensing. Furthermore, commercially available materials are preferable.

This chapter describes the development of a cheap, reliable, simple and fast assay for β-haematin inhibition that makes use of cheap readily available UV-visible detection. The assay is based on a classical and well-known method for quantitation of haematin known as the pyridine ferrihaemochrome method. This method has in the past been used for determining haematin, both protein bound [181] and free [182]. Surprisingly, this old and established method hardly appears to have been investigated for use in studies involving β-haematin or haemozoin. The only exception is an early study in which haemozoin was shown to react with dithionite and pyridine to form a pyridine ferrohaemochrome [183].

4.2 MATERIALS AND METHODS

4.2.1 Materials

Various substituted quinolines were obtained from a library of compounds previously prepared in our laboratory [184]. All other compounds which are listed in chapter 2 were from commercial suppliers.

4.2.2 Measurements

Unsterilized U bottomed and flat bottomed Bio-ne 96 well plates were purchased from Greiger. Spectroscopic measurements on 96 well plates were carried out on an Anthos Labtec HT2 plate reader.

For X-ray powder diffraction determination, the samples were prepared using a method described previously [164], but using scaled-up quantities of reactants (180 mg of haemin and volumes scaled up accordingly). The sample was incubated for 60 minutes. The product was then quenched on ice,

filtered and washed four times with distilled water. After drying, the β-haematin was finely ground and placed in a glass sample holder.

Infrared Spectroscopy was also used to characterise β-haematin formation as described in chapter 2.

4.2.3 Preparation of 200 mM HEPES buffer stock solution

The buffer used in this work is HEPES (pH 7.5). In preparation of the stock solution, 4.776 g of HEPES was weighed out and dissolved in less than 100 ml of water. A slurry of NaOH was used to adjust the pH to 7.5. The solution was made up to 100 ml with water.

4.2.4 Preparation of 2 M HEPES buffer stock solution

23.84 g of HEPES as weighed out and dissolved in less than 50 ml of distilled water. A slurry of NaOH solution was used to adjust the pH to 8.2. The solution was made up to 100 ml with water.

4.2.5 Preparation of pyridine stock solution

Two solutions of 5% pyridine solution were prepared. In the first, 5 ml of pure pyridine was added to a 100 ml volumetric flask using a 5 ml pipette, followed by 10 ml of 200 mM HEPES (pH 7.5) buffer solution. The solution was made up to 100ml with water.

A second 5% pyridine solution was prepared in a 100 ml volumetric flask in a similar manner, but using the same volume of the 2 M, pH 8.2 HEPES buffer solution.

4.2.6 Preparation of 12.9 M sodium acetate stock solution

Acetate stock solution was prepared by dissolving 63.14 g of sodium acetate trihydrate (obtained from Sigma) in a beaker containing 47.28 ml of glacial acetic acid in a water bath thermostated at 60°C. The paste mixture was stirred vigorously with a glass rod until a clear sodium acetate solution was formed. The resulting solution was 12.9 M in sodium acetate/acetic acid with a measured pH of 5.

4.2.7 Preparation of haematin solutions

A stock solution of haematin was prepared regularly every hour by dissolving 10.9541 mg of haemin in 10 ml of 0.1 M sodium hydroxide solution, and kept in the dark. Frequent preparation of solutions is necessary as haematin is susceptible to oxidation under these pH conditions.

4.2.8 Preparation of stock solutions of drugs and related compounds

Stock solutions were prepared by weighing out required masses of each drug or related compound and dissolving in 100 μl of 1.0 M HCl or methanol in Eppendorf tubes. The concentration was determined by measuring the solution volume by sucking up the drug solution with a micro pipette and adjusting the knob to read off the approximate total volume of the drug solution. Solutions containing different concentrations were pre-prepared in Eppendorf tubes, so as to give concentrations ranging between 16.8 mM and 168 mM. When 2.02 μl is dispensed to the reaction mixture, they give 1-10 equivalents of the compound relative to haematin.

4.2.9 Inhibition of β-haematin formation by drugs and related compounds carried out in Eppendorf tubes

A 20.2 μl volume of a 1.680 mM haematin stock solution (prepared by dissolving bovine haemin in 0.1 M NaOH and used within 60 minutes of

preparation) was dispensed in each of a series of Eppendorf tubes (33.94 nmol/ Eppendorf tube) containing 2.02 μl of drug solutions (prepared by dissolving the drug in 1.0 M HCl or methanol) with concentrations predetermined to give 0 – 10 equivalents relative to haemin in the final solution. After mixing the solutions, 11.74 μl of a 12.9 M acetate solution (pH 5.0) which was pre-incubated in a thermostated water bath at 60°C was added. The final haemin concentration was 1 mM and the final solution pH was 4.5. The reaction mixtures were incubated at 60°C for 60 minutes. The mixtures were quenched at the end of the reaction by adding 900 μl of 5% (v/v) pyridine solution (0.2 M HEPES, pH 8.2) to buffer the mixtures to a final pH which ranges between 7.2 – 7.5 followed by 1100 μl of a 5% (v/v) pyridine solution (0.02 M HEPES, pH 7.5). These solutions were shaken to ensure complete dissolution of haematin and the β-haematin was allowed to settle for at least 15 minutes. The supernatants were carefully transferred to a cuvette. The data collection was carried out using a Uv-Vis spectrophotometer to measure absorbance at 405 nm. The sigmoidal dose response curve was analysed by non-linear least squares fitting to determine the number of equivalents of drug required to inhibit β-haematin formation by 50% (IC_{50}).

4.2.10 Microassay of β-haematin formation

Serial dilutions of the drug solutions were carried out in triplicate in the wells of a 96 well plate using a multichannel pipette to give concentrantions of drug solution so as to ensure that 0–10 equivalents relative to haematin were present in the final mixture. Each well contained 10.12 μl of drug solution. Then 101.2 μl of haematin stock solution (1.680 mM haematin in 0.1 M NaOH) was added to each well. After mixing the solutions, 58.7 μl of the acetate buffer (12.9 M, pH 5.0) that was pre - incubated at 60°C was added to each of the 96 wells and the plate incubated for 60 minutes at 60°C. The reaction mixtures were quenched by adding 80 μl of a 30% (v/v) pyridine solution in situ (prepared by mixing 30 ml of pyridine with 10 ml HEPES buffer (pH 7.5; 200 mM) and made to 100 ml with water). The plate was gently

agitated from side to side and then β-haematin was allowed to settle for 15 minutes. A small volume of the mixture (38 μl) was transferred to another plate and then diluted with 30% (v/v) pyridine solution to give a total of 250 μl. The data was collected using a microplate reader and analysed as described above to obtain the IC_{50}.

4.2.11 Screening of antimalarial drugs and related compounds

The screening process was carried out in duplicate with both 1 and 5 equivalents of different drugs or related compounds relative to haematin. A 20.2 μl volume of haematin stock solution (1.680 mM haematin in 0.1 M NaOH) was mixed with 2.02 μl solutions of different drugs and related compounds that were pre- prepared in Eppendorf tubes by dissolution in 1.0 M HCl or methanol. Then 11.74 μl of acetate solution (12.9 M, pH 5.0) pre-warmed in a water bath at 60°C was added to the wells. After 60 minutes of incubation at 60°C, the reaction was stopped by adding 250 μl of 12% (v/v) pyridine solution (prepared by mixing 12 ml of pyridine with 10 ml of HEPES buffer (pH 7.5; 200 mM) in a 100 ml volumetric flask and made up to 100 ml with water). After settling, supernatants were transferred to a second plate. The compounds that inhibit β-haematin formation exhibited a distinct orange-pink colour while those which do not inhibit remained clear. Detection of β-haematin inhibition was both by visual inspection and measurement of absorbance at 405 nm using a 96-well plate reader.

4.3 RESULTS AND DISCUSION

4.3.1 Association of pyridine with haematin.

Pyridine has been used to determine the concentration of haemochrome in blood [185] and from uroporphyrinogen and coproporphyrinogen [186]. It is referred to as the pyridine haemochrome method. Pyridine was used to determine the concentration of both ferrihaemochrome and ferrohaemochrome formed by interaction of amino acids and amino acid esters with haem [182]. Furthermore, it has been a classical method used in measuring haemin concentration [187] and haemoglobin concentration [181].

Figure 4.1(A) shows the spectral changes observed with increasing pyridine concentration. When hematin is dissolved in purely aqueous medium it exhibits a broad and a relatively weak Soret band that is a characteristic of an aggregated state. Addition of pyridine at pH 7.5 gives a spectrum of a bis pyridyl low spin complex implying that in this pH range, pyridine coordinates to the iron [188]. Upon addition of pyridine, the Soret band shows a red shift from 389 nm to 404 nm. The Soret band also sharpens upon titration with pyridine and becomes more intense, consistent with monomerisation of iron porphyrin. There is considerable change in the Q-band region of the spectrum which gives a signal characteristic of a low spin Fe(III)-porphyrin IX complex, namely a prominent absorption band is at 527 nm. By contrast, it was observed that at high pH values, the spectrum of haematin in aqueous pyridine shows that it promotes the formation of μ-oxo dimer which is in agreement with earlier studies [79, 88]. Thus it is essential to perform pyridine titrations in buffered solutions. A pH of 7.5 was chosen to prevent μ-oxo dimer formation and to ensure direct proportionality of absorbance to concentration. The observed change in the spectrum of haematin upon titration with aqueous pyridine is central to assaying haematin concentration [185].

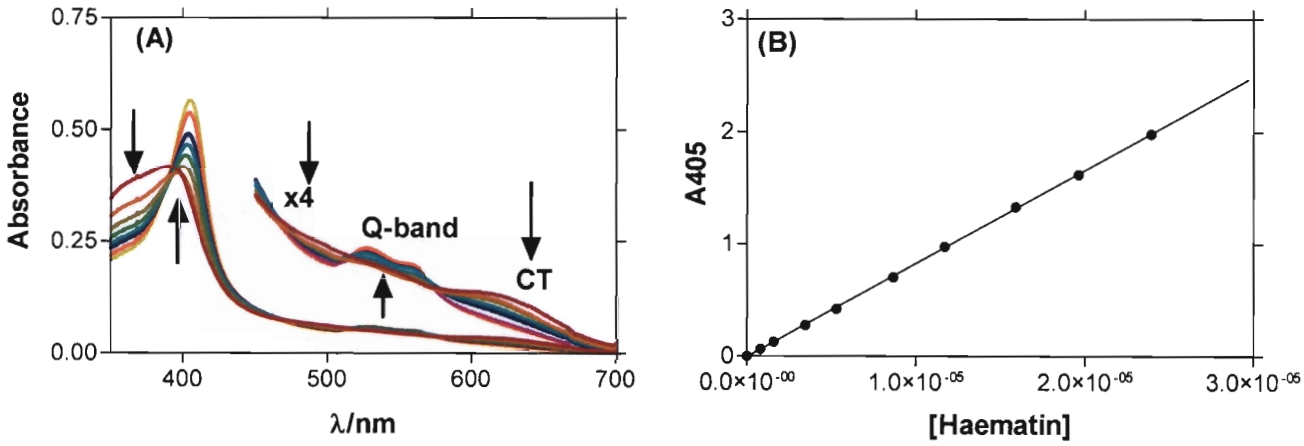

Figure 4.1 The interaction of pyridine with haematin. **(A)** Shows spectral changes due to increasing pyridine concentration on the spectrum of haematin in aqueous solution. The arrows indicate the direction of change as pyridine concentration is increased (CT- charge transfer band). **(B)** Beer's law plot of the Soret band of haematin (measured at 405 nm) in 5% (v/v) aqueous pyridine, pH 7.5 (0.020 M) (r^2 = 0.9998)

This is demonstrated in a Beer's law plot Figure 4.1(B). Such a proportionality is not observed in an aggregated state of Fe(III) porphyrin where dilution favours monomerisation while increasing concentration favours aggregation with resultant changes in extinction coefficient. Under such conditions, deviations from Beer's law are observed in porphyrins and their compounds [189]. Additional advantages owing to pyridine coordination are the red shift observed in the spectrum which is useful in minimising interference from β-hematin particles that may remain suspended in solution. Furthermore, the coordination of pyridine to the Fe(III) center can be expected to displace other molecules that might be coordinated and could give rise changes in molar extinction coefficient of the iron porphyrin making quantitation difficult. Finally, the increased intensity of the Soret band is also important as in improves the sensitivity of the assay.

4.3.2 Effect of aqueous pyridine on β-haematin and mixtures of β-haematin with haematin

In the order for pyridine to be useful in assaying inhibition of β-haematin formation, it was necessary for conditions to be found in which pyridine reacts with haematin but not β-haematin. Pure pyridine solution is capable of decomposing β-haematin to form haematin-pyridine complex because of the coordination properties of pyridine. Such behaviour has previously been observed with imidazole, a heterocycle with similar coordination properties [190]. It was found however, that aqueous solutions of pyridine between 5 and 10% (v/v) buffered close to neutral pH do not react with β-haematin. These solutions are capable of dissolving haematin and forming a complex with it. To investigate this further, mixtures of β-haematin and haematin ranging from 0% (m/m) haematin to 100% (m/m) haematin were prepared. Equal volumes of 5% (v/v) pyridine pH 7.5 (0.02 M HEPES) were added to each of the samples. The samples were shaken and the unreacted β-haematin was allowed to settle for 15 minutes by gravitation. The absorbance was read at 405 nm. Results are shown in figure 4.2. This shows a low absorbance when a sample of β-haematin is used (this absorbance probably arises from a small fraction of unconverted haematin, probably around 10% of the sample). As the percentage of haematin in the mixture increases the absorbance increases in direct proportion. And thus the absorbance can be used to quantify the percentage of haematin in the mixture.

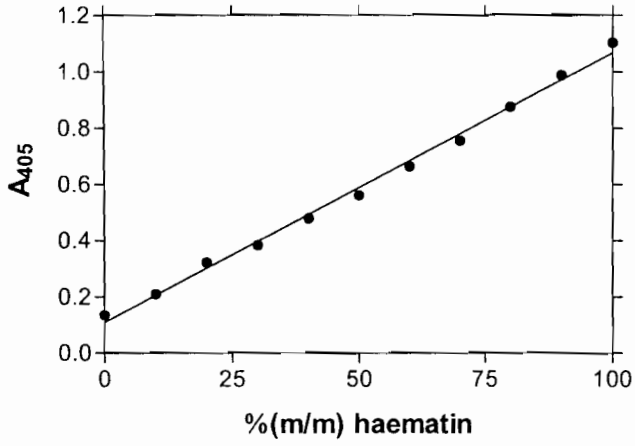

Figure 4.2 Linear dependence of the Soret band measured at 405 nm on the fraction of haematin in pre-prepared haematin/β-haematin mixtures (r^2 = 0.996). The solid material was shaken in 5% (v/v) pyridine, pH 7.5 (0.020 M HEPES) and then allowed to settle for 15 minutes before measurement of absorbance values.

4.3.3 Characterisation of the dried and wet products of the β-haematin formation process

The method used to prepare *β*-haematin was the so called thermal method in aqueous acetate solution and was described earlier [73, 191]. Egan et al. have previously demonstrated by infrared spectroscopy, Mössbauer spectroscopy [54, 191], X-ray diffraction and elemental analysis [90] that this product is *β*-haematin and is chemically and structurally identical to parasite haemozoin. The only difference that has been confirmed between materials prepared in this way and the natural product is the size of the microcrystals. These are smaller and irregular in shape, suggesting poorer crystallinity than haemozoin [90]. Given controversies over the identity of this product produced in aqueous acetate solution [192, 193], the product used in this study was characterised by X-ray diffraction as suggested by Bohle and co-workers who noted phase heterogeneity in some preparations of *β*-haematin [109]. Recent evidence shows that *β*-haematin can exist in various states of hydration [194], probably accounting for much of the controversy. The X-ray diffraction pattern is shown figure 4.3A. This pattern is identical to that reported for both lyophilised parasitized red blood cells and *β*-haematin prepared in non-

aqueous medium [39] except the peaks are broader. This broadening stems from several predictable causes. Firstly this product was characterised by conventional X-ray source, while Bohle and co-workers used synchrotron radiation to observe the diffraction pattern. Synchrotron radiation has greatly superior resolution to a conventional X-ray source. Secondly, the smaller size of β-haematin crystals formed in acetate solution causes peak broadening. Thirdly poor crystallinity of the sample may also contribute to broadening. Nonetheless, as a given diffraction pattern arises from the scattering power of the atoms making up the sample as well as their spatial arrangement in the crystal lattice [195], it provides definitive evidence for the chemical and structural identity of any crystalline solid. This diffraction pattern thus constitutes incontrovertible evidence that the solid in this case is indeed β-haematin.

It has been suggested that the process of β-haematin formation does not occur during the incubation of haematin at pH 4.5 in 4.5 M acetate solution, but rather during the drying process of the washed product of β-haematin over phosphorus pentoxide [193]. For this reason a sample of wet material from the β-haematin preparation was obtained and characterised by X-ray diffraction and IR (figure 4.3). The diffraction pattern of the wet material shows unequivocally that β-haematin is formed during the acetate incubation process and was found to be identical to that of the dried product except for a broad peak centred near a 2θ value of approximately 30^{o} (d = 2.98 Å) characteristic of the pair distribution function of water (figure 4.2B). An IR spectrum of the wet product was obtained as a Nujol mull (figure 4.3C). This was also virtually identical to that of the dried product. IR spectra obtained as Nujol mulls are unsuited to quantitation, and amounts of materials used for X-ray diffraction analysis also make accurate quantitation impractical. As a result, these observations themselves cannot preclude the possibility that additional β-haematin may be formed during drying process, but substantial amounts of β-haematin are certainly present before drying

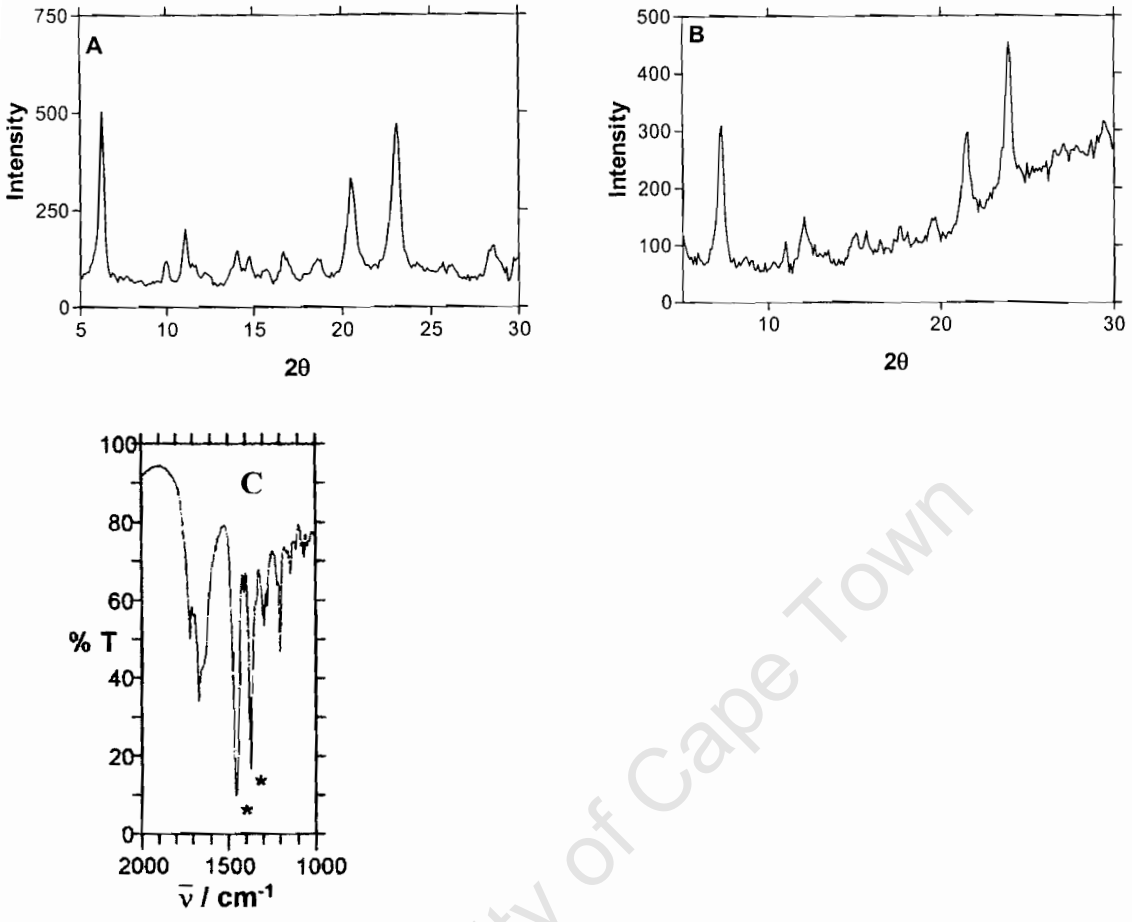

Figure 4.3 XRD pattern of **(A)** the dried product of β-haematin and **(B)** wet β-haematin obtained after 60 minutes of reaction carried out in 4.5 M acetate at pH 4.5 and 60°C. The rising background seen above 20° (2θ) was found to reach a maximum intensity at approximately 30° and is caused by H_2O. Cu Kα radiation (λ = 1.541 Å) was used in this experiment. The diffraction pattern is identical to that of dried β-haematin. IR spectrum **(C)** of the same wet material obtained as a Nujol mull. Peaks marked with asterisk are due to Nujol.

4.3.4 Measurement of β-haematin inhibition using the pyridine assay and evaluation of the assay

Having established that 5 – 10% aqueous pyridine solutions are suitable for quantitative and selective determination of haematin in haematin/β-haematin mixtures it was investigated whether they can be used to quantify inhibition of β-haematin formation. Fifteen quinoline antimalarials and related compounds

were tested (Table 4.1). The process of β-haematin formation was performed in 4.5 M acetate solution at pH 4.5 and at 60°C for one hour in Eppendorf tubes. The only difference between this method and that reported previously by Egan et al. [73] is that the reaction was allowed to proceed for one hour instead of thirty minutes and conducted unstirred. Egan et al. have shown that the rate of β-haematin formation is dependent on stirring rate with the process being slower when conducted without stirring [196], but the process nonetheless proved to be optimal under these conditions. It is possible however, that there could be some unreacted haematin remaining, even in control Eppendorf tubes. This is evident from the non-zero absorbance observed in the control sample where there is no drug added. By conducting the process in the presence of varying concentrations of drug and assaying unreacted haematin with pyridine, the IC_{50} values for the inhibition of β-haematin formation were determined. As noted in the methods, assay solutions were not filtered prior to measurement and separation of haematin from β-haematin was by gravity (centrifugation showed no change on the IC_{50} values). From here onwards this pyridine based assay is abbreviated as Phiβ (pyridine haemichrome inhibition of β-haematin).

Figure 4.4 shows typical inhibition curves obtained by fitting the data to sigmoidal dose response curves using the program GraphPad Prism [197]. The IC_{50} values were obtained from these curves (Table 4.1). Figure 4.4(G) and (H) show examples of non-inhibitors. The results were compared to those reported in the BHIA assay [113, 161] for ten of the compounds investigated.

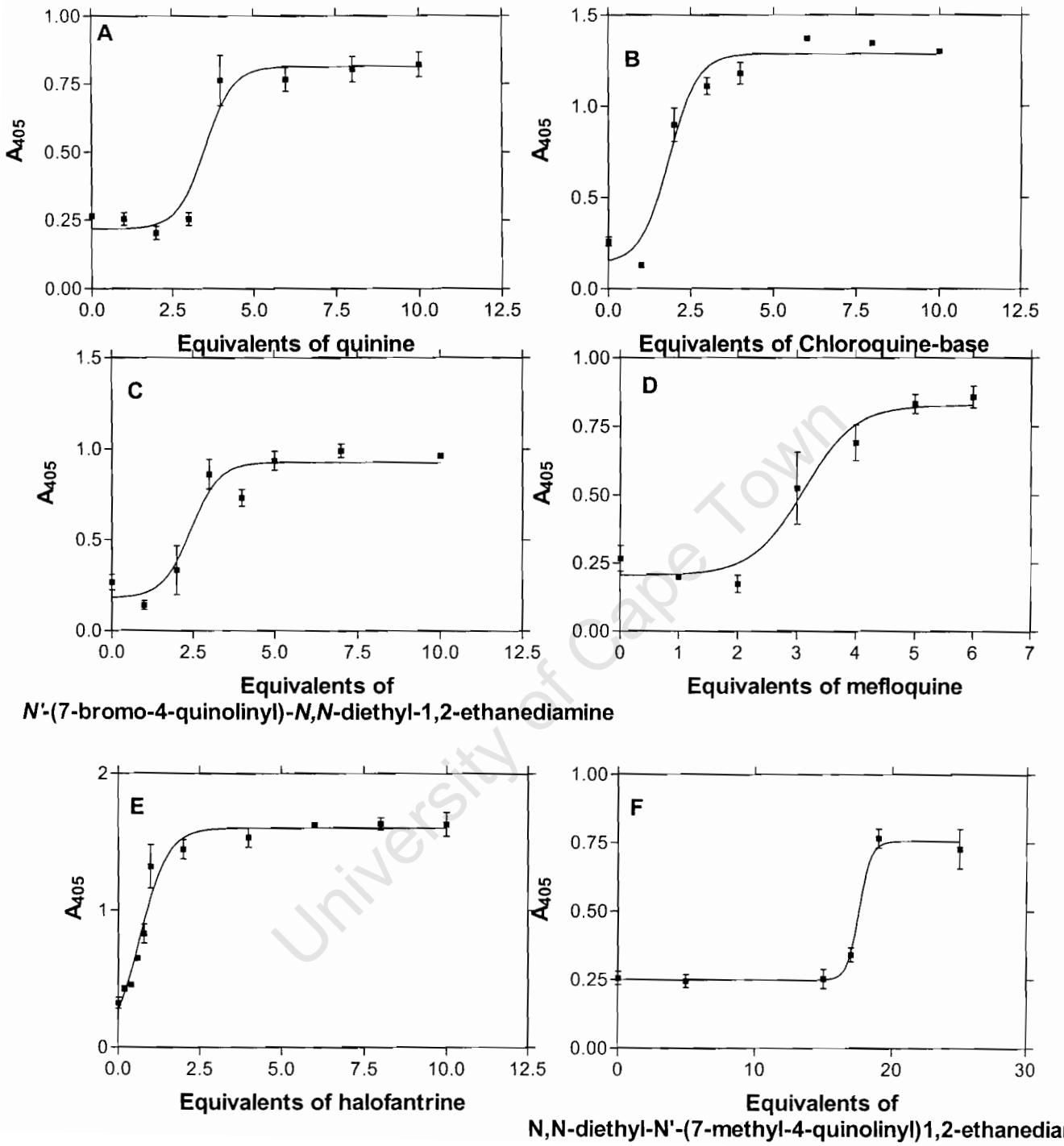

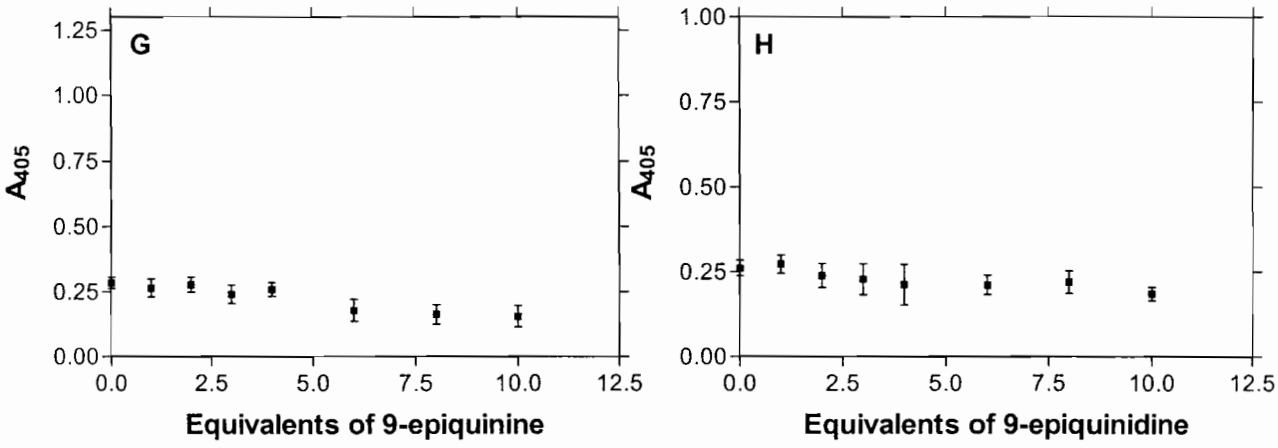

Figure 4.4 Examples of plots of absorbance versus drug concentrations fitted to sigmoidal dose response curves using non-linear least square fitting. The example shown in **(A)** is quinine **(B)** chloroquine base **(C)** N'-(7-bromo-4-quinolinyl)-N,N-diethyl-1,2-ethanediamine **(D)** mefloquine **(E)** halofantrine **(F)** N,N-diethyl-N'-(7-methyl-4-quinolinyl)-1.2-ethanediamine **(G)** 9-epiquinine and **(H)** 9-epiquinidine.

The results show a good correlation between the IC_{50} values obtained in the Phiβ and BHIA assays (figure 4.5(A)). The correlation coefficient is acceptable with an r^2 value of 0.9 (r^2 = 0.98 if open circle data points are omitted). Most deviations are within three standard errors of mean from the best fit in the BHIA IC_{50} values. Deviations are mainly a reflection of larger errors in the BHIA data. The reproducibility of repeat experiments on individual compounds was better in Phiβ assay than in BHIA assay. There are three compounds that correlated poorly when these two assays are compared (quinine, mefloquine and a short chain bromo analogue of chloroquine, compound 3 in Table 4.1 i.e. *N'* –(7-bromo-4-quinolinyl)-*N,N*-diethyl-1.2-ethanediamine)), but only mefloquine deviated by more than two standard deviations from the correlation line. This strongly indicates that these deviations stem from poor determination in the BHIA assay, rather than any systematic difference in the results of the two assays. This is further supported by the observation that the slope of the linear correlation between the two assays is unity after removal of these three points.

The results from the Phiβ assay (Table 4.1) were then compared with the data reported by Dorn et al. [74] using the haem polymerisation assay (HPA). Figure 4.5(B) shows a good correlation between the two assays. Only one compound (chloroquine) shows relatively poor agreement. With chloroquine included r^2 is 0.88 but it improved to 0.97 if chloroquine is omitted. The data point for chloroquine is not included in the correlation line shown in figure 4.5 (B). However, its value deviates from the correlation line by less than 3 standard deviations. In addition, the HPA assay reported by Dorn et al. appears to give a low IC_{50} for chloroquine. This suggests that it is an outlier in this case.

Table 4.1 Properties of quinolines and related compounds for which quantitative β-haematin inhibitory activities have been determined[a]

No.	Compound	pK_{a1}	pK_{a2}	IC_{50} for β-haematin inhibition				IC_{50} /nM[e]	VAR[f]
				Phiβ/ equiv.[b]	BHIA/ equiv.	HPA/μM[c]	HPA/ μM[d]		
1.	amodiaquine	7.08[g]	8.14[g]	1.45 ± 0.08	0.85 ± 0.25[h]	60 ± 1	15.1	7.8[d] ,—[i]	73335
2.	chloroquine	8.38[j]	10.18[j]	1.91 ± 0.3	1.63 ± 0.64[h]	45 ± 9*	24.4	14.0[d] ,38[k]	22749
3.	X = Br[l]	7.93[k]	7.97[k]	2.4 ± 0.2	4.4 ± 0.7[k]	—[i]	—[i]	—[i], *36*[k]	18308
4.	mefloquine	?[m]	9.2[n]	2.9 ± 0.1	6.18 ± 0.53[h,*]	120 ± 1	46.9	23.4[d],—[i]	157
5.	X = I[l]	7.48[k]	8.83[k]	3.0 ± 0.1	2.8 ± 0.2[k]	—[i]	—[i]	—[i] ,35[k]	13566
6.	quinine	4.12[j]	8.58[j]	3.5 ± 0.2	5.48 ± 1.31[h]	160 ± 10	64.8	34.2[d], —[i]	161
7.	X = Cl[l]	7.56[k]	7.79[k]	3.6 ± 0.2	2.2 ± 0.2[k]	—[i]	—[i]	—[i],37[k]	12783
8.	X = F[l]	7.62[k]	9.24[k]	8.9 ± 0.5	9.7 ± 0.8[k]	—[i]	—[i]	—[i],138[k]	15649
9.	X = CF_3[l]	7.50[k]	7.65[k]	9.9 ± 0.2	8 ± 2[k]	—[i]	—[i]	—[i],99[k]	11265
10.	X = CH_3[l]	8.12[k]	9.51[k]	17.6 ± 0.2	17 ± 4[k]	—[i]	—[i]	—[i],82[k]	21082
11.	pyronaridine	?[m]	?[m]	0.67 ± 0.1	—[i]	30 ± 2	64.4*	5.7[d], —[i]	?
12.	halofantrine	10.0[n]	NA[o]	0.168 ± 0.002	—[i]	30 ± 2	84.5*	5.8[d], —[i]	158
13.	quinidine	4.42[j]	8.58[j]	1.5 ± 0.1	—[i]	—[i]	24.0	21.5[d], —[i]	173
14.	9-epiquinine	9.54[j]	4.08*j*	>10	>10	—[i]	—[i]	3471[p] 1179[q]	169.2
15.	9-epiquinidine	9.39[j]	4.15[j]	>10	>10	—[i]	—[i]	2700[p] 1024[q]	170.8

[a]* represents reported β-haematin inhibitory data that are odds with ranking of at least two other independent investigations; [b]This study ± standard error of mean on three determinations; [c]From Dorn et al. [74]; [d]From Hawley et al. [75]; [e]In vitro antimalarial activity for 3D7 and D10 strains respectively; [f]Calculated vacoular accumulation ratio based on pH trapping and assuming a FV pH of 5.2 and external pH of 7.4 [113]; [g]From Hawley et al. [198]; [h]From Parapini et al. [161]; [i]not investigated ; [j]From Warhurst et al. [199]; [k]From Kaschula et al. [113]; [l]N,N-diethyl-N'-(7-X-4-quinolinyl)-1,2-ethanediamine; [m]unknown; [n]Calculated value obtained using ADME Boxes software; [o]Not applicable, [p] and [q]IC_{50} for chloroquine sensitive and chloroquine resistant parasites respectively [199].

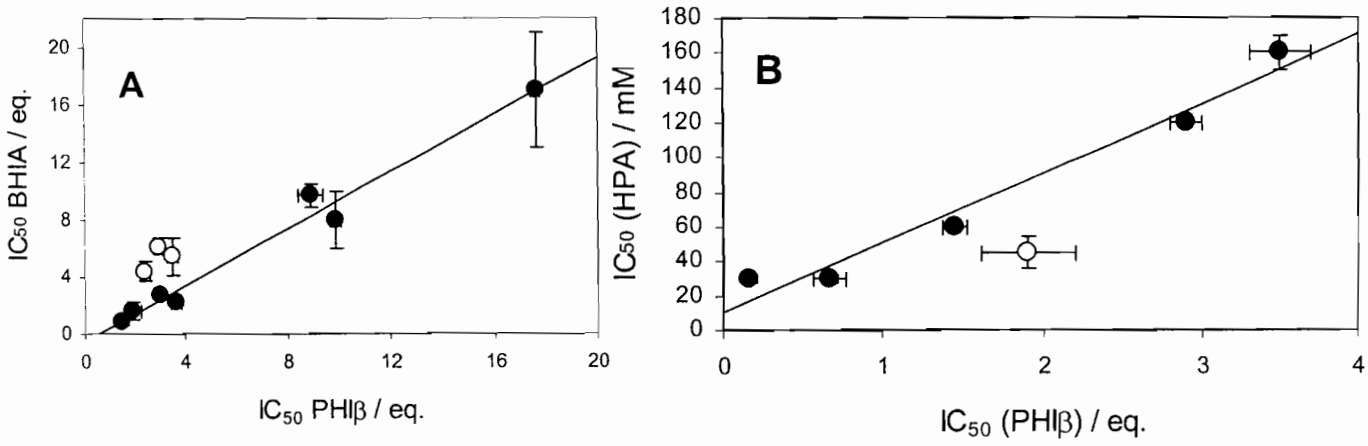

Figure 4.5 The Phiβ IC_{50} values for β-haematin inhibition by quinoline antimalarials and related compounds with known in vitro antimalarial activity correlated with IC_{50} values reported in other studies. The error bars represent the standard error of the mean on three determinations for compounds, referred to in Table 4.1. **(A)** Correlation of the IC_{50} values obtained from the Phiβ assay with those reported using so called BHIA assay. The regression line is obtained using data points represented by black circles. The open circles represent probable outliers, in this case compounds 3, 4 and 6 in Table 4.1. The errors in the BHIA assay are quite large so that these points lie within 2 standard errors of the correlation line for 3 and 6. Excluding the data represented by open circles $r^2 = 0.98$. If all data points are used in the correlation $r^2 = 0.90$. The correlation line shown permits conversion from Phiβ IC_{50} to BHIA IC_{50} using the equation IC_{50} (BHIA) = IC_{50} (Phiβ) -0.63. **(B)** Correlation of Phiβ IC_{50} values with IC_{50} values for β-haematin inhibition by the so -called haem polymerisation assay (HPA) as reported by Dorn et al. [74]. The solid line is a linear regression obtained using the data points shown in black. The open circle represents a probable outlier. The value of r^2 is 0.97 if the outlier is excluded and 0.88 if it is included. Error bars represent one standard error of the mean on three determinations in the Phiβ data and three standard deviations in the HPA data. The correlation line permits conversion of Phiβ IC_{50} values to HPA IC_{50} values (in μM) according to the equation IC_{50}(HPA) = 39.9μM x IC_{50}(Phiβ) + 10.6μM

Hawley et al. [75] used a slightly modified version of the HPA assay to measure β-haematin inhibitory activity of 27 compounds. Seven of these measurements were for compounds used in this study. Two of these compounds, halofantrine and pyronaridine, were found to correlate poorly.

Both were reported to give high IC_{50} values by Hawley et al. [75] which does not agree with results obtained by Dorn et al. [74] for these compounds using the same assay. Results from Dorn et al. showed halofantrine and pyronaridine to be the strongest inhibitors [74]. The Phiβ assay confirmed that halofantrine is indeed one the strongest inhibitors of β-haematin formation. It is difficult to be certain of the origin of the contradictory findings of Hawley et al. for halofantrine and pyronaridine, but their weak activity may stem from poor water solubility, which is exceptionally low in the case of halofantrine. Figure 4.6(A) shows that the correlation line between the data reported by Hawley et al. and the Phiβ assay for the five remaining compounds is excellent (r^2 = 0.97) [75]. All points are within one standard error of the correlation line. Chong and Sullivan have recently reported a new assay for β-haematin inhibition involving growth of β-haematin onto pre-formed *β*-haematin crystallites [108], but only four quinoline antimalarials were reported. These give a good correlation with the data from the Phiβ assay with r^2 = 0.999 (figure 4.6(B)). The data available for comparison all show excellent agreement in relative strength of *β*-haematin inhibition between the Phi*β* assay and other β-haematin inhibition assays. Indeed, the Phiβ assay appears to correlate well with the other assays, even when there is disagreement between them (Table 4.1), usually agreeing with the consensus values for the remaining assays. Direct quantitative comparison can be made with the BHIA and HPA assays, allowing conversion of Phi*β* values to BHIA and HPA values.

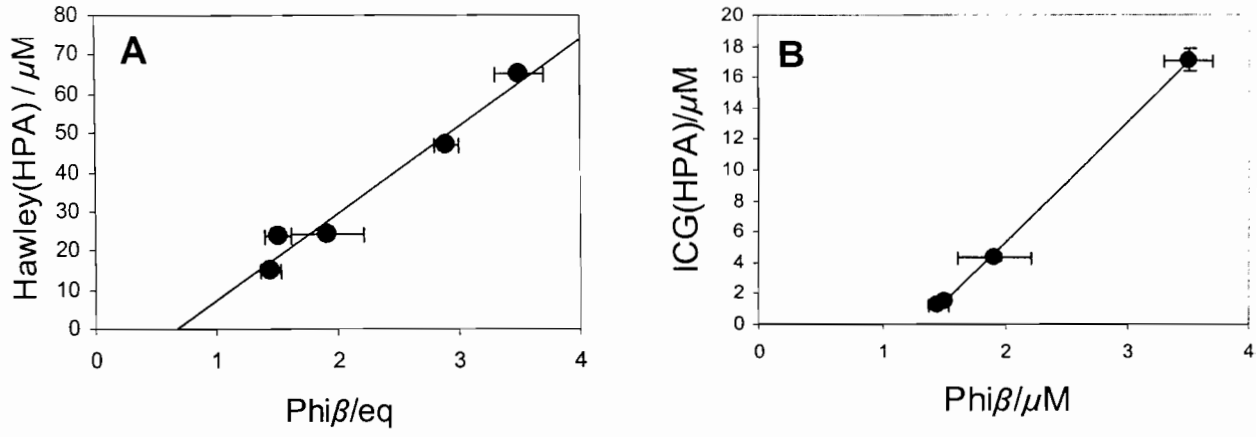

Figure 4.6 The IC_{50} values for β-haematin inhibition by quinoline antimalrials and related compounds with known in vitro antimalarial activity correlated with IC_{50} values reported in other studies. **(A)** Correlation of the IC_{50} values obtained from the Phiβ assay with those reported by Hawley et al. [75], using the so-called haem polymerisation assay (HPA)(r^2 = 0.97). **(B)** Correlation of Phiβ IC_{50} values with IC_{50} values obtained using inhibition of crystal growth (ICG) assay reported by Chong and Sullivan [108] (r^2 = 0.999).

4.3.5 The Phiβ assay conducted in 96 well plates

The results shown above demonstrate that the Phiβ assay requires no centrifugation and requires only one hour of incubation time. It thus has a considerable advantage over all of the prevoiusly reported assays. For improved throughput however, it was necessary to adapt the method for use in 96-well plates. The quantitative study of β-haematin inhibition in 96-well plates, uses approximately 10 micromole of each compound.

Figure 4.7 shows plots of absorbance versus equivalents of drugs obtained in 96-well plates. The absorbance was measured at 405 nm, and the IC_{50} was obtained by fitting the data using non-linear least squares fitting to a sigmoidal dose response curve. The low absorbance observed at saturation in the dose response curve in figure 4.7(D), is due limited solubility of pyronaridine-haematin complex. This does not appear to interfere with the IC_{50} value.

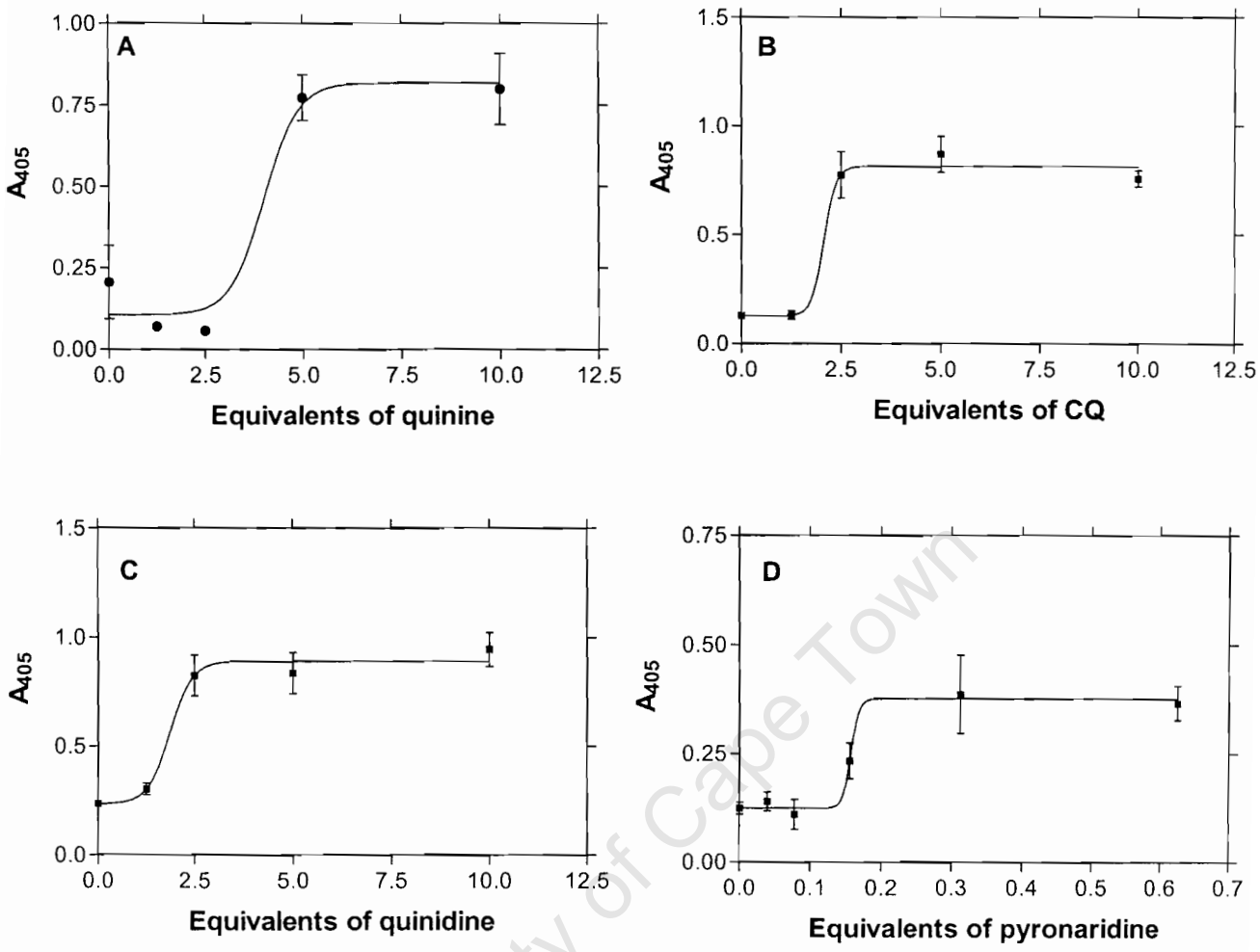

Figure 4.7 Examples of sigmoidal dose response curves obtained from a plot absorbance versus concentration using 96 well plates. **(A)** quinine; **(B)** chloroquine; **(C)** quinidine and **(D)** pyronaridine

Figure 4.8 shows the observed correlation between results produced by the Eppendorf method with that of the 96-well plate method. Results are essentially identical. The slope of the plot is 1 and the intercept zero within the limits of the scatter. The slightly larger standard errors in the values obtained using the 96 well plate format were found to be due to the fact that there were fewer data points obtained in the region of maximum curvature. This is because of the use of serial dilution, rather than evenly spaced points used in the 96 well plate, but not in the Eppendorf format.

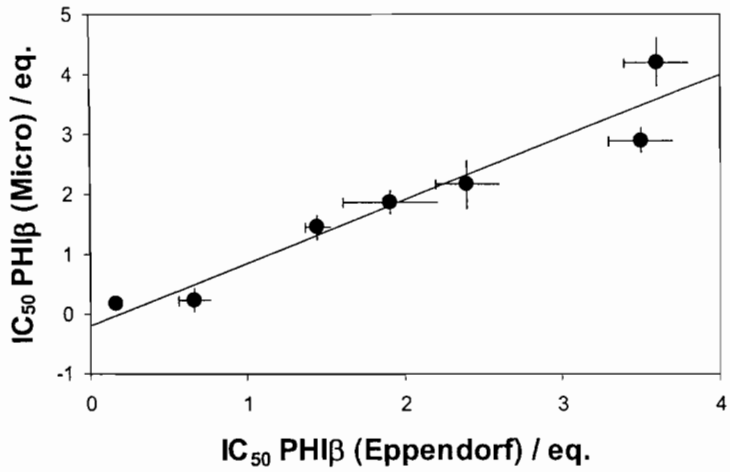

Figure 4.8. The correlation between Phiβ IC_{50} values obtained using 96 well plates (indicated as "micro") with those obtained using the Eppendorf method (r^2 = 0.92). The slope and intercept lie within one standard deviation of unity and zero respectively.

4.3.6 Potential for high-throughput screening

The quantitative determination of β-haematin inhibitory activity described above for use in 96 well plates can only be used to determine six compounds per plate if done in triplicate. This is suitable for medium throughput screening. For high throughput screening, it is not probably necessary to obtain IC_{50} values for inhibition of β-haematin formation. It is likely to only be necessary to find compounds that show inhibitory activity below a certain cut-off concentration. The choice of the cut-off value is somewhat arbitrary, but a value of 5 equivalents of the drug relative to haematin was chosen for this study. This corresponds to 200 μM in the HPA assay. A large variety of known antimalarial compounds that have been proposed to inhibit β-haematin formation appear to have IC_{50} values below this cut-off value [74, 75, 108, 161], whereas compounds with weak inhibitory activity and with poor biological activity lie above this value [113]. The advantage of using the Phiβ assay in this way is that it can be used to screen 96 compounds per plate per hour. In this study 47 known compounds, including 4-aminoquinoline

antimalarials and related 4-aminoquinolines that have been shown previously to inhibit β-haematin formation, quinoline methanol antimalarials and non-antimalarial quinolines known not to inhibit β-hematin formation, related antimalarials, salts previously found to interfere with the HPIA assay [119, 161] and common solvents that are likely to be used to solubilize hydrophobic compounds were investigated (scheme 4.1). One well was used as a control for β-haematin formation. The same compounds were also tested at one equivalent relative to haematin for comparison. After one hour of the incubation time and the addition of aqueous pyridine solution to the wells, the inhibitors of β-haematin could be identified by visual inspection (figure 4.9) or by using a 96 well plate reader (Table 4.2). In this study, a cut-off absorbance value of 0.250 was found to be suitable for detecting inhibitors with the plate reader. This value clearly distinguished the β-haematin formation inhibitors from the non-inhibitors. The method is well suited to high throughput screening and is easy to handle. It should be easily adapted for automated techniques, as no centrifugation is required and detection can be done in situ. Detection can be either by visual inspection using digitally captured images or by spectrophotometric measurements.

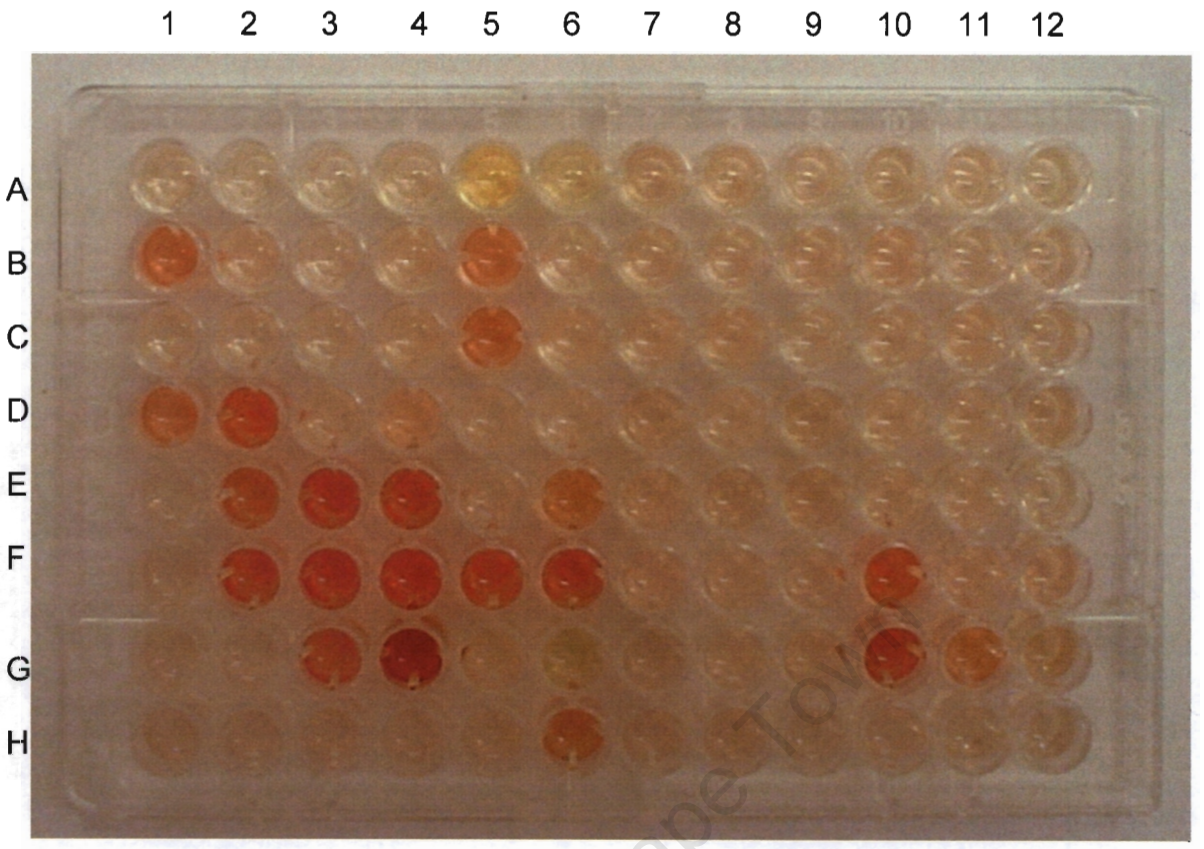

Figure 4.9 A digital photograph of a 96-well plate in which the β-haematin formation process has been conducted in the presence of quinoline antimalarials, quinoline analogues, and various salts at 5 rquivalents relative to haematin and solvents (shown in the left wells). The same materials present at 1 equivalent are shown in the right wells of the plate. See Table 4.2 and scheme 4.1 for compound identities.

This screening assay conducted at 5-equivalents relative to haematin successfully identified all the compounds that inhibit β-haematin formation except halofantrine. But inhibition halofantrine is observed when the assay is performed at one equivalent relative to haematin. This can be traced to the poor water solubility of halofantrine, which appears to trap unreacted haematin in the solid state when present at 5 equivalents. No false positives were observed in the case of compounds that are known to be incapable of inhibiting β-haematin formation. No evidence of the interaction of pyridine and test compound. Even the common salts do not interfere with the assay. A repeat of the assay produced the same observations.

The compound in well 6C was expected to give a positive result based on previous infrared evidence indicating β-haematin inhibition at four equivalents relative to haematin [112]. After observing no activity in the screening assay the quantitative β-haematin inhibition activity of this compound was investigated using the Phi*β* assay. An IC_{50} of 6.7 ± 0.2 equivalents was observed, which confirms the accuracy of the screening result (figure 4.10). A similar discrepancy has previously been noted between the Infrared assay and BHIA assay with the compound in well 5E. This also gave a positive infrared result at 4 equivalents relative to haematin, but has a value of 8 equivalents [113] in the BHIA assay. That latter result is confirmed by the Phiβ assay in Table 4.2.

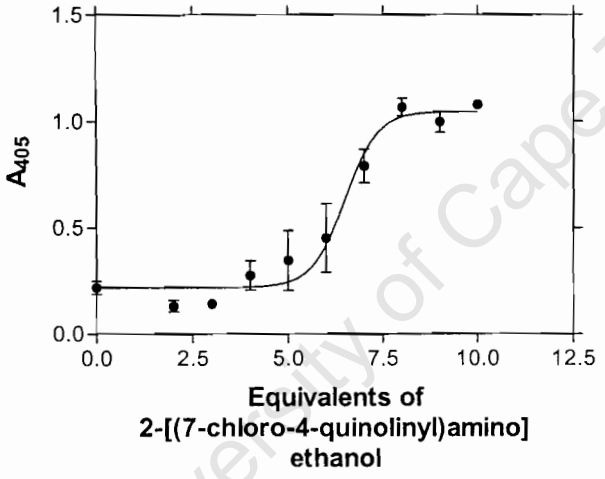

Figure 4.10 Shows a plot of absorbance versus the drug concentration fitted to a sigmoidal dose response curve using non-linear square fitting. The example is 2-[(7-chloro-4-quinolinyl)amino]ethanol with an IC_{50} value of 6.7 ± 0.2

Table 4.2 compounds used in high throughput screening mode in figure 4.6. The positive and negative signs in parenthesis indicate expected β-haematin inhibition based on previous observations. Numbers indicate A_{405} in the plate reader (boldface if >cut-off A of 0.250)

	1	2	3	4	5	6
A	Quinoline (-[a],0.083)	2-quinolinamine (-[a],0.070)	3-quinolinamine (-[a],0.073)	4-quinolinamine (-[a],0.083)	5-quinolinamine (-[a],0.105)	6-quinolinamine (-[a],0.071)
B	7-chloro-*N*-methyl-4-quinolinamine (+[a],**0.492**)	4.7-dichloroquinoline (-[a],0.098)	*N*-methyl-4-quinolinamine (-[a],0.0669)	*N*-methyl-2-quinolinamine (-[a],0.079)	7-chloro-4-quinolinamine (+[a],**0.711**)	*N*-4-quinolinyl-1,2-ethanediamine (-[a],0.130)
C	2-(4-quinolinylamino)-ethanol (-[a],0.072)	*N*,*N*-diethyl-*N*'-4-quinolinyl-1,2-ethanediamine (-[a],0.074)	*N*-[2-(4-quinolinylamino) ethyl]acetaminde (-[a],0.072)	*N*-2-quinolinyl-1.2-ethanediamine (-[a],0.082)	*N*-(7-chloro-4-quinolinyl)-1,2-ethanediamine (+[a],**0.513**)	2-[(7-chloro-4-quinolinyl)amino]ethanol (+[a],0.180)
D	*N*'-(7-chloro-4-quinolinyl)-*N*,*N*-dimethyl-1,2-ethanediamine (+[a],**0.517**)	7-chloro-*N*-propyl-4-quinolinamine (+[b],**0.475**)	N^4-[2-(diethylamino)ethyl]-4,7-quinolinediamine (-[c],0.194)	Dimethylsulfoxide (-[d],0.109)	*N*,*N*-diethyl-*N*'-(7-methoxy-4-quinolinyl)-1,2-ethanediamine (+[c],0.107)	*N*,*N*-diethyl-*N*'-(7-methyl-4-quinolinyl)-1,2-ethanedimamine (-[c],0.084)
E	*N*,*N*-diethyl-*N*'-(7-fluoro-4-quinolinyl)-1,2-ethanediamine (-[c],0.067)	*N*'-(7-chloro-4-quinolinyl)-*N*,*N*-diethyl-1,2-ethanediamine (+[c],**0.499**)	*N*'-(7-bromo-4-quinolinyl)-*N*,*N*-diethyl-1,2-ethanediamine (+[c],**0.450**)	*N*,*N*-diethyl-*N*'-(7-iodo-4-quinolinyl)-1,2-ethanediamine (+[c],**0.415**)	*N*,*N*-diethyl-*N*'-[7-trifluoromethyl)-4-quinolinyl]-1,2-ethanediamine (-[c],0.145)	*N*,*N*-diethyl-*N*'-(7-nitro-4-quinolinyl)-1,2-ethanediamine (+[c],**0.333**)
F	8-quinolinol (-[e],0.110)	Chloroquine phosphate (+[f],**0.565**)	Chloroquine base (+[d],**0.728**)	Amodiaquine dihydrochloride (+[d],**0.391**)	Quinine sulphate (+[e],**0.401**)	Quinidine sulphate (+[f],**0.300**)
G	9-epiquinine hydrochloride (-[e],0.103)	9-epiquinidine hydrochloride (-[g],0.084)	Mefloquine hydrochloride (-[f],**0.400**)	Pyronaridine (+[h],**0.888**)	Halofantrine hydrochloride (+[f],0.085)	Primaquine diphosphate (-[e],0.209)
H	Sodium chloride (-[d],0.097)	Sodium hydrogen phosphate (-[d],0.111)	Sodium hydrogen sulphate (-[d],0.053)	Negative control (0.055)	Methanol (-[d],0.0470)	*N*-{2-[(7-chloro-4-quinolinyl)amino]ethyl}-2-(4-methyl-1-piperazinyl)acetamide (+[i],**0.613**)

[a]Egan et al. [112]; [b]Kaschula [184]; [c]Kaschula et al. [113]; [d]Parapini et al. [161]; [e]Egan et al. [73]; [f]Egan et al.; [90] [g]Mavuso [164]; [h]unpublished observations;

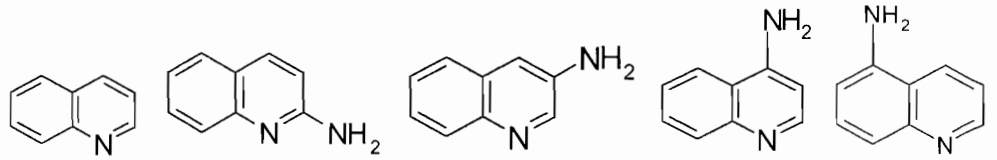

1A **2A** **3A** **4A** **5A**

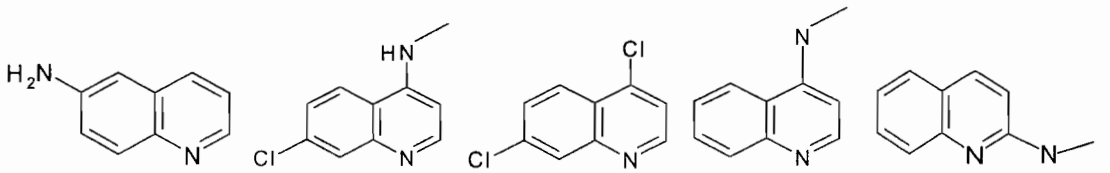

6A **1B** **2B** **3B** **4B**

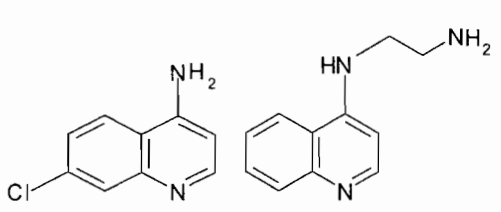

5B **6B** **1C** **2C**

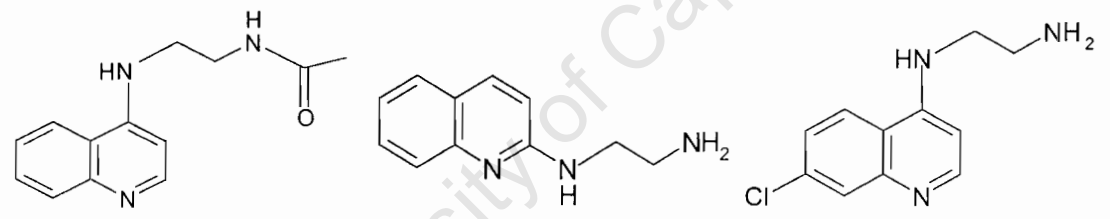

3C **4C** **5C**

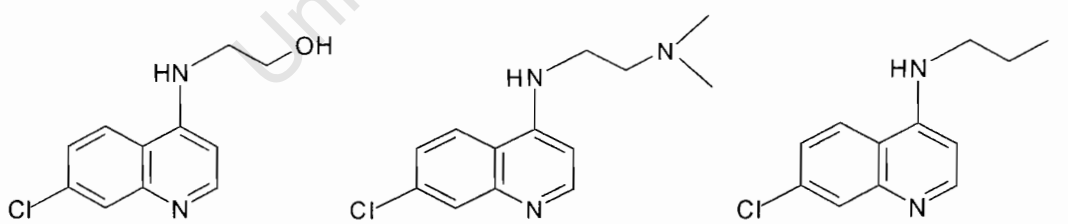

6C **1D** **2D**

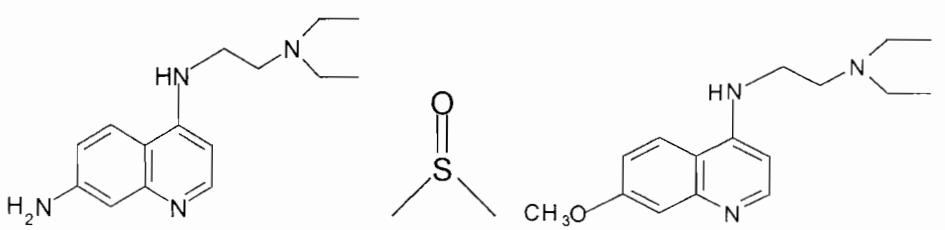

3D **4D** **5D**

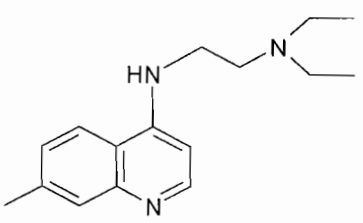

6D

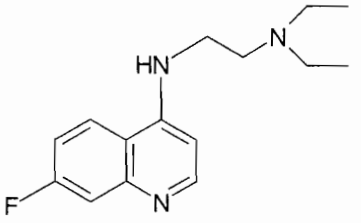

1E

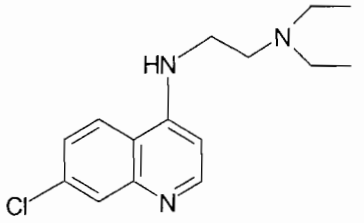

2E

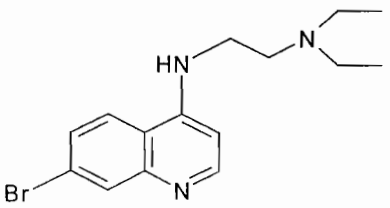

3E

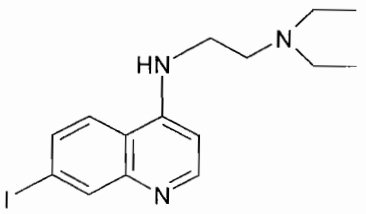

4E

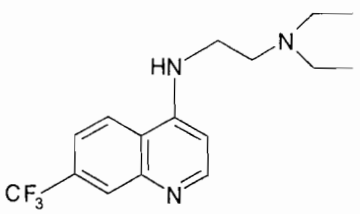

5E

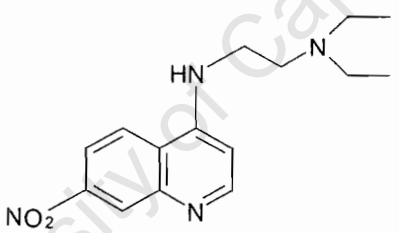

6E

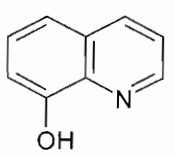

1F

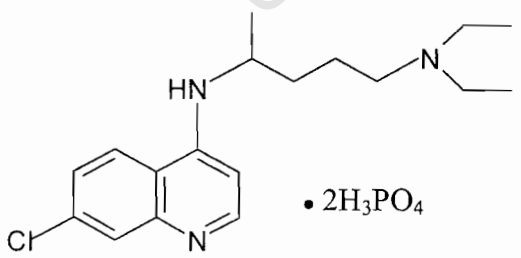

2F

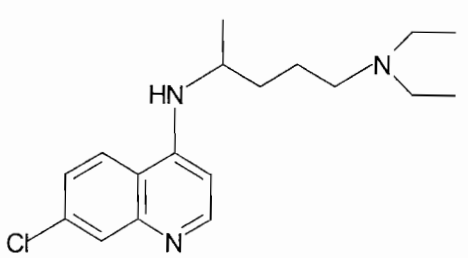

3F

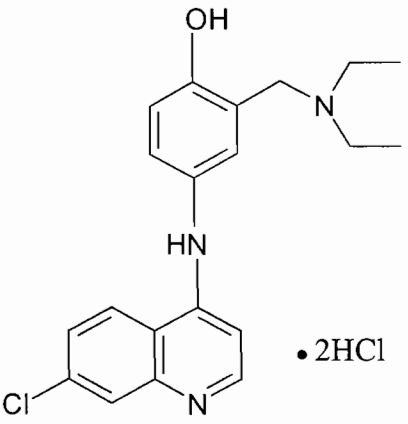

4F

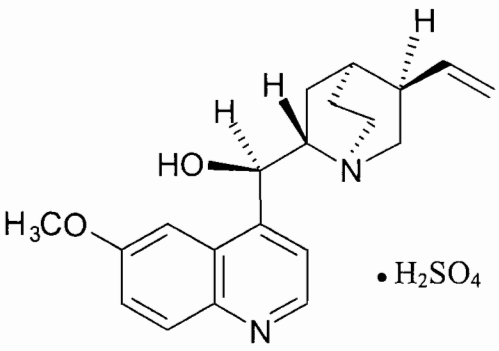

5F

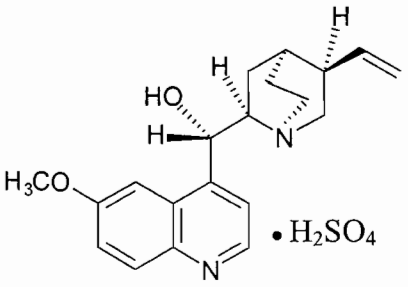

6F

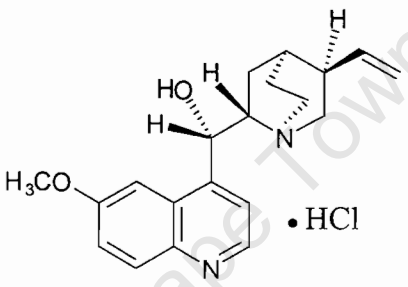

1G

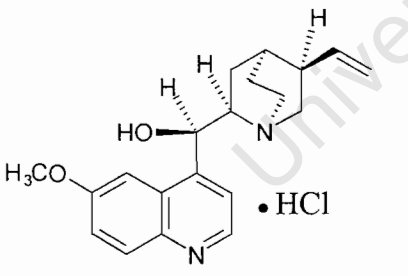

2G

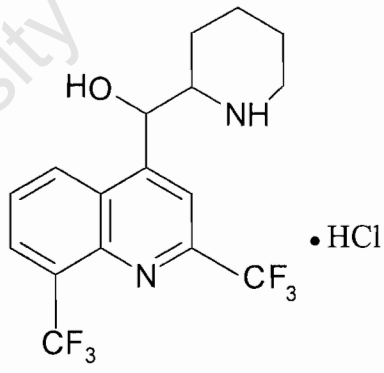

3G

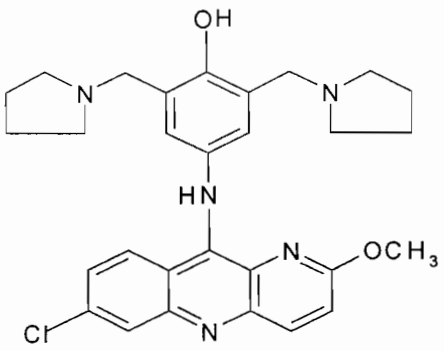

4G

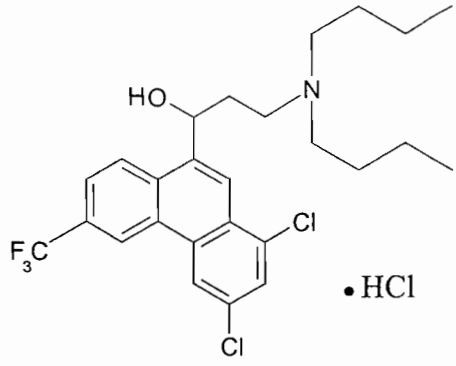

5G

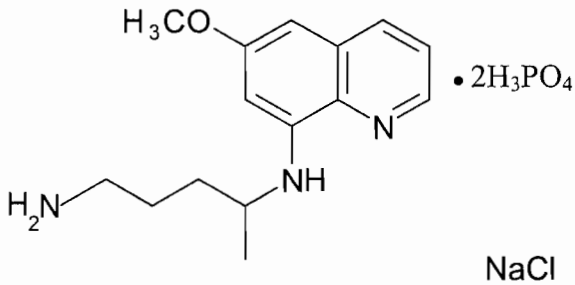

6G

NaCl	$NaHPO_4$	$NaHSO_4$	H_2O	CH_3OH
1H	**2H**	**3H**	**4H**	**5H**

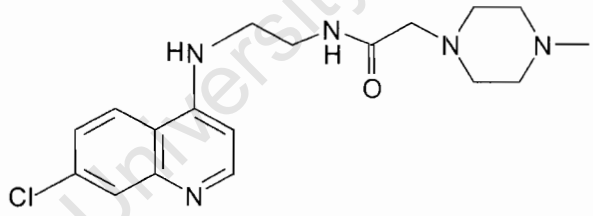

6H

Scheme 4.1 Structures of quinoline and other compounds, salts and organic solvents used for high-throughput screening in the 96 well-plate are shown in figure 4.6. The number of the compounds corresponds with the wells in figure 4.8. The name of the compound is given in table 4.2

4.3.7 Correlation of β-haematin inhibition with biological activity

IC_{50} values for β-haematin inhibition for a wide range of antimalarial and antiplasmodial compounds have been collected. Thus it was investigated whether there is a correlation between β-haematin inhibitory strength and biological activity.

Figure 4.11(A) shows the correlation between biological activity for chloroquine sensitive parasites and IC_{50} values from Phiβ assay. There is a significant increase in biological activity as the ability of compounds to inhibit β-haematin formation increases (P = 0.0005). The biological activity data used in the correlation were from two different sources (Table 4.1) and so each subset of data was also separately correlated. The Phiβ data correlates with biological activity data reported by Kaschula et al. [113] (P = 0.018, r^2 =0.71, n = 7) and by Hawley et al. (P = 0.025, r^2 = 0.67, n = 7) [75]. Figure 4.11(B) also shows a good correlation with vacuolar accumulation normalised activity [113] (P=0.0042, r^2=0.62, n=11 with mefloquine and pyronaridine omitted as pK_a values are not available). However, the correlation is not as good as that in figure 4.10(A). If the vacuolar accumulation ratio is used together with the IC_{50} from the Phiβ assay in multiple correlation as seen in figure 4.11(C), P<0.0001 and r^2=0.84, n=11. This confirms that vacuolar accumulation is critically important, but suggests that vacuolar accumulation probably does not play as big role in activity as previously thought. Nonetheless, in all cases activity is strongly correlated with β-haematin inhibition, confirming that knowledge of such activity is a good indicator of in vitro antimalarial activity.

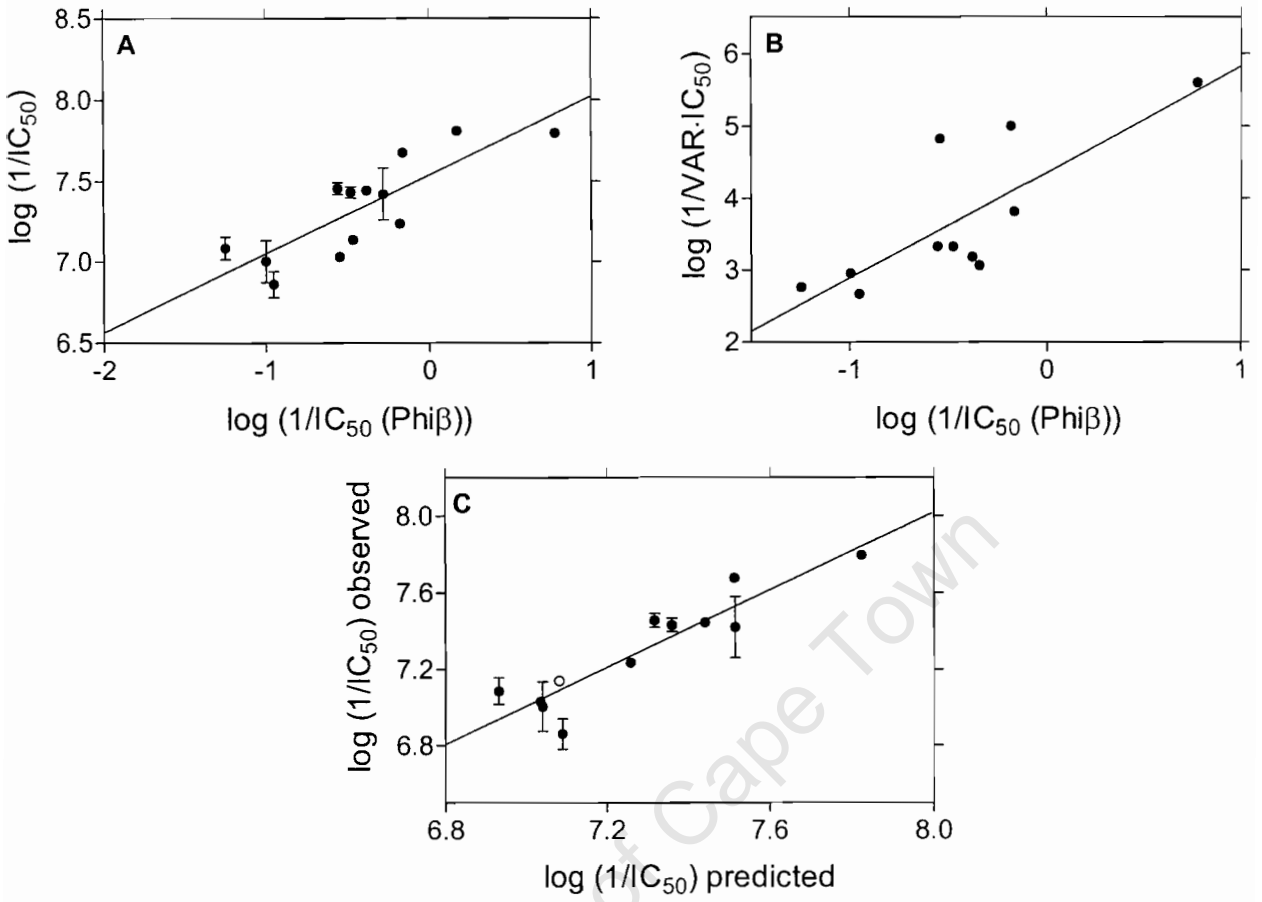

Figure 4.11 (A) Correlation between biological activity (IC_{50}) for chloroquine sensitive parasites and IC_{50} values for β-haematin formation from the Phiβ assay. **(B)** Shows a good correlation with vacoular accumulation normalised activity [113] (P = 0.0042, r^2 = 0.62, n = 11). Mefloquine and pyronaridine were omitted as pK_a values were not available. **(C)** Shows observed biological activity compared with that predicted on the basis of the vacuolar accumulation ratio together with IC_{50} from the Phiβ assay in multiple correlation analysis. The P value is less than 0.0001 and r^2 = 0.84, n = 11, (F =21.3 > F_{crit} = 8.65 at 99% confidence level). This indicates that vacuolar accumulation probably does play a role in activity. As observed in all cases biological activity correlated strongly with β-haematin inhibition. The open circle represents the estimated value for mefloquine.

4.4 CONCLUSIONS

The interaction of aqueous pyridine with haematin produces a spectrum that shows excellent properties that can be used to determine haematin concentration because the absorbance increases in direct proportion with the concentration of haematin. The pyridine solution is unable to disrupt β-haematin, but can dissolve haematin in a mixture of the two. This allows aqueous pyridine solution to be used as an assay method for determination of unreacted haematin present when *β*-haematin inhibition occurs. This assay provides β-haematin inhibitory activity data that correlated well with reported data obtained by other methods. In addition the pyridine based assay correlates well with the consensus order where there is disagreement in the data between the different existing assays.

For β-haematin inhibitory activity, the pyridine based assay has an advantage of being fast, requires no centrifugation and involves easy detection methods. The assay uses cheap materials and is suitable for use in small laboratories especially in Third World countries. Two problems that are likely to be encountered in this Phiβ assay are that the low water solubility of some compounds appear to prevent solubilisation of haematin in aqueous pyridine medium. False negative results may be obtained in such cases. Preliminary investigations suggest that inclusion of organic solvents may be able to alleviate the problem. Coloured compounds can also interfere with the assay, but this can be solved by carrying out blank measurements.

Correlation of the observed β-haematin inhibitory activity with biological activity of compounds investigated in this study suggest that discovery of new antimalarials of this class partly reduces to finding compounds capable of inhibiting β-haematin formation, validating the assay as a screening method for discovering new antimalarials.

CHAPTER 5

EFFECT OF QUINOLINE ANTIMALARIALS ON THE RATE OF β-HAEMATIN FORMATION

5.1 INTRODUCTION

Studies conducted over the years (see chapter 1) have shown that antimalarial drugs chloroquine, amodiaquine and quinine inhibit β-haematin formation, and have suggested that these may act in the malaria parasite by inhibiting haemozoin formation via complexation with Fe(III)PPIX [90]. In early studies carried out by Egan et al. it was shown that incubation of haematin in acetate solution for 30 minutes in the presence of 3 molar equivalents of these drugs relative to haematin lead to absence of the characteristic peaks of *β*-haematin at 1210 cm^{-1} and 1660 cm^{-1} in the infrared spectrum [73].

The formation of *β*-haematin from haematin appears to be a thermodynamically spontaneous process under acidic conditions, which requires a suitable catalyst (for example acetic acid when prepared synthetically in aqueous medium) [73, 191, 196]. There is no evidence that this product spontaneously converts back to haematin to any measurable extent under acidic conditions. Thus this process is probably thermodynamically irreversible. In contrast, the interaction of chloroquine and related compounds with haematin and possibly with the surface of the *β*-haematin crystal [111] is a reversible equilibrium process [86]. This suggests these drugs are unlikely to be able to thermodynamically block *β*-haematin formation.

In the present study the newly developed method of analysis of inhibition of *β*-haematin formation which employs 5% (v/v) pyridine solution was used to demonstrate that these quinoline antimalarials slow down but do not in fact prevent the process of *β*-haematin formation.

5.2 MATERIALS AND METHODS

All materials used in this study are as described in chapter 2. The compounds investigated are chloroquine, amodiaquine, quinine and quinidine.

5.2.1 Measurement of the inhibition of β-haematin formation by assaying in Eppendorf tubes

The inhibition of *β*-haematin formation was measured in Eppendorf tubes as described in chapter 4 (section 4.2.7) except that the reactions were allowed to proceed for between1 and 24 hours.

5.2.3 Analysis of results

The results were analysed using the same method indicated in chapter 4 (section 4.2.7)

5.2.4 Inhibition of β-haematin formation monitored by IR and XRD

A product was prepared by dissolving 75 mg of haemin in 15 ml of 0.1 M NaOH in a reaction vessel. The solution was allowed to stand for 5 minutes at 60^{o}C for complete dissolution of haemin. A 1.5 ml volume of 1.0 M HCl was added to the solution of haematin. After 3 minutes, 3 or 5 molar equivalents of chloroquine, or quinine relative to haematin were added and dissolved, followed by 8.7 ml of a 12.9 M acetate buffer solution (preparation described in section 4.2.4), pre-incubated under the same conditions, so that the final acetate concentration is 4.5 M. The mixture was incubated for 1 to 24 hours. The reaction was stopped by diluting with cold water and cooled on ice for 5 minutes. The solid material was collected by filtration on a cellulose nitrate disc (0.22 μm) and washed extensively with water and dried over silica gel and phosphorus pentoxide. The product was analysed by X-ray diffraction and

FTIR spectroscopy. Conditions and equipment used for IR and XRD are described in chapter 2 (section 2.3.3 and 2.3.4)

5.3 RESULTS AND DISCUSION

5.3.1 Effect of incubation time on β-haematin inhibition by chloroquine monitored by the Phiβ assay

The inhibition of the β-haematin formation process was conducted unstirred in 4.5 M acetate solution at pH 4.5 and 60°C in Eppendorf tubes (2 ml) for 1 to 24 hours. Sigmoidal dose response curves for inhibition of *β*-haematin formation by amodiaquine, chloroquine, quinine and quinidine were obtained. This assay has been described and validated in chapter 4. As can be seen in figure 5.1(A) using a 1 hour incubation time at 60°C and 4.5 M acetate concentration, 5 equivalents of chloroquine is sufficient to completely inhibit *β*-haematin formation. However, if the incubation time is increased, the absorbance arising from the haematin-pyridine complex formed upon addition of pyridine at the end of the reaction decreases. The decrease is time-dependent as shown in figure 5.1(B). This decrease is ascribed to *β*-haematin formation in the presence of 5-equivalents of chloroquine if the incubation is continued for more than 60 min at this temperature, resulting in a decrease in the quantity of haematin that can react with pyridine. It should be noted in figure 5.1(B) that data points before 1 hour are absent because the haematin process is not yet complete, even in the absence of the drug. It is likely that there is an induction period at the beginning of the process and that the reaction should display sigmoidal behaviour as observed for *β*-haematin in the absence of drugs, rather than exponential behaviour suggested by the line passing through the data in figure 5.1 (B) [196]. These data suggest that *β*-haematin in fact forms in the presence of 5 equivalents of chloroquine if the incubation is continued for more that 60 minutes at this temperature, resulting in decreasing quantities of haematin to react with the pyridine.

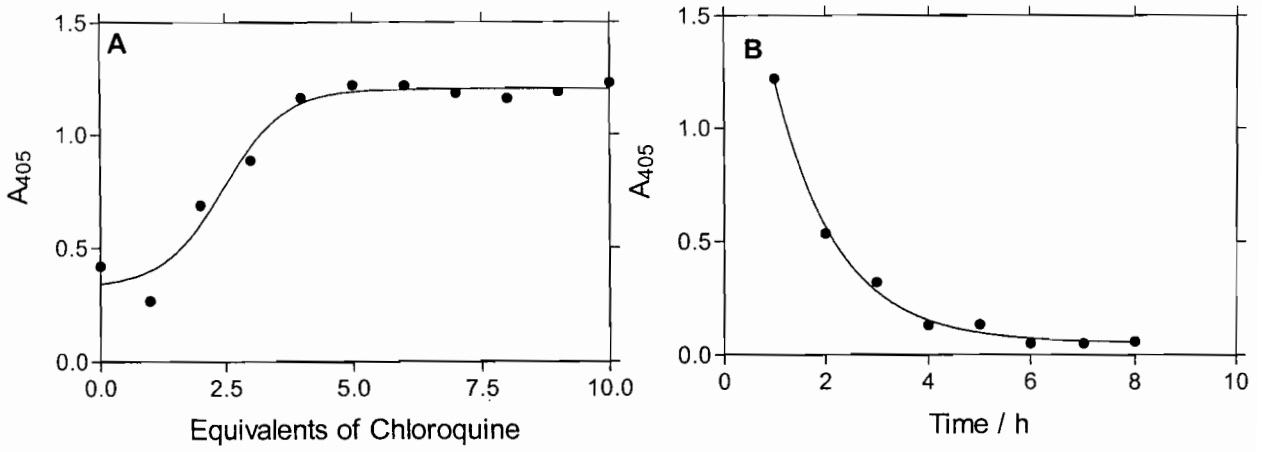

Figure 5.1 The inhibition of β-haematin formation by chloroquine is a consequence of its decreased rate of formation. **(A)** Shows a dose response curve for inhibition of β-haematin formation in the presence of increasing quantities of chloroquine in 4.5 M acetate, pH 4.5 at 60°C for 1 hour. **(B)** Shows the decrease in absorbance values in the presence of 5 equivalents of chloroquine at various incubation times.

5.3.2 Confirmation of β-haematin formation by IR spectroscopy and XRD

The decreased absorbance observed at 405 nm when the incubation time is increased does not provide definitive evidence that β-haematin formation occurs. Other explanations could be envisaged for this behaviour. It could be attributed to slow crystallisation of haematin-chloroquine complex resulting in a product that does not react readily with pyridine, or haematin may be degraded over time in the presence of chloroquine. For this reason, infrared spectroscopy and X-ray diffraction has been used to characterise the product. Figure 5.2(A) shows the infrared spectra obtained when haematin is incubated in 4.5 M acetate at pH 4.5 and 60°C in the presence of 3 equivalents of chloroquine for 1, 6 and 24 hours. The final spectrum of this material when incubated in the presence of chloroquine is identical to that of β-haematin previously reported by Egan et al. [73]. It is also identical to that reported by Bohle and Helms [201] where β-haematin was prepared by base abstraction of HCl from haemin in dry methanol. The spectral changes resulting from the conversion of haematin to β-haematin involve not only the appearance of sharp and intense peaks at 1660 cm^{-1} and 1208 cm^{-1}, but also a sharpening of

many other peaks in the spectrum, as can be seen by comparing the spectrum with that of haematin incubated for 1 hour. At 6 hours the prominent peaks at 1660 and 1208 cm^{-1} are already discernable, indicating significant formation of β-haematin. These findings are confirmed by XRD in figure 5.2B. The diffraction pattern of the product formed in the presence of 5 equivalents of chloroquine definitively demonstrates the presence of β-haematin both at the 6 and 24 hour time point. Thus, these results unequivocally demonstrate that the observed decrease in A_{405} does indeed correspond to β-haematin formation in the presence of chloroquine.

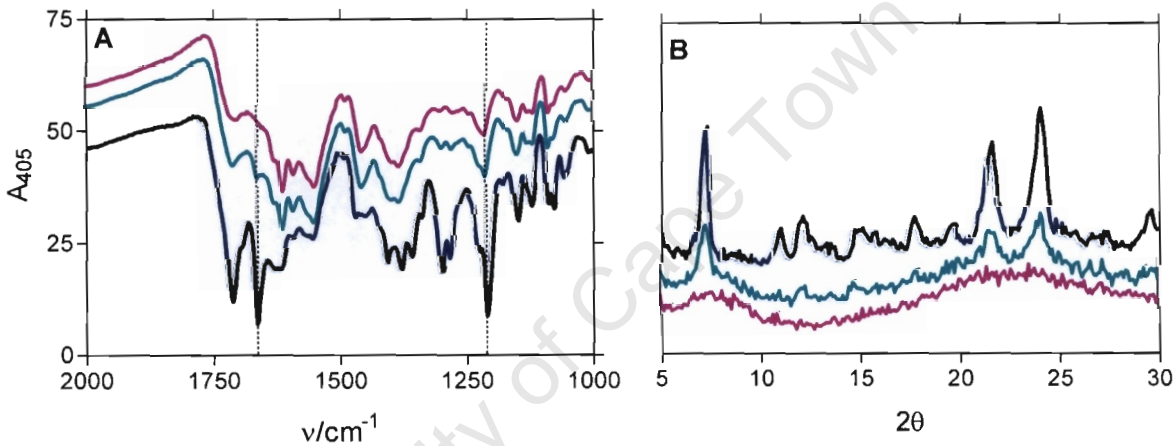

Figure 5.2 Infrared and XRD evidence confirming β-haematin formation in the presence of chloroquine. The XRD data and the infrared spectra were obtained at 1(—), 6(—) and 24(—) hours. **(A)** Shows infrared spectra in the presence of 3 equivalents of chloroquine, the dotted lines mark the positions of the most prominent bands expected for β-haematin at 1660 and 1210 cm^{-1}. **(B)** XRD data obtained in the presence of 5 equivalents of chloroquine. Conditions are as described in figure 5.1.

5.3.3 Effect of incubation time on IC_{50} for β-haematin inhibition by chloroquine

Chong and Sullivan [108] have also recently noted that β-haematin formation eventually occurs in the presence of chloroquine under conditions where crystal growth is brought about on preformed β-haematin crystallites at 37°C. These authors did not however report whether the IC_{50} values seen when a

longer incubation time is used are different. Consequently, the effect of incubation time on IC_{50} of chloroquine was investigated. Curves for β-haematin inhibition are shown in figure 5.3A. The dependence of IC_{50} on incubation time is shown in figure 5.3B. The data confirms that the IC_{50} values obtained for the inhibition of β-haematin formation by chloroquine become larger as the incubation time is increased. Furthermore, the IC_{50} increases steeply with incubation time at short times, but more gradually at longer times.

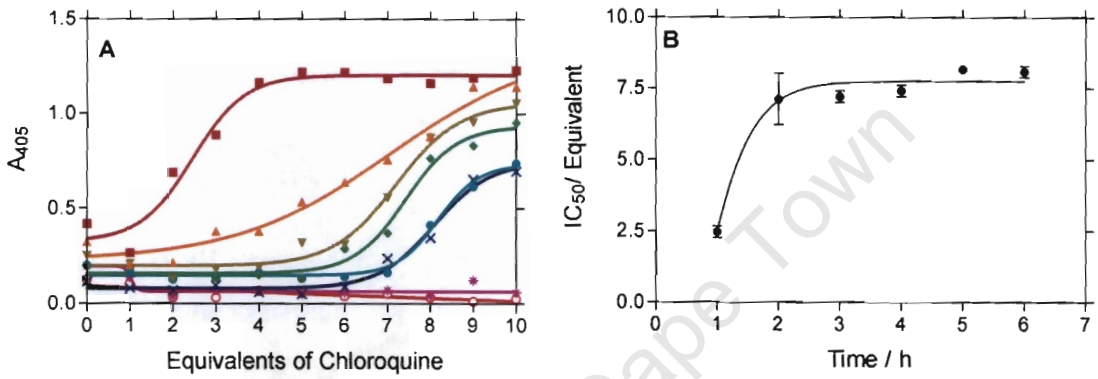

Figure 5.3 The effect of incubation time on the inhibition of β-haematin formatin by chloroquine. **(A)** The dose response curves obtained with incubation times of 1(■), 2(▲), 3(▼), 4(♦), 5(●), 6(x), 7(*) and 8(o) hours. **(B)** The dependence of IC_{50} on incubation time. The solid line is shown for clarity but has no theoretical significance. Incubation conditions are as described in figure 1.

5.3.4 Scanning electron microscopy

The external morphology of β-haematin crystallites was examined by scanning electron microscopy (SEM). Previous studies have shown that synthetic β-haematin produced in acetate solution exhibits smaller, less ordered crystals that natural haemozoin [90, 109, 202]. Better formed crystals are observed when β-haematin is synthesised under non-aqueous conditions, [109] or when it is grown onto pre-existing haemozoin crystals [202]. This is also observed when β-haematin forms in the presence of chloroquine (Figure 5.4(B)). After 1 hour of incubation time in the presence of 3 equivalents of chloroquine, the haematin product consists of relatively large seemingly

amorphous or possibly nanocrystalline fragments (figure 5.4(A)). These are probably glass-like in structure, as they do not give rise to a sharp diffraction pattern (figure 5.2(B), bottom trace). After 6 hours, a mass of small, needle-like crystals is formed (figure 5.4(B)). These crystals appear to be considerably more uniform, well formed and larger than those produced in the absence of the drug (figure 5.4(D)). However, further incubation to 24 hours does not appear to result in much additional growth of these crystals (figure 5.4(C)). Rather, they appear simply to aggregate in large in clumps.

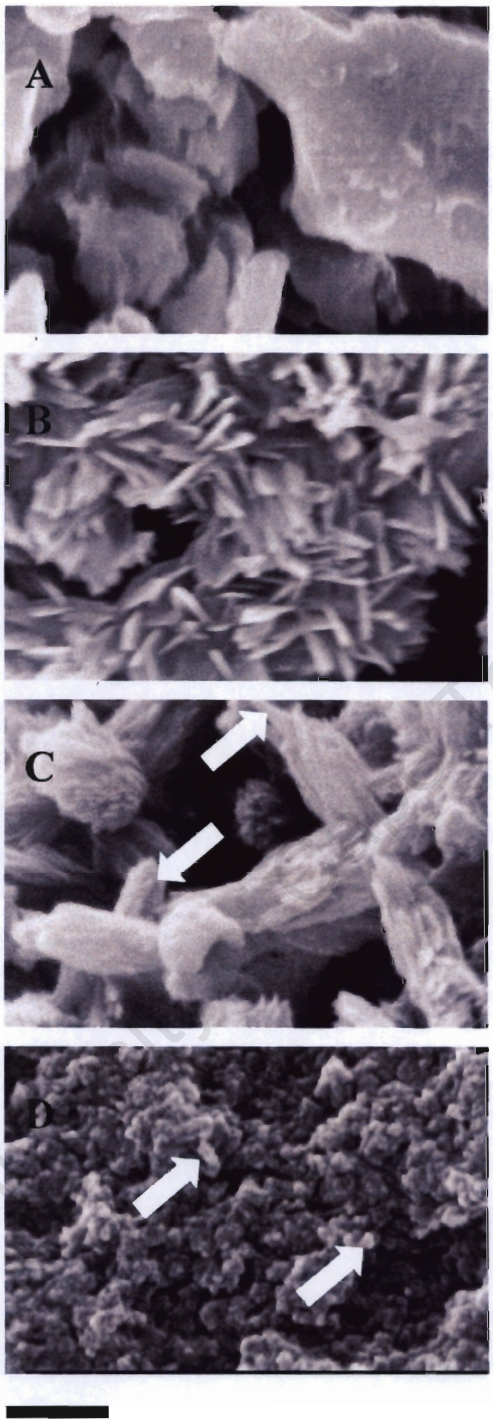

Figure 5.4 Scanning electron micrographs of haematin and β-haematin products. The SEMs obtained in the presence of 3 molar equivalents of chloroquine are shown in **(A)**, **(B)** and **(C)** with corresponding incubation times of 1, 6 and 24 hours respectively. **(D)** Shows the external morphology of β-haematin prepared by incubation in the absence of drug for 1 hour [196]. The conditions are as described in figure 5.1. The thick scale bar corresponds to a length of is 1 μm. Crystallites are indicated by arrows in (C) and (D).

5.3.5 Effect of incubation time on β-haematin inhibition by amodiaquine, quinidine and quinine

Amodiaquine shows a dependence of IC_{50} on incubation time for inhibition of β-haematin formation which increases significantly with increasing incubation time (figure 5.5A). The initial steep increase seen with chloroquine however, is not observed with amodiaquine but rather the IC_{50} appears to increase linearly over the time range. Behaviour of the 4-aminoquinolines appears to be somewhat different to that of the quinoline methanols, quinine and quinidine in that β-haematin formation is far slower in the presence of the latter two drugs. The IC_{50} values of these two compounds are less sensitive to incubation time, but an increase in IC_{50} is nonetheless evident (figure 5.3C and figure 5.6(B) and C). The slow increase in IC_{50} in the case of quinine mirrors the far slower rate of β-haematin formation in the presence of this drug compared to chloroquine (figure 5.6B).

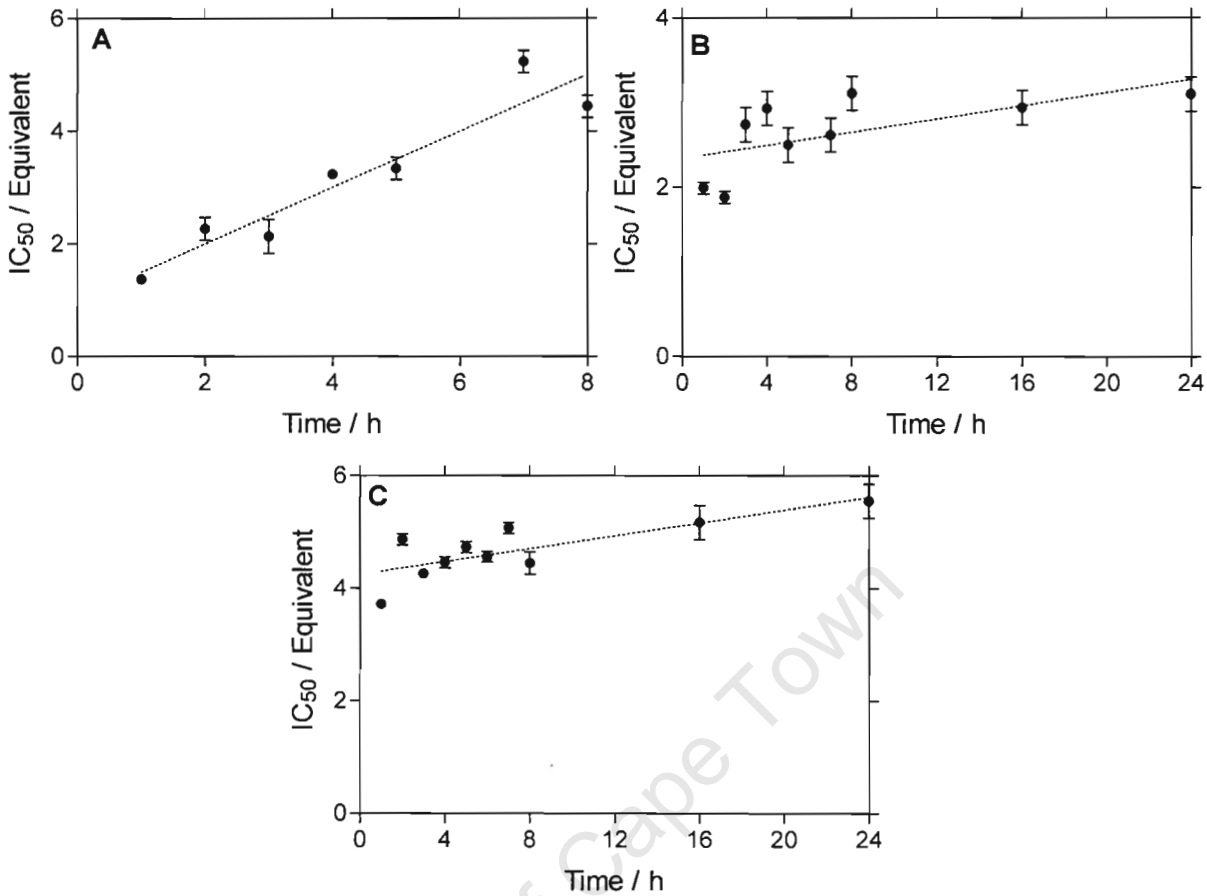

Figure 5.5 The effect of incubation time on the IC_{50} values for inhibition of β-haematin formation by amodiaquine, quinidine and quinine are shown in **(A)**, **(B)** and **(C)** respectively. The dotted lines are linear regression lines. Incubation conditions are as described in figure 5.1

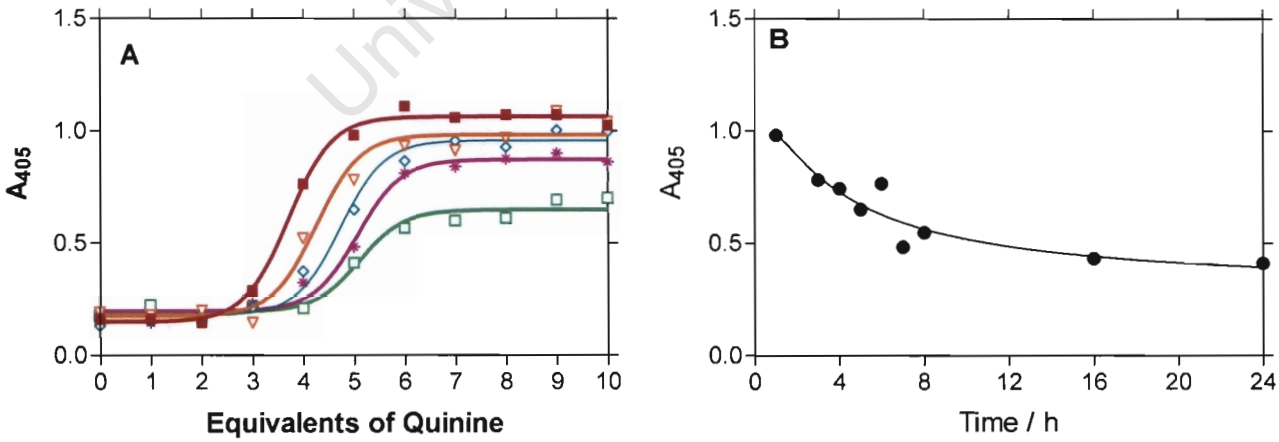

Figure 5.6 (A) Shows a dose response curves for quinine obtained with incubation times of 1(■), 3(▼), 5(●), 7(*) and 24(□) hours. **(B)** Shows the decrease in absorbance values in the presence of 5 equivalents of quinine at various incubation times. Incubation conditions are as described in figure 1.

Infrared spectroscopy shown in figure 5.7(A) confirms that conversion of haematin to β-haematin does occur in the presence of quinine and the XRD pattern in figure 5.7(B) unequivocally shows that β-haematin is formed. The kinetic trace in figure 5.6B shows that only about 50% conversion of haematin to β-haematin occurs in 24 hours in the presence of 5 equivalents of quinine, compared to almost 100% within 8 hours in the presence of chloroquine. This is supported by the XRD data which confirm incomplete conversion in the presence of quinine (compare the 24 hour trace for quinine in figure 5.7B with the corresponding trace for chloroquine in figure 5.2B).

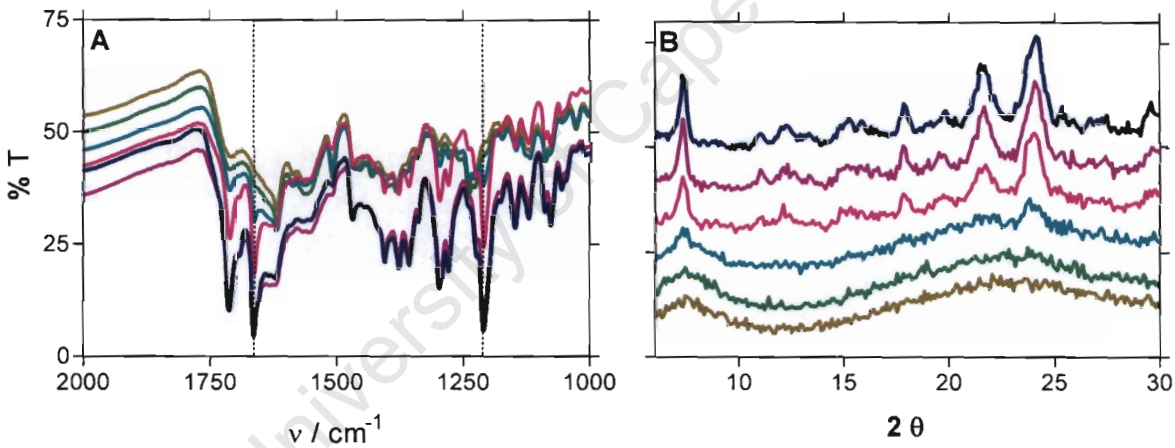

Figure 5.7 Infrared and XRD evidence demonstrating that β-haematin formation occurs in the presence of 5 equivalents of quinine. (A) Shows infrared spectra with corresponding incubation times of 1(—), 4(—), 5(—), 8(—), 16(—) and 24(—) hours. The dotted vertical lines are described in figure 5.2A. (B) Shows XRD data. Diffraction patterns correspond to incubation times of 2(—), 4(—), 5(—), 8(—), 16(—) and 24(—) hours. Incubation conditions are as described in figure 5.1.

Chong and Sullivan [108] have recently reported that inhibition of β-haematin formation by chloroquine and quinidine is reversible. This study has confirmed their observation and also demonstrated that these compounds act by slowing the rate of β-haematin formation rather than inhibiting the process by

competitive equilibrium binding. On the basis of this behaviour, it appears that β-haematin formation in acidic medium is essentially irreversible, while haematin-drug interactions are reversible. This supports the idea that β-haematin formation is a far more favourable thermodynamic process than haematin-drug complex formation (and probably also adsorption of drugs onto β-haematin surface). Consequently, this evidence suggests that the inhibitory effect is kinetic.

5.4 CONCLUSION

At this stage the mechanism of β-haematin inhibition is still unknown. Certainly, the quinoline antimalarials form complexes with haematin in solution [72, 74, 86, 100]. Kaschula et al. [113] have however, shown that there is no direct correlation between the strength of such complexes and the ability to inhibit β-haematin formation. It remains to be seen whether there are correlations with the solution structures of these complexes and their inhibitory activity. It is interesting that these drugs have been proposed to interact with the growing β-haematin crystal surface [111], as such an hypothesis appears to be consistent with the findings that were observed by Chong and Sullivan [108] that the strength of β-haematin inhibition by chloroquine and quinidine decreases as a results of increasing quantity of β-haematin seed crystals.

Intriguingly, there is an observation in this study is the marked effect of chloroquine on the external morphology of β-haematin crystals that is especially apparent in figure 5.4B. This appears to be confined to the external appearance of the crystals, as there is no evidence from the XRD traces of crystalline material other than β-haematin (figure 5.2B). This observation seems to further support the hypothesis that chloroquine interacts with the surface of the β-haematin crystal. This is the first observation in which a quinoline antimalarial has been directly shown to affect the growth of the crystal faces of β-haematin and to influence the final external appearance of the crystal. Further observations of this type may be able to provide more

detailed information on the process of inhibition and the crystal face with which chloroquine interacts most strongly. It would also be of interest to investigate whether other quinolines give rise to similar changes in crystal morphology.

Whatever the mechanism of inhibition of β-haematin formation is, it is clear that the IC_{50} depends on the incubation time used. This has not been appreciated previously and it has important implications for the strengths of inhibition of β-haematin formation. The strength of inhibition using a 1 hour incubation time at 60°C in 4.5 M acetate, pH 4.5 follows the order amodiaquine > quinidine > chloroquine > quinine. With two hour incubation the order is quinidine > amodiaquine > quinine > chloroquine and at five hours it is quinidine > quinine > amodiaquine > chloroquine. It is thus demonstrated that chloroquine is a strong inhibitor at short periods of incubation time and quinine is weaker, but the reverse is observed over longer incubation times. On the basis of the fact that IC_{50} data collected using one hour incubation correlate well with values obtained using various methods (chapter 4), it would appear that most quantitative β-haematin inhibition data collected to date refer to the early part of the process. Despite this, data correlate with biological activity (chapter 4) and also, the action of the drugs may well emerge from the early part of the inhibitory process, at least in 4-aminoquinolines.

The antimalarials such as 4-aminoquinilines and the quinoline methanols appear to act by slowing rather than irreversibly blocking haemozoin formation. The IC_{50} for inhibition of β-haematin formation by the 4-aminoquinolines in particular, depend strongly on incubation time. The above conclusion is an important consideration when investigating β-haematin inhibitors. In addition it is unclear whether the initial slowing of haemozoin formation or longer lasting activity is more important for biological activity. Further investigation is required to make a definitive conclusion.

CHAPTER 6

OVERALL CONCLUSIONS AND FURTHER STUDIES

6.1 CONCLUSIONS

A number of proposals have been made over the years about the mechanism of action of quinoline antimalarials. One of these is that quinoline drugs act by association with haematin, thereby blocking haemozoin formation by forming a complex with haematin. A number of studies have indicated that these interactions are due to $\pi - \pi$ stacking, but the role of electrostatic and hydrophobic interactions in this association have not been probed. The possible nature of these interactions between the metalloporphyrin and the quinoline antimalarial drugs has been investigated in this work. A number of important conclusions could be drawn:

(i) It was found that the electrostatic contribution to the interaction is small as the ionic strength has little effect on the interaction strength.

(ii) To further probe this question the association constants of chloroquine, amodiaquine, quinine, quinidine and 9-epiquinine with haematin at five different concentrations of DMSO were converted to molar free energy of association and showed a linear increase in ΔG with decreasing water fraction. This suggests that water plays a significant role in the stability of these complexes.

(iii) This was confirmed by measuring association constants of chloroquine base in five organic solvents. It was found that stability of these interactions depend on the solvent polarity and hydrogen bond donor strength, suggesting that these interactions are mainly hydrophobic.

(iv) The important role of solvent is also indicated by the large desolvation indicated to occur upon complex formation by thermodynamic compensation plots.

There is considerable evidence that quinoline drugs form complexes with haematin and act by inhibiting haemozoin formation. Thus, there is an interest in determining the β-haematin inhibitory activity of these compounds using a cheap and fast method. It was found that the interaction of aqueous pyridine with haematin in solution produces spectra that show excellent properties for analytical determination of haematin. These include a linear dependence on haematin concentration and high extinction coefficient. In addition β-haematin is insoluble in 5 – 10% (v/v) aqueous pyridine at pH 7.5. Thus, this pyridine solution can quantitate haematin in a mixture of the two. Aqueous pyridine solution was successfully used to assay β-haematin formation in 4.5 M acetate at pH 4.5, 60°C by removal of aliquots at the end of the reaction. In this assay, trends in inhibitory activity correlated well with other reported methods. Thus relative strengths of various inhibitors are very similar to those reported in other studies. For quantitative determination of β-haematin inhibitory activity the assay has the advantage of being fast, requiring no centrifugation and using an easy detection method. The method can be used qualitatively for high throughput screening, in which case detection can even be by visual inspection.

Although the mechanism of inhibition of β-haematin formation is still unclear it was found that the 4-aminoquinoline and quinoline methanols act by slowing down haemozoin formation, rather than irreversibly blocking the process. When incubated for long times. β-haematin formation eventually occurs. The observed IC_{50} for β-haematin formation is dependent on incubation time and inhibition of haemozoin formation thus needs to be considered as a kinetic phenomenon.

6.2 FURTHER STUDIES

Further understanding of haematin – quinoline interactions will require the use of computational methods. Based on the results obtained in chapter 3, further study of the interaction of quinoline antimalarials with haematin using any computational model would seem to need to explicitly include solvent molecules, since water plays a critical role in these interactions. The electrostatic and orbital interactions will however need to be included as they may contribute to the geometry of the complex. As this is likely to be a formidable task, experimental methods such as NMR relaxation measurements may also be able to assist in structure determination by providing experimental constraint distances which might permit modelling in the absence of explicit solvent molecules.

Further development of the β-haematin inhibition assay is also warranted. Compounds with low solubility that inhibit haemozoin formation in water may interfere with dissolution of the haematin-drug complex in aqueous pyridine and could lead to false negative results as observed with halofantrine. Preliminary studies have suggested the use of organic solvents overcome this problem. At this stage it is unclear to what extent this would be likely to cause problems in a high-throughput screening study or whether the use of organic solvents will obviate the problem. Coloured compounds may interfere with the assay although the problem may be alleviated by carrying out blank measurements. The only way to test the potential of this assay will be to attempt a high throughput screening exercise. This will require access to a suitable compound library.

As regards the mechanism of β-haematin inhibition, although evidence from this study has shown that chloroquine and related compounds decrease the rate of haemozoin formation, the intimate mechanism of this process remains obscure. It is also unclear whether the initial slowing of haemozoin formation or longer lasting inhibitory activity is crucial for biological activity. This will require further investigation. However, the poor understanding of the mechanism of haemozoin formation *in vivo* will make definitive conclusions

difficult. The observation of external morphological changes in β-haematin brought about by chloroquine also deserves further investigation.

In order to rationally design new antimalarials other than 4-aminoquinolines, it would be necessary in future to determine what structural features in the complex lead to β-haematin inhibition. The assay described in chapter 4 can be used as a tool in discovering these new compounds and in the future could be used to determine what structural changes lead to β-haematin inhibition. In this regard, it will be necessary to study the molecular interactions in the complex using computational methods, taking into account electrostatic interactions molecular orbitals and solvent interactions of different polarity. This may answer the question of why some compounds inhibit haemozoin formation but others do not, even when they form complexes with haematin. Such studies may eventually lead to the *in silico* design of new antimalarials of this class.

REFERENCES

[1] World Health Organisation report on infectous disease, removing obstacles to the healthy development. WHO Geneva (1999)

[2] I. W. Sherman, Comp. Biochem. Physiol. 53B (1976) 447-450.

[3] WHO Expert committee on malaria. Technical report series. Twentieth report. World Health Organisation. Geneva. (2000), 1-83

[4] T. J. Egan, H. M. Marques, Coord. Chem. Rev. 190-192 (1999) 493-517.

[5] P. I. Trigg, A. V. Kondrachine, in: I. W. Sherman (Ed.), The Current Global Malaria Situation, ASM Press, 1998, pp. 11-22.

[6] S. W. Lindsay, W. J. Martens, Bull World Health Organ. 76 (1998) 33-45.

[7] S. R. Phillips in: Malaria, E Arnold, London, 1983, pp.

[8] W.H. Wernsdorfer, I. McGregor (Eds.), Malaria: Principles and practice of Malariology, Churchill - Livingstone, Edinburgh, 1998.

[9] www.wooster.edu/biology/Ciliates/disease/student%20Web%20pages/nelson,%20L.%20/nelson_life%20Cycle.html

[10] M. A. Rudzinska, W. Trager, R. S. Bray, J. Protozool. 12 (1965) 563-576.

[11] M. Krugliak, F. Zhang, H. Ginsburg, Mol. Biochem. Parasitol. 119 (2002) 249-256.

[12] D. E. Goldberg, A. F. G. Slater, A. Cerami, G. B. Henderson, Proc. Natl. Acad. Sci. USA 87 (1990) 2931-2935.

[13] D. E. Goldberg, A. F. G. Slater, R. Beavis, B. Chait, A. Cerami, G. B. Henderson, J. Exp. Med. 173 (1991) 961-969.

[14] L. Tyas, I. Gluzman, R. P. Moon, K. Rupp, J. Westling, R. G. Ridley, J. Kay, D. E. Goldberg, C. berry, FEBS Lett. 454 (1999) 210-214.

[15] R. P. Moon, L. Tyas, U. Certa, Eur. J. Biochem. 244 (1997) 552-560.

[16] M. D. Wyatt, C. Berry, FEBS Lett. 513 (2002) 159-162.

[17] C. Berry, M. J. Humphreys, P. Matharu, R. Granger, P. Horrocks, R. P. Moon, U. Certa, R. G. Ridley, D. Bur, J. Kay, FEBS Lett. 447 (1999) 149-154.

[18] R. Banerjee, J. Liu, A. Beatty, L. Pelosof, M. Klemba, E. D. Goldberg, Proc. Natl. Acad. Sci. USA 99 (2002) 990-995.

[19] A. L. Omara-Opyene, M. A. Pedro.;, R. C. Sulsona, B. J. Alfredo.;, A. C. Yowel, H. Fujioka, A. D. Fidock, B. J. Dame, J. Biol. Chem. 279 (2004) 54088-54096.

[20] P. J. Rosenthal, P. S. Sijwali, A. Singh, B. R. Shenai, Curr. Pharm. Des. 8 (2002) 1659-1672.

[21] K. K. Eggleson, K. L. Duffin, D. E. Goldberg, J. Biol. Chem. 274 (1999) 32411-32417.

[22] P. J. Rosenthal, in: P. J. Rosenthal (Ed.), Protease Inhibitors, Humana Press, 2001, pp. 325-345.

[23] H. Ladan, Y. Nitzan, Z. Malik, FEMS Microbiol. Lett. 112 (1993) 173-178.

[24] L. W. Scheibel, I. W. Sherman, in: W. H. Wernsdorfer, I. McGregor (Ed.), Churchill-Livingstone, 1998, pp. 219-252.

[25] M. F. Oliveira, J. R. Silva, M. Dansa-Petretski, W. de Souza, U. Lins, C. M. S. Braga, H. Masuda, P. L. Oliveira, Nature 400 (1999) 517-518.

[26] M. F. Oliveira, J. R. Silva, M. Dansa-Petretski, W. de Souza, C. M. S. Braga, H. Masuda, P. L. Oliveira, FEBS Lett. 477 (2000) 95-98.

[27] M. Oliveira, J. C. P. d'Avila, C. R. Torres, P. L. Oliveira, A. J. Tempone, F. D. Rumjanek, C. M. S. Braga, J. R. Silva, M. Dansa-Petretski, M. A. Oliveira, W. de Souza, S. T. Ferreira, Mol. Biochem. Parasitol. 111 (2000) 217-221.

[28] M. M. Chen, L. Shi, D. J. Sullivan, Mol. Biochem. Parasitol. 113 (2001) 1-8.

[29] T. J. Egan, Targets 2 (2003) 115-124.

[30] W. Brown, J. Exp. Med. 13 (1911) 290-299.

[31] B. N. Ghosh, J. A. Sinton, Rec. Mal. Survey India 4 (1934) 43-59.

[32] J. O. Ashong, I. P. Blench, D. C. Warhurst, Trans R. Soc. Trop. Med. Hyg. 83 (1989) 167-172.

[33] P. Goldie, E. F. Roth, J. Oppenheim, J. P. Vanderberg, Am. J. Trop. Med. Hyg. 43 (1990) 584-596.

[34] C. D. Fitch, P. Kanjananggulpan, J. Biol. Chem. 262 (1987) 15552-15555.

[35] A. F. G. Slater, W. J. Swiggard, B. R. Orton, W. D. Flitter, D. E. Goldberg, A. Cerami, G. B. Henderson, Proc. Natl. Acad. Sci. USA 88 (1991) 325-329.

[36] S. Pagola, P. W. Stephens, D. S. Bohle, A. D. Kosar, S. K. Madsen, Nature 404 (2000) 307-310.

[37] R. B. Wood, J. S. Langford, M. B. Cooke, J. Lim, K. F. Glenister, M. Duriska, K. J. Unthank, D. McNaughton, J. Am. Chem. Soc. 126 (2004) 9233-9239.

[38] R. B. Wood, J. S. Langford, M. B. Cooke, K. F. Glenister, J. Lim, D. McNaughton, FEBS Lett. 554 (2003) 247-252.

[39] D. S. Bohle, R. E. Dinnebier, S. K. Madsen, P. W. Stephens, J. Biol. Chem. 272 (1997) 713-716.

[40] A. F. G. Slater, Pharmac. Ther. 57 (1993) 203-235.

[41] K. Bendrat, B. J. Berger, A. Cerami, Nature 378 (1995) 138-139.

[42] C. D. Fitch, G.-z. Cai, Y.-F. Chen, J. D. Shoemaker, Biochim. Biophys. Acta 1454 (1999) 31-37.

[43] A. Dorn, S. R. Vippagunta, H. Matile, A. Bubendorf, J. L. Vennerstrom, R. G. Ridley, Biochem. Pharmacol. 55 (1998) 737-747.

[44] A. Dorn, R. Stoffel, H. Matile, A. Bubendorf, R. G. Ridley, Nature 374 (1995) 269-271.

[45] D. J. Sullivan, I. Y. Gluzman, D. G. Russell, D. E. Goldberg, Proc. Natl. Acad. Sci. USA 93 (1996) 11865-11870.

[46] C. Y. H. Choi, J. F. Cerda, H.-A. Chu, G. T. Babcock, M. A. Marletta, Biochemistry 38 (1999) 16916-16924.

[47] A. Lynn, S. Chandra, P. Malhotra, V. S. Chauhan, FEBS Lett. 459 (1999) 267-271.

[48] J. Ziegler, R. T. Chang, D. W. Wright, J. Am. Chem. Soc. 121 (1999) 2395-2400.

[49] T. J. Egan, J. Inorg. Biochem. 91 (2002) 19-26.

[50] D. J. Sullivan, Int. J. Parasitol. 32 (2002) 1645-1653.

[51] T. J. Egan, Drug Design Revs Online 1 (2004) 93-110.

[52] H. Ginsburg, O. Famin, F. Zhang, M. Krugliak, Biochem. Pharmacol. 56 (1998) 1305-1313.

[53] P. Loria, S. Miller, M. Foley, L. Tilley, Biochem. J. 339 (1999) 363-370.

[54] T. J. Egan, J. M. Combrinck, J. Egan, G. R. Hearne, H. M. Marques, S. Ntenteni, B. T. Sewell, P. J. Smith, D. Taylor, D. A. van Schalkwyk, J. C. Walden, Biochem. J. 365 (2002) 343-347.

[55] C. D. Fitch, R. Chevli, Y. Gonzalez, Antimicr. Agents Chemother. 6 (1974) 757-762.

[56] D. J. Krogstad, P. H. Schlesinger, I. Y. Gluzman, J. Cell Biol. 101 (1985) 2302-2309.

[57] C. A. Homewood, D. C. Warhurst, W. Peters, V. C. Baggaley, Nature 235 (1972) 50-52.

[58] K. Raynes, P. G. Bray, G. E. Ward, Drug Resist. updates 2 (1999) 97-103.

[59] F. S. Parker, J. L. Irvin, J. Biol. Chem. 199 (1952) 897-909.

[60] M. W. Davidson, B. G. Griggs, D. W. Boykin, D. W. Wilson, Nature 254 (1975) 632-634.

[61] G. C. Kirby, M. J. O' Neill, D. Phillipson, D. C. Warhurst, Biochem. Pharmacol. 38 (1989) 4367-4374.

[62] C. A. Homewood, D. C. Warhurst, V. C. Baggaley, Trans R. Soc. Trop. Med. Hyg. 65 (1971) 10.

[63] N. Surolia, G. Padmanaban, Proc. Natl. Acad. Sci. USA 88 (1991) 4786-4790.

[64] A. C. Chou, R. Chevli, C. D. Fitch, Biochemistry 19 (1980) 1543-1549.

[65] C. D. Fitch, R. Chevli, H. S. Banyal, G. Phillips, M. A. Pfaller, D. J. Krogstad, Antimicr. Agents Chemother. 21 (1982) 819-822.

[66] C. D. Fitch, R. Chevli, P. Kanjananggulpan, P. Dutta, K. Chevli, A. C. Chou, Blood 62 (1983) 1165-1168.

[67] E. Königk, S. Mirtsch, B. Putfarken, S. Abdel-Rasoul, Trop. Parasit. 32 (1981) 73-76.

[68] D. C. Warhurst, Biochem. Pharmacol. 30 (1981) 3323-3327.

[69] M. Hollemans, R. O. Elferink, P. G. De Groot, A. Stritjiland, J. M. Tager, Biochim. Biophys. Acta. 643 (1981) 140-151.

[70] H. Ginsburg, M. Krugliak, Biochem. Pharmacol. 43 (1992) 63-70.

[71] F. N. Gyang, B. Poole, W. Trager, Mol. Biochem. Parasitol. 5 (1982) 263-273.

[72] S. N. Cohen, K. O. Phifer, K. L. Yielding, Nature 202 (1964) 805-806.

[73] T. J. Egan, D. C. Ross, P. A. Adams, FEBS Lett. 352 (1994) 54-57.

[74] A. Dorn, S. R. Vippagunta, H. Matile, C. Jaquet, J. L. Vennerstrom, R. G. Ridley, Biochem. Pharmacol. 55 (1998) 727-736.

[75] S. R. Hawley, P. G. Bray, M. Mungthin, J. D. Atkinson, P. M. O' Neill, S. A. Ward, Antimicr. Agents Chemother. 42 (1998) 682-686.

[76] A. F. G. Slater, A. Cerami, Nature 355 (1992) 167-169.

[77] G. Blauer, H. Ginsburg, Biochem. Internatl. 5 (1982) 519-523.

[78] P. A. Adams, P. A. M. Berman, T. J. Egan, P. J. Marsh, J. Silver, J. Inorg. Biochem. 63 (1996) 69-77.

[79] D. H. O' Keeffe, C. H. Barlow, G. A. Smythe, W. H. Fuchsman, T. H. Moss, H. R. Lilienthal, W. S. Caughey, Bioinorg. Chem. 5 (1975) 125-147.

[80] J. Silver, B. Lucas, Inorg. Chim. Acta 78 (1983) 219-224.

[81] S. Moreau, B. Perly, C. Chachaty, C. Deleuze, Biochim. Biophys. Acta 840 (1985) 107-116.

[82] G. Blauer, Arch. Biochem. Biophys. 251 (1986) 306-314.

[83] G. Blauer, Arch. Biochem. Biophys. 251 (1986) 315-322.

[84] G. Blauer, Biochem. Internatl. 17 (1988) 729-734.

[85] D. C. Warhurst, Ann. Trop. Med. Parasitol. 81 (1987) 65-67.

[86] T. J. Egan, W. W. Mavuso, D. C. Ross, H. M. Marques, J. Inorg. Biochem. 68 (1997) 137-145.

[87] T. H. Davies, J. Biol. Chem. 135 (1940) 597-622.

[88] W. A. Gallagher, W. B. Elliot, Ann. N. Y. Acad. Sci. 206 (1973) 463-482.

[89] W. Graf, K. Pommerening, W. Scheler, Acta Med.Ger. 26 (1971) 895-909.

[90] T. J. Egan, E. Hempelmann, W. W. Mavuso, J. Inorg. Biochem. 73 (1999) 101-107.

[91] H. M. Marques, K. Voster, T. J. Egan, J. Inorg. Biochem. 64 (1996) 7-23.

[92] S. Moreau, B. Perly, J. Biguet, Biochimie 64 (1982) 1015-1025.

[93] I. Constantinidis, J. D. Satterlee, J. Am. Chem. Soc. 110 (1988) 4391-4395.

[94] I. Constantinidis, J. D. Satterlee, J. Am. Chem. Soc. 110 (1988) 927-932.

[95] J. A. Shelnutt, J. Phys. Chem. 87 (1983) 605-616.

[96] J. A. Shelnutt, J. Am. Chem. Soc. 103 (1981) 4275-4277.

[97] J. A. Shelnutt, J. Am. Chem. Soc. 105 (1983) 774-778.

[98] J. A. Shelnutt, Inorg. Chem. 22 (1983) 2535-2544.

[99] P. M. O' Neill, D. J. Willock, S. R. Hawley, P. G. Bray, R. C. Storr, S. A. Ward, B. K. Park, J. Med. Chem. 40 (1997) 437-448.

[100] A. Leed, K. DuBay, L. M. B. Ursos, D. Sears, A. C. de Dios, P. D. Roepe, Biochemistry 41 (2002) 10245-10255.

[101] D. De, F. M. Krogstad, F. B. Cogswell, D. J. Krogstad, Am. J. Trop. Med. Hyg. 55 (1996) 579-583.

[102] S. R. Vippagunta, A. Dorn, H. Matile, A. K. Bhattacharjee, J. M. Karle, W. Y. Ellis, R. G. Ridley, J. L. Vennerstrom, J. Med. Chem. 42 (1999) 4630-4639.

[103] T. J. Egan, K. R. Koch, P. L. Swan, C. Clarkson, D. A. Van Schalkwyk, P. J. Smith, J. Med. Chem. 47 (2004) 2926-2934.

[104] Y. Inoue, T. Wada, Adv. Supramolec. Chem. 4 (1997) 55-96.

[105] B. E. C. Banks, V. Damjanovic, C. A. Vernon, Nature 240 (1972) 147-148.

[106] Y. Inoue, T. Hakushi, Y. Liu, L.-H. Tong, B.-J. Shen, D.-S. Jin, J. Am. Chem. Soc. 115 (1993) 475-481.

[107] Y. Inoue, Y. Liu, L.-H. Tong, B.-J. Shen, D.-S. Jin, J. Am. Chem. Soc. 115 (1993) 10637-10644.

[108] C. R. Chong, D. J. Sullivan, Biochem. Pharmacol. 66 (2003) 2201-2212.

[109] D. S. Bohle, A. D. Kosar, P. W. Stephens, Acta Cryst. D58 (2002) 1752-1756.

[110] D. J. Sullivan, H. Matile, R. G. Ridley, D. E. Goldberg, J. Biol. Chem. 273 (1998) 31103-31107.

[111] R. Buller, M. L. Peterson, Ö. Almarsson, L. Leiserowitz, Cryst. Growth Des. 2 (2002) 553-562.

[112] T. J. Egan, R. Hunter, C. H. Kaschula, H. M. Marques, A. Misplon, J. C. Walden, J. Med. Chem. 43 (2000) 283-291.

[113] C. H. Kaschula, T. J. Egan, R. Hunter, N. Basilico, S. Parapini, D. Taramelli, E. Pasini, D. Monti, J. Med. Chem. 45 (2002) 3531-3539.

[114] M. Mungthin, P. G. Bray, R. G. Ridley, S. A. Ward, Antimicr. Agents Chemother. 42 (1998) 2973-2977.

[115] P. G. Bray, O. Janneh, K. Raynes, M. Mungthin, H. Ginsburg, S. A. Ward, J. Cell Biol. 145 (1999) 363-376.

[116] C. Portela, C. M. M. Afonso, M. M. M. Pinto, M. J. Ramos, FEBS Lett. 547 (2003) 217-222.

[117] R. S. Cheruku, S. Maiti, A. Dorn, B. Sconeaux, A. K. Bhattacharjee, Y. W. Ellis, J. L. Vennerstrom, J. Med. Chem. 46 (2003) 3166-3169.

[118] N. Basilico, D. Monti, P. Olliaro, D. Taramelli, FEBS Lett. 409 (1997) 297-299.

[119] N. Basilico, E. Pagani, D. Monti, P. Olliaro, D. Taramelli, J. Antimicr. Chemother. 42 (1998) 55-60.

[120] D. De, F. M. Krogstad, L. D. Byers, D. J. Krogstad, J. Med. Chem. 41 (1998) 4918-4926.

[121] D. De, L. D. Byers, D. J. Krogstad, J. Heterocyclic Chem. 34 (1997) 315-320.

[122] T. J. Egan, Minirev. Med. Chem. 1 (2001) 114-124.

[123] S. J. Foote, J. K. Thompson, A. F. Cowman, D. J. Kemp, Cell 57 (1989) 921-930.

[124] M. Duraisingh, C. J. Drakeley, O. Muller, R. Bailey, G. Snounou, G. A. Targett, B. M. Greenwood, D. C. Warhurst, Parasitol. 114 (1997) 205-211.

[125] S. J. Foote, D. E. Kyle, R. K. Martin, A. M. J. Oduola, K. Forsyth, D. J. Kemp, A. F. Cowman, Nature 345 (1990) 255-258.

[126] L. K. Basco, J. Le Bras, Z. Rhoades, C. M. Wilson, Mol. Biochem. Parasitol. 74 (1995) 157-166.

[127] J. Cox Singh, B. Singh, A. Alias, M. S. Abdullah, Trans R. Soc. Trop. Med. Hyg. 89 (1995) 436-437.

[128] I. S. Adagu, F. Dias, L. Pinheiro, L. Rombo, V. do Rosario, D. C. Warhurst, Trans R. Soc. Trop. Med. Hyg. 90 (1996) 90-91.

[129] L. von Seidlein, M. T. Duraisingh, C. J. Drakeley, R. Bailey, B. M. Greenwood, M. Pinder, Trans R. Soc. Trop. Med. Hyg. 91 (1997) 450-453.

[130] M. Mungthin, P. G. Bray, S. A. Ward, Am. J. Trop. Med. Hyg. 60 (1999) 469-474.

[131] K. R. McCutcheon, J. A. Freese, J. A. Frean, B. L. Sharp, M. B. Markus, Trans R. Soc. Trop. Med. Hyg. 93 (1999) 300-302.

[132] P. R. Battacharya, C. R. Pillai, Ann. Trop. Med. Parasitol. 93 (1999) 679-684.

[133] P. R. Battacharya, S. Biswas, L. Kabilan, Trans R. Soc. Trop. Med. Hyg. 91 (1997) 454-455.

[134] L. Basco, P. Ringwald, Am. J. Trop. Med. Hyg. 59 (1998) 577-581.

[135] L. Basco, P. E. de Pecoulas, J. Le Bras, C. M. Wilson, Exp. Parasitol. 82 (1996) 97-103.

[136] T. E. Wellems, L. J. Panton, I. Y. Gluzman, V. E. do Rosario, R. W. Gwadz, A. Walker-Jonah, D. J. Krogstad, Nature 345 (1990) 253-255.

[137] R. N. Price, C. Cassar, A. Brockman, M. Duraisingh, M. van Vugt, N. J. White, F. Nosten, S. Krishna, Antimicr. Agents Chemother. 43 (1999) 2943-2949.

[138] A. F. Cowman, D. Galatis, J. K. Thompson, Proc. Natl. Acad. Sci. USA 91 (1994) 1143-1147.

[139] S. A. Peel, P. Bright, B. Yount, J. Handy, R. S. Baric, Am. J. Trop. Med. Hyg. 51 (1994) 648-658.

[140] C. M. Wilson, S. K. Volkman, S. Thaithong, R. K. Martin, D. E. Kyle, W. K. Milhous, D. F. Wirth, Mol. Biochem. Parasitol. 57 (1993) 151-160.

[141] A. F. Cowman, S. Karcz, D. Galatis, J. G. Culvenor, J. Cell Biol. 113 (1991) 1033-1042.

[142] R. A. Cooper, M. T. Ferdig, X. Z. Su, L. M. B. Ursos, J. Mu, T. Nomura, H. Fujioka, D. A. Fidock, P. D. Roepe, T. E. Wellems, Mol. Pharmacol. 61 (2002) 35-42.

[143] D. A. Fidock, T. Nomura, A. K. Talley, R. A. Cooper, S. M. Dzekunov, M. T. Ferdig, L. M. B. Ursos, A. b. S. Sidhu, B. Naudé, K. W. Deitsch, X.-z. Su, J. C. Wootton, P. D. Roepe, T. E. Wellems, Molec. Cell 6 (2000) 861-871.

[144] K. L. Waller, R. A. Muhle, L. M. B. Ursos, P. Horrocks, D. Verdier-Pinard, A. b. S. Sidhu, H. Fujioka, P. D. Roepe, D. A. Fidock, J. Biol. Chem. 278 (2003) 33593-33601.

[145] A. b. S. Sidhu, D. Verdier-Pinard, D. A. Fidock, Science 298 (2002) 210-213.

[146] C. D. Fitch, Science 169 (1970) 289-290.

[147] C. D. Fitch, Antimicr. Agents Chemother. 3 (1973) 545-548.

[148] C. P. Sanchez, S. Wünsch, M. Lanzer, J. Biol. Chem. 272 (1997) 2652-2658.

[149] S. Wünsch, C. P. Sanchez, M. Gekle, L. Grosse-Wortmann, J. Wiesner, M. Lanzer, J. Cell Biol. 140 (1998) 335-345.

[150] J. A. Martiney, A. S. Ferrer, A. Cerami, S. M. Dzekunov, P. D. Roepe, Novartis Found. Symp. 226 (1999) 265-280.

[151] P. G. Bray, M. Mungthin, R. G. Ridley, S. A. Ward, Mol. Pharmacol. 54 (1998) 170-179.

[152] S. M. Dzekunov, L. M. B. Ursos, P. D. Roepe, Mol. Biochem. Parasitol. 110 (2000) 107-124.

[153] P. G. Bray, K. J. Saliba, J. D. Davies, D. G. Spiller, M. R. White, K. Kirk, S. A. Ward, Mol. Biochem. Parasitol. 119 (2002) 301-304.

[154] C. P. Sanchez, W. Stein, M. Lanzer, Biochemistry 42 (2003) 9383-9394.

[155] H. Ginsburg, W. Stein, Biochem. Pharmacol 41 (1991) 1463-1470.

[156] E. R. Martin, K. Kirk, Mol. Biol. Evol. 21 (2004) 1938-1949.

[157] R. G. Ridley, W. Hofheinz, H. Matile, C. Jaquet, A. Dorn, R. Masciadri, S. Jolidon, W. F. Richter, A. Guenzi, M. A. Girometta, H. Urwyler, W. Huber, S. Thaithong, W. Peters, Antimicr. Agents Chemother. 40 (1996) 1846-1854.

[158] C. Biot, G. Glorian, L. A. Maciejewski, J. S. Brocard, J. Med. Chem. 40 (1997) 3715-3718.

[159] K. Chibale, J. R. Moss, M. Blackie, D. van Schalkwyk, P. J. Smith, Tetrahedron Lett. 41 (2000) 6231-6235.

[160] Y. Kurosawa, A. Dorn, M. Kitsuji-Shirane, H. Shimada, T. Satoh, H. Matile, W. Hofheinz, R. Masciadri, M. Kansy, R. G. Ridley, Antimicr. Agents Chemother. 44 (2000) 2638-2644.

[161] S. Parapini, N. Basilico, E. Pasini, T. J. Egan, P. Olliaro, D. Taramelli, D. Monti, Exp. Parasitol. 96 (2000) 249-256.

[162] E. Deharo, R. N. Garcia, P. Oporto, A. Gimenez, M. Sauvain, V. Jullian, H. Ginsburg, Exp. Parasitol. 100 (2002) 252-256.

[163] G. S. Collier, J. M. Pratt, C. R. De Wet, C. F. Tshabalala, Biochem. J. 179 (1979) 281.

[164] W. W. Mavuso, Ph.D. Thesis, University of Cape Town, 2001

[165] S. B. Brown, T. C. Dean, P. Jones, Biochem. J. 117 (1970) 733-739.

[166] T. Mizutani, K. Wada, S. Kitagawa, J. Org. Chem. 65 (2000) 6097-6106.

[167] S. B. Brown, I. R. Lantzke, Biochem. J. 115 (1969) 279-285.

[168] S. R. Vippagunta, A. Dorn, R. G. Ridley, J. L. Vennerstrom, Biochim. Biophys. Acta 1475 (2000) 133-140.

[169] D. B. Smithrud, F. Diederich, J. Am. Chem. Soc. 112 (1990) 339-343.

[170] C. Reichardt, D. Che, G. Heckenkemper, G. Schäfer, Eur. J. Org. Chem. (2001) 2343-2361.

[171] T. J. Egan, Exp. Opin. Ther. Patents 11 (2001) 185-209.

[172] J. M. Karle, I. L. Karle, L. Gerena, W. K. Milhous, Antimicr. Agents Chemother. 36 (1992) 1538-1544.

[173] M. S. Cubberley, B. L. Iverson, J. Am. Chem. Soc. 123 (2001) 7560-7563.

[174] A. F. Lagalante, R. J. Jacobson, T. J. Bruno, J. Org. Chem. 61 (1996) 6404-6406.

[175] M. Terada, R. H. Marchessault, Int. J. Biol. Macromol. 25 (1999) 207-215.

[176] L. J. Hughes, G. E. Britt, J. Appl. Polym. Sci. 5 (1961) 337-348.

[177] V. Guttman in: Coordination Chemistry in Nonaqueous Solutions, Springer-Verlag, Berlin, 1968, pp.

[178] J. Ziegler, L. Pasierb, K. A. Cole, D. W. Wright, J. Inorg. Biochem. 96 (2003) 478-486.

[179] R. Baelmans, E. Deharo, G. Bourdy, V. Munoz, C. Quenevo, M. Sauvain, H. Ginsburg, J. Ethnopharm. 73 (2000) 271-275.

[180] M. Kalkanidis, N. Klonis, L. Tilley, L. W. Deady, Biochem. Pharmacol. 63 (2002) 833-842.

[181] R. D. Barr, M. Koekebakker, Am. J. Hematol. 30 (1989) 27-31.

[182] J. H. A. Akoyunoglou, H. S. Olcott, W. D. Brown, Biochemistry (Moscow) 2 (1963) 1033-1041.

[183] T. Deegan, B. G. Maegraith, Ann. Trop. Med. Parasitol. 50 (1956) 194-211.

[184] C. H. Kaschula, Ph.D. Thesis, University of Cape Town, 2002

[185] O. Schales, Ber. 70B (1937) 1874-1880.

[186] T. Heikel, Scandinavian Journal of Clinical and Laboratory Investigation 10 (1958) 193-195.

[187] S. Ohkuma, Yakugaku Zasshi 95 (1975) 1504-1506.

[188] W. I. White, in: D. Dolphin (Ed.), Chapter 7. Aggregation of Porphyrins and Metalloporphyrins, Academic Press, 1978, pp. 303-339.

[189] O. Q. Munro, H. M. Marques, Inorg. Chem. 35 (1996) 3768-3779.

[190] E. Hempelmann, H. M. Marques, J. Pharm. Toxicol. Meth. 32 (1994) 25-30.

[191] P. A. Adams, T. J. Egan, D. C. Ross, J. Silver, P. J. Marsh, Biochem. J. 318 (1996) 25-27.

[192] A. V. Pandey, B. L. Tekwani, FEBS Lett. 393 (1996) 189-192.

[193] G. Blauer, M. Akkawi, Biochem. J. 346 (2000) 249-250.

[194] D. S. Bohle, A. D. Kosar, P. W. Stephens, Can. J. Chem. 81 (2003) 1285-1291.

[195] P. W. Atkins in: Physical Chemistry, Oxford University Press, Oxford, 1990, pp. 621-640.

[196] T. J. Egan, W. W. Mavuso, K. K. Ncokazi, Biochemistry 40 (2001) 204-213.

[197] Graphpad Prism, 3.0, GraphPad Software Inc., 10855 Sorrento Valley Rd. #203, San Diego. CA 92121

[198] S. R. Hawley, P. G. Bray, B. K. Park, S. A. Ward, Mol. Biochem. Parasitol. 80 (1996) 15-25.

[199] D. C. Warhurst, J. C. Craig, I. S. Adagu, D. J. Meyer, S. Y. Lee, Malaria J. 2 (2003) preprint online at http://www.malariajournal.com/content/2/1/26.

[200] J. D. Van der Merwe, MSc. Thesis, University of Cape Town, 2004

[201] D. S. Bohle, J. B. Helms, Biochem. Biophys. Res. Commun. 193 (1993) 504-508.

[202] G. S. Noland, N. Briones, D. J. Sullivan, Mol. Biochem. Parasitol. 130 (2003) 91 - 99.